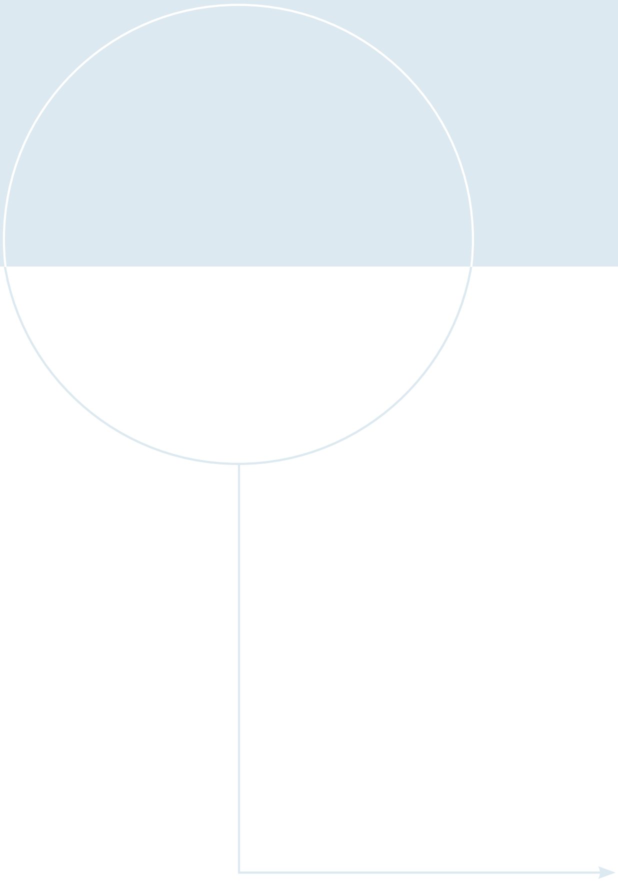

NTNU
Norwegian University of
Science and Technology

Master's thesis

Firstname Lastname

Master's thesis

NTNU
Norwegian University of
Science and Technology
Faculty of Architecture and Design
Department of Design

Firstname Lastname

NTNU
Norwegian University of
Science and Technology

NTNU
Norwegian University of
Science and Technology

Soil-water influences on trace elements and organic matter in Arctic

shuangwu

Environmental Toxicology and Chemistry
Submission date: May 2019
Supervisor: Øyvind Mikkelsen
Co-supervisor: Shazia N Aslam

Norwegian University of Science and Technology
Department of Chemistry

Preface

This thesis was carried out in the Environmental Chemistry and Toxicology (ENVITOX) program from the autumn semester 2018 until the spring semester 2019. Field work and sampling was performed in August 2018 in Ny-Ålesund. The project can be found at the RIS database with the number 10962.

The analysis of background soil samples from Svalbard has also been performed by two other NTNU students, Carolin Elisabeth Huber and Katarina Halbach (2016). The objectives of this work are given below.

- Study the impact of pH on elemental leaching from surface soils.
- Study the distribution profile of trace elements between organic and mineral soils.
- Identify sources of origin of trace elements leading to the current levels in Svalbard soils.
- Study correlations of soil organic matter and inorganic elements in soil.

Trondheim, 2019-05-15

Signature

Shuang Wu

Acknowledgment

I would like to thank the following persons for their great help during the time of accomplishing this work:

My main supervisor Øyvind Mikkelsen, for guidance throughout the project and helpful feedback on the results and thesis and for support during sampling in Svalbard. My co-supervisor Shazia N Aslam, for guidance throughout the thesis and helpful feedback on the results.

I also thank Syverin Lierhagen, for the ICP-MS analysis. Xiaoxue Zhang, for helpful lab work.

List of contents

List of Figures

List of Tables

Acronyms

ADME	Atmospheric mercury depletion events
AMAP	Arctic monitoring and assessment program
Al	Aluminium
B	Boron
BDL	Blank detection limit
Br	Bromium
Ca	Calcium
Cd	Cadmium
Cl	Chloride
Co	Cobalt
Cu	Copper
DOC	Dissolved organic carbon
DOM	Dissolved organic matter
EFs	Enrichment factors
Fe	iron
GEM	Gaseous elemental mercury
GOM	Gaseous oxidized mercury
HA	Humic acid
Hg	Mercury
IDL	Instrumental detection limit
K	Potassium
K_{OA}	Partition coefficient between octanol and air
LRAT	Long range atmospheric transport
LOI	Loss on ignition
MC	Moisture content
MeHg	Methylmercury
Mg	Magnesium
Mn	Manganese
Na	Sodium
Ni	Nickel
OH	Hydroxyl
OM	Organic matter
P	Phosphorus
Pb	Sulfur
PCA	Principal component analysis
Rb	Rubidium
S	Sulfur
Se	Selenium
Si	Silicon
SOM	Soil organic matter
STD	Standard deviation

THg	Total mercury
Zn	Zinc

Abstract

In this study, the impact of pH on leaching of elements from soils was tested. Samples were taken from Bayelva / Stuphalle, Svalbard in August 2018. Overall, the impact of three pH levels, 2, 7 and 10 was investigated in Svalbard soils. Leached elements namely, Cd, Co, Cr, Cu, Fe, Ni, S and Zn showed V-shaped leaching curves. The concentrations of Cd, Co, Ni, Cu, Zn, Fe, Al were higher in pH 2 leachates, while the concentrations of S and Cr, Hg, Pb, Se, U were greater in pH 10 leachates. The concentrations of Cd, Co, Cr, Ni, Cu, Zn, Fe and S were lowest in pH 7 leachates. Among, the concentrations of elements Cd, Co, Cr, Ni, Zn and Fe decreased with increasing pH from 2 to 7 and increased again from pH 7 to 10; only element Al decreased with increasing pH value from 2 to 10. Conversely, the elements Hg, Pb, Se and U increased with raising pH value. In addition to this, current burden of background pollution of inorganic pollutants (trace elements) in organic and mineral soils was also investigated. SOM contents were significantly higher in organic soils (47.33 ± 16.56%) compared to mineral soils (6.07 ± 4.76%). Conversely, pH value of organic soils (6.495 ± 0.66) were significantly lower than mineral soils (7.22 ± 1.15). The levels of 11 trace elements (Cd, Cr, Co, Cu, Hg, Ni, Pb, Rb, Se, U, Zn) and 11 macro/micro elements (Al, B, Ca, Fe, K, Mg, Mn, Na, P, Si, S) for samples from both organic soils and mineral soils were investigated. The concentrations of Cd, Hg, Pb, Se and Zn were significantly higher in organic soils, whereas concentrations of Cr, Cu, Ni and Rb were significantly higher in mineral soils. Additionally, SOM positively correlated with Cd, Hg, Ca, S, Si and negatively related with Al, Fe, Mn, Cr, Cu, Ni, Rb, Co, Na, Mg, K, B. Cd, Hg and S had strongly positive correlation with each other. Al, Fe, K and Co, Cr, Cu Ni, Rb had significantly positive association with each other.

Key words: Elemental composition; Soil organic matter; Bayelva / Stuphalle, Svalbard; Surface soils; Mineral soils; pH; Leachates

Chapter 1

Introduction

1.1 General introduction

Arctic is considered relatively pristine due to minimum local anthropic activities. However, remote human activity occurring in temperate and industrial areas have significantly influenced the polar environment. Svalbard (74-81ºN) is a remote archipelago in the Arctic, and as a gateway to further Arctic, Svalbard is considered a reservoir for contaminants (Kozak et al., 2016). Among others, toxic elements are of particular concern in Arctic environment. Arctic significantly promote deposition of trace metals because of its high latitude and low temperature, sunlight shortage and snow covering with perennial years (AMAP, 2002).

Although trace elements naturally occur and accumulate throughout the environment over geological time period, the considerable quantities should be concerned in the environment due to human activities. The contaminants which released by anthropogenic sources can be distinguished from natural sources through calculating enrichment factors (EFs) for trace elements. EFs values >10 represent anthropogenic inputs (Wedepohl, 1995). Local anthropogenic activities of Svalbard include coal mining, power plants, airport and local traffic (Halbach et al., 2017) lead to small proportion for trace elemental deposition. Distant sources such as fossil fuel combustion, non-ferrous metal production and waste incineration (AMAP 1997) from Europe, North America and Asia are significantly impacting polar environment. Fossil fuel combustion is the major source of trace elemental emission. For example, coal combustion contributes chromium (69%), mercury (66%), manganese (85%) and selenium (98%) to atmospheric emission; combustion of leaded, low-leaded and unleaded gasoline contributes to 74% of total lead emission; Oil combustion contributes to 90% of nickel emission (AMAP, 2002). Non-ferrous metal industry is another major source result in emission of cadmium (73%), copper (70%) and zinc (72%) (AMAP. 2002).

Soils and glaciers may also be major sources of trace elements to aquatic ecosystems. Snow melting possibly promotes production of MeHg which can be uptake by biota and transported to soil by plant roots and thus transferred to water through soil runoff. Zaborska et al (2017) reported that high sedimentary concentration of some trace elements, such as Pb, Cd and Zn were found closed to glaciers, this might result from melting of deposition on glaciers' surface. There was an important influence in trace elemental concentration due to melting glacier water in fjords, Svalbard (Steffen et al; 2013; Beldowski et al., 2015).

1.2 Impact of pH on trace elements in soils

Dissolved organic carbon (DOC) plays a key role in mobility of trace elements which is controlled by their distribution between colloidal and dissolved phases (Pédrot et al., 2009). Humic substances can bind to mineral surface and then react with adsorption properties (e.g. cations) to control organic functional groups and size of organic matter (Gangloff et al., 2016). The important governed mechanism for binding of organic matter to mineral surface is considered as specific adsorption by ligand exchange. This binding can impact on colloidal and dissolved phases and therefore affecting the mobility of trace elements (Pédrot et al., 2009).

pH is the most important factor that affects mobilization and chemical speciation of trace elements through two ways. firstly, pH promotes competition between trace elements and protons and secondly pH affects separation of colloids (Pédrot et al., 2009).

Pédrot et al (2009) tested the leaching of 12 elements (Co, Cr, Mn, Ni, Pb, Rb, U, Al, Ca, Fe, Mg, Zn) released in soils leachates during the pH changes. Inorganic elements namely, Co, Mn, Ni, Rb and Zn, Mg and Ca were released more at pH 4. Other elements namely Cr, Pb, U, Al and Fe had higher concentration in solutions at pH 7.2, this was attributed by binding of metals to anionic ligands at pH 7.2 rather than promotion of neutral pH (Pédrot et al., 2009).

Pédrot et al (2009) also indicated that the concentrations of elements Co, Mn, Zn and Mg, Ca released from soil sharply increased with pH decrease due to their dissolved state at acidic pH, while these elements released from soil with DOM at pH 7.2. The concentrations of Ni and Rb slowly increased with lowering pH. Ni and Rb released as soluble ions or molecules at pH 4 and as colloids at pH 7.2. The trace elements Cr, Pb and U bound with anionic ligands released in pH 7.2 solutions. Similarly, Grybos et al (2007) showed increase in concentrations of Cr, Pb and U with pH increase from 5.3 to 7 over 160 hours. Higher concentrations of Al and Fe released from soil to neutral pH solution in this study were attributed by Fe-/Al-oxyhydroxides formation at pH 4, which enhanced binding ability of elements on humic substances, however, increased pH weakened binding ability of humic matters.

Dijkstra et al (2004) reported “V-shaped” leaching curves reflecting a strong pH dependence of the leached concentration of trace elements. The concentration of leached trace elements (Ni, Cu, Zn, Cd, Pb) reduced with rising pH from high concentration at pH 2 and reach to lowest points at neutral pH value, then increased again from neutral pH to alkaline pH values (Figure 1.1). The elemental speciation which was strongly dependent on pH explained V-shaped leaching (Figure 1.2). It can be divided into three groups, including “free metal”, “inorganic complex” and “organic complex”. The free metal mostly dominates below pH 4 and Iron and Aluminum (hydr)oxides significantly contribute to adsorption at neutral pH, while the binding of trace elements to DOC generally dominate from neutral to high pH value. OH complex predominantly appears at pH 12 (Dijkstra et al., 2004). The stronger sorption of trace elements to variable surface appears at neutral pH conditions compare to low pH values. Cation sorption increases from neutral pH to slightly alkaline pH, while organic complex of cations increases in solutions at alkaline pH value and thereby decreasing sorption to the solid surfaces. The increased DOC concentrations in solution at strongly alkaline pH values result in strong binding of complex to DOC (Dijkstra et al., 2004).

Figure 1.1: Leached concentrations and model predictions as a function of pH of Ni, Cu, Zn, Cd, and Pb from the soil samples (Dijkstra et al., 2004).

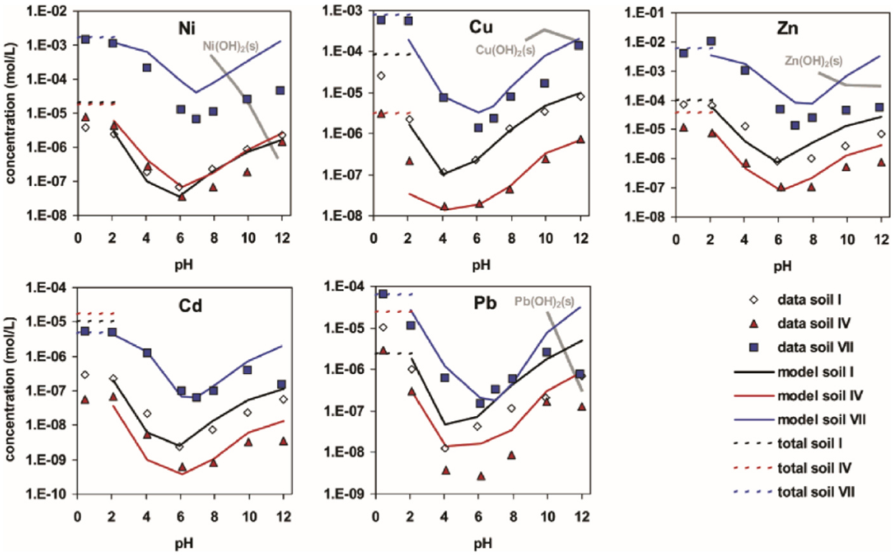

Figure 1.2: Calculation of the distribution of Ni, Cu, Zn, Cd, and Pb among the different surfaces considered in the model. In the solid phase, SOM = solid organic matter; Fe+Al = sum of amorphous iron (hydr)oxide, crystalline iron (hydr)oxide, and amorphous aluminum (hydr)oxide; Clay = clay surfaces. In solution, DOM = dissolved organic matter; Inorg = inorganic complexes such as OH species; Free = free ions (Me^{2+}) (Dijkstra et al., 2004).

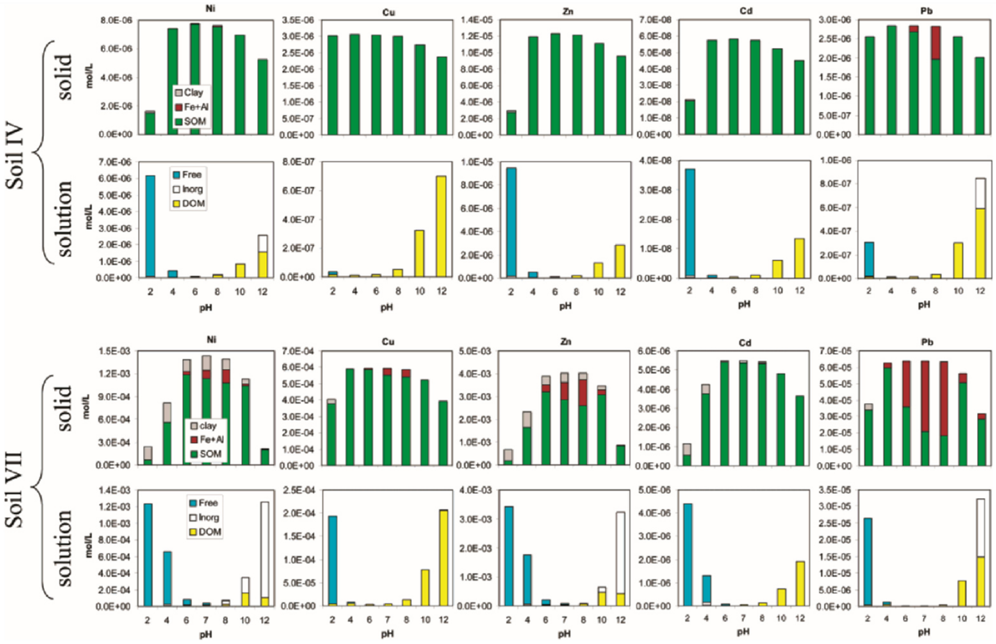

Objectives

It is important to study the trace elements because certain form and level of some trace elements can be toxic and can pose a risk to people and animals (AMAP, 1997). Moreover, pH is the critical factor to affect their mobility and chemical speciation of trace elements (Pédrot et al., 2009), and their mobility and chemical speciation determine their transportation; therefore, the study of effects of pH value on trace elements is also essential.

Main objectives of the study are given below

- Study the impact of pH on elemental leaching from surface soils.
- Study correlations of soil organic matter and inorganic elements in soil.
- Study current burden of background pollution of inorganic pollutants (trace elements) in Svalbard soils.
- Study the distribution profile of trace elements between organic and mineral soils.
- Identify sources of origin of trace elements leading to the current levels in Svalbard soils.

The elemental accumulation was measured in five sampling sites with geological differences and mineral variation. In this study, Inductively Coupled Plasma Mass Spectrometry (ICP-MS) was used to measure the concentrations of elements in soils and pH leachates. The traditional statistical analysis (Student t-test, Mann Whitney U-test, one-way ANOVA and Kruskal Wallis test) was used to detect significant difference and variance. Principal component analysis was used to study pH, soil organic matter (SOM) and elemental profiles in different types of soils (organic-rich soils and mineral soils).

Chapter 2

Background

2.1 General introduction of soil in Svalbard

2.1.1 Characteristics of soils

Soil is the mixture of organic matter, minerals, gases, liquids as well as organisms, and plays a key role in biogeochemical cycling of organic and mineral matter (Bockheim et al., 2006). The formation of soil is dependent on the interactions between physical, chemical, biological, anthropogenic processes and soil parent materials (Szymanski et al., 2013). The distinct layers formed in soils are called horizons. Soil forming processes are affected by physical and chemical weathering, silt translocation, aeolian deposition and rill erosion (Szymański, 2017). However, both physical and chemical weathering are dominantly controlled by soil moisture availability. In addition, spatial soil variation is attributed by soil age and morphological position (Marijin van der Meij et al., 2016).

Svalbard is covered by permafrost which is ground, including rock or soil at or below the freezing point of water 0°C for two or more years (Osterkamp, 2001). The cryogenic process, which involves input and output, transfer, transformation of energy, water and soil material, is the dominant process of permafrost formation (McGuire et al., 2009). Cryogenic processes can also control the carbon cycle in permafrost; the carbon is transferred from permafrost to terrestrial vegetation and microbes, then reaches to the atmosphere and back vegetation again, finally back to permafrost through sediments (McGuire et al., 2009). Cryopedogenic processes are natural and characteristic of permafrost (Bockheim et al., 2006). These processes produce the irregular and broken horizons for crysols (crysols is defined as permafrost within 1m of land surface by Food and Agriculture Organization (FAO)). Cryoturbation, which is used to describe soil movements, is the most important cryopedogenic process in cryosols (Bockheim, 2015). It impacts on chemical weathering due to refresh soil material and increase surface area of soil, also affects the distribution of soil organic carbon to relate with soil parent materials (Bockheim et al., 2006). Soil parent materials are also the factor that influences in variable physical and chemical properties of soil surface horizons. In Svalbard, most surface horizons are characterized by sand, sandy loam and loamy sand texture classes, whereas, SiO_2, Al_2O_3, Fe_2O_3 and K_2O are main chemical components of surface horizons (Szymanski et al., 2016).

2.1.2 Micro-ecosystem of soils – Biological soil crusts (BSCs)

Biological soil crusts (BSCs) are communities of living organisms on the soil surface play an important ecological role, such as carbon and nitrogen fixation as well as soil stabilization. They also impact on germination and nutrient levels of plants. BSCs are mainly composed of fungi, lichens, cyanobacteria, bryophytes and algae (Bettina et al., 2016). However, the species and composition depend on the soil characteristics and climate as well as disturbance (Bawker, 2007). For example, the abundances of lichens and mosses increase with rising content of clay and silt and reducing sand. Moreover, moist habitats also contribute to growth of liches and mosses. The soils which suffer low chemical weathering and thus low contents of nutrient generally have more BSCs (Willianms et al., 2017).

BSCs influence ecosystem functioning. Firstly, BSCs can affect biogeochemical cycling due to its contribution to carbon cycle through respiration and photosynthesis of crust microorganisms. Secondly, they can also affect geophysical and geomorphological properties because they contribute to the nitrogen cycle that varied with crust compositions (Belnap, 2003). BSCs are considered as important ecosystem engineer in Svalbard where the variability of BSCs coverage is ranged from 18 to 90% in different locations. Ny-Ålesund is reported to be covered by higher variability of BSCs with up to 90%. The regions closer to the coast have greater proportions of bryophytes and lichens compare to mountain regions. BSCs development in the regions closed to coast is dependent on water availability. In addition, the short growing seasons and little summer rainfall in Svalbard positively influence BSCs development. Snow melt also contribute to BSCs development in the areas with limited precipitation (Willianms et al., 2017).

2.2 Soil organic matter (SOM)

Soil organic matter (SOM), consists of decomposed plant and animal residues, and microbial materials influences soil formation and soil properties, such as pH value (Szymanski, 2017). It also plays a key role in transportation, sorption of water, elements and pollutants, as well as their reactivity and bioavailability. The SOM is mainly composed of humic substances, including fulvic acid, humic acid and humin, liquid-soluble materials, proteins and carbohydrates (Pignatello, 1998). The variation of SOM composition is influenced by soil forming factors, such as parent materials, biota, input chemistry, energy level and climate, and their interactions (Wang et al., 2016). SOM is an important consideration in High Arctic because soils in these regions are permafrost-affected that maybe easily decomposed due to climate change. Soils covered by tundra vegetation in Svalbard contain more SOM (Szymanski, 2017). The formation and stability of SOM can be contributed by plant roots, this is attributed by decomposition, closure in soil aggregates and interactions with soil materials.

SOM is the important source of organic carbon and nitrogen (Szymanski, 2017). SOM decomposition is affected by increased plant primary production in deeper layers of permafrost soils due to increased temperature. However, increased plant productivity impacts on rising available organic carbon and nitrogen and thus SOM also affects organic carbon and nitrogen storage in soil layers (Wild et al., 2014; Henkner et al., 2016). SOM also acts as sink of organic carbon and nitrogen and plays crucial role to control carbon cycling. Poirier et al (2018) reported that organic carbon stored in soils was three or four times greater than in vegetation or atmosphere overall the world.

SOM acts as a sink and determines the retention of trace elements in Arctic soils (Marques et al., 2017), because trace elements have strong correlation with SOM. Trace elements can be absorbed by SOM, which contributes on their stability to accumulate in soils; therefore, these organic matters can control elemental distribution and levels. While trace elements can also be absorbed by dissolved organic matter (DOM). DOM is defined as organic matter that can pass through a filter size ranging from 0.22 to 0.7 μm. DOM impact on metal transport because and affect mobility of trace metals. Humic substances, are considered as reactive fraction of dissolved organic carbon (DOC), which can bind to mineral surface; thereby modifying their particle charge and colloidal stability and hence influence in mobility of trace elements (Pédrot et al., 2009).

2.3 Pathways for transportation of trace elements to Arctic

The trace elements can enter Arctic ecosystem through several pathways, including ocean current, migratory birds and pelagic organisms and atmospheric transport (Pacyna and Ottar, 1985; Ziółek et al., 2017). Among, atmospheric transport is the most important long-range transport for the trace elements (Flanner at el., 2008). Air-octanol partitioning coefficient of Log K_{OA} <10 is defined as having a tendency for long-range atmospheric transport; otherwise, the metals mainly deposit on atmospheric particle before they enter Arctic. Cadmium, mercury, lead and zinc have been reported as elements that experience long range atmospheric transport (Li et al., 2003; Halbach et al., 2017).

Zaborska et al (2017) indicated that trace metals in Svalbard atmosphere were transported from Europe and Russia. However, the pathway of transportation changes with seasonal shift (Bazzano et al., 2016). Levels of Cd, Mn and Pb were higher around Ny-Ålesund regions in spring compared to summer. Pb isotopic ratios also showed changes in the geographic input related with seasonal shifts. Significant atmospheric inputs in Ny-Ålesund were from the north Eurasia during spring and South America during summer. The mean lead isotopic ratio $^{208}Pb/^{206}Pb$ was 2.103 ± 0.003 in spring and 2.085 ± 0.008 in summer; while mean Pb isotopic ratio $^{207}Pb/^{206}Pb$ was 0.8638 ± 0.004 in spring and 0.8564 ± 0.006 in summer; this was consistent with previously published report (Bazzano et al. 2015). Lead (Pb) stable isotopic ratios are usually used to identify original sources of heavy metals deposited in Arctic atmosphere (Bollhöfer and Rosman, 2002; Bazzano et al., 2014), as Pb isotopic composition is not affected by physical or chemical fraction processes. Lead has four stable isotopes, ^{204}Pb, ^{206}Pb, ^{207}Pb and ^{208}Pb. The relative abundance of Pb isotopes in ores is correlated with both the abundance of their parent nuclide of the ore formation at the moment and the age of the rocks; therefore, the distinct geographical areas have distinctive Pb isotopic ratios (Komarek et al. 2008). For this source variation with seasonal shift, it could be combined with back trajectory (BT) analysis for further explanation. BT analysis which indicated the movement of air masses was used to detect source areas of atmospheric particulate matter by model of HYSPLIT (Kozak et al. 2016). In addition, distant residence time (DRT) is used to evaluate long-range transport potential of chemicals by characterizing persistence of chemicals. Comparing chemicals with distant regions and specific target compartment within these regions (Reid and Mackay, 2008).

These trace elements can release in air and then deposit (wet/dry) on snow, ice, soil, sediment from where plants and animals consume these elements. And if something goes into sediments or water in ocean, it's already a part of marine system. Atmospheric deposition relates with some trace elemental accumulation in surface soil (AMAP 2005; Pédrot et al., 2009). According to existing literature (Halbach et al., 2017), trace elements namely Cd, Hg and Pb are more abundant in surface soils. Terrestrial ecosystem also plays a key role in receiving atmospheric deposition and is an important source of trace elements to aquatic ecosystem or release of some trace elements back to atmosphere, the latter contribution is from re-emission of these trace elements (Douglas et al., 2010). According to Halbach et al (2017), the accumulation of mercury into surface soils in Svalbard was a result of atmospheric deposition. Other studies also provide evidence that the direct sources of mercury in soils are snow and ice deposition (Larose et al., 2010; Chételat et al., 2015; Bazzano et al., 2016). Snow and ice have been considered as "key reservoirs" of trace elements (Gamberg et al 2015). Søndergaard et al (2012) showed that the major fraction of mercury deposited into snow during winter/spring. The mercury is released to soils when snow and ice are melting in summer. Mercury can also be reduced to gaseous elemental mercury (GEM) by photolytic reduction after Atmospheric mercury depletion events (AMDEs) and thus return to atmosphere. Approximately 20%-50% of deposited mercury during AMDEs quickly returned to atmosphere within 24 hours (Gamberg et al 2015). However, a large quantity of mercury stored in snow. Dommergue et al (2010) reported that snow melting contributed to 1.5-3.6 kg/year of mercury input in the fiord around regions of Spitsbergen, Svalbard.

Trace elements can be stored in snow or ice and then transport to soil or water through melting snow or soil runoff. Snow is a key media to transfer trace elements between atmosphere and landscape. The highest concentration of mercury was found in surface snow during early spring (Steffen et al., 2008; Larose et al., 2010; Durnford et al., 2012). This is attributed by AMDEs promoting mercury deposition. Peak concentration ranged from 35-198 ng/L when AMDE happened, while ranged from 17-74 ng/L when it did not happen (Larose et al., 2010). The deposited concentration was variable with seasonal shift (Sharp et al., 2002; Faïn et al., 2008). In addition, snow crystal type and age of flowers can influence in mercury distribution in snowpack (Douglas et al., 2008). Melting snow affects soil moisture and properties, such as pH, redox. Soil organic matter is also affected by snowpack due to OH formation (Edwards et al., 2007).

2.4 The trace elements in Svalbard soils

2.4.1 Mercury (Hg)

Mercury (Hg) has been an element of great concern in Arctic, because it can bioaccumulate and biomagnify through food chain and its concentration can reach toxic levels in high trophic level species (AMAP, 2005). Hg is released in environment both from natural (such as volcanoes and rock weathering) and anthropogenic sources. The major local anthropogenic source of Hg release includes power plant, fossil fuel combustion and coal mining (AMAP, 2011). Svalbard has a long history of coal mining (Vidar, 1998).

Figure 2.1 features mercury cycling. Hg exists in nature as elemental mercury as well as inorganic and organic compounds (AMAP, 2011). It has long retention time in atmosphere (approx. 1 year), which allows its long-range transportation to Arctic (Durnford et al., 2010). The chemical forms of mercury determine its pathway to enter Arctic. The important pathways are air and oceanic current. The form of Hg that reaches to Arctic through atmosphere is gaseous elemental mercury (GEM, Hg(0)) (Gauchard et al., 2005). GEM is oxidized or absorbed to form gaseous oxidized mercury (GOM) [Hg (II)] or particulate mercury (HgP)[Hg (II)]. These two forms of mercury [Hg (II)] can be transported and deposited into other Arctic environmental media, such as snow, ice and soil by dry or wet deposition (Cole et al. 2013; Obrist et al. 2017). Hg enters to Arctic through oceanic current as inorganic Hg, methylated mercury and dissolved gaseous mercury (AMAP, 2011).

Atmospheric mercury depletion events (AMDEs) happen during polar spring after sunrise before air temperature reaches to 0°C (Figure 2.2), which relates with sea ice melting and increases the total deposition of mercury in Arctic environment. This is attributed by decreasing GEM and increasing GOM or HgP during AMDEs (Figure 2.3) (Schroeder et al., 1998). The processes are described by equations (1-4). Hg (0) is rapidly oxidized to form Hg (II) in the atmosphere and hence quickly deposit in ice and snow surface. AMDEs also result in important Hg speciation change, Hg(II) temporarily dominates Arctic atmosphere when AMDEs occur.

$$Br_2 + hv \rightarrow 2Br- \ (1)$$

$$Br^- + O_3 \rightarrow BrO + O_2 \ (2)$$

$$BrO + Hg\,(0) \rightarrow HgO + Br \ (3)$$

$$HgBr + O$$

$$HgBrO$$

$$2Br^- + Hg\,(0) \rightarrow HgBr_2 \ (4)$$

Climate change can slow down the oxidation rate of Hg(0) to Hg(II) during AMDEs due to increased rate of HgBr dissociation and reduction of Br release, consequently decrease Hg deposition. However, rising temperature results in melting sea ice, glaciers and thawing of permafrost, where mercury stored can be released. As a result, mercury available for methylation will increase and re-emitted mercury from sea surface will also increase transportation of mercury (AMAP, 2011).

In addition, mercury can methylate and de-methylate abiotically and biotically, as well as be strongly bound to organic matter (Skyllberg et al., 2000), thus organic matter contribute to enhance Hg(II) retention in soils. The higher concentration of Hg is commonly found in organic soils compared to mineral soils. Strong correlation between Hg and organic matter in organic soils was reported by Låg and Steinnes (1978). In addition, Hg concentration varies with soil depth (Låg & Steinnes, 1978). Hg has strong ability to form stable complex through binding with hydroxyl ($Hg(OH)_2$ above pH7, as well as binding to sulphide anion (HgS) (Alloway, 2013). The strong ability of soil to fix Hg^{2+} species leads to stability of Hg in soils (Gilmour et al., 1973). Johansson et al (1988) reported that less than 1% of Hg on humus colloids transported to lake from forest soils in Sweden per year.

Figure 2.1: Mercury cycling (AMAP, 2011).

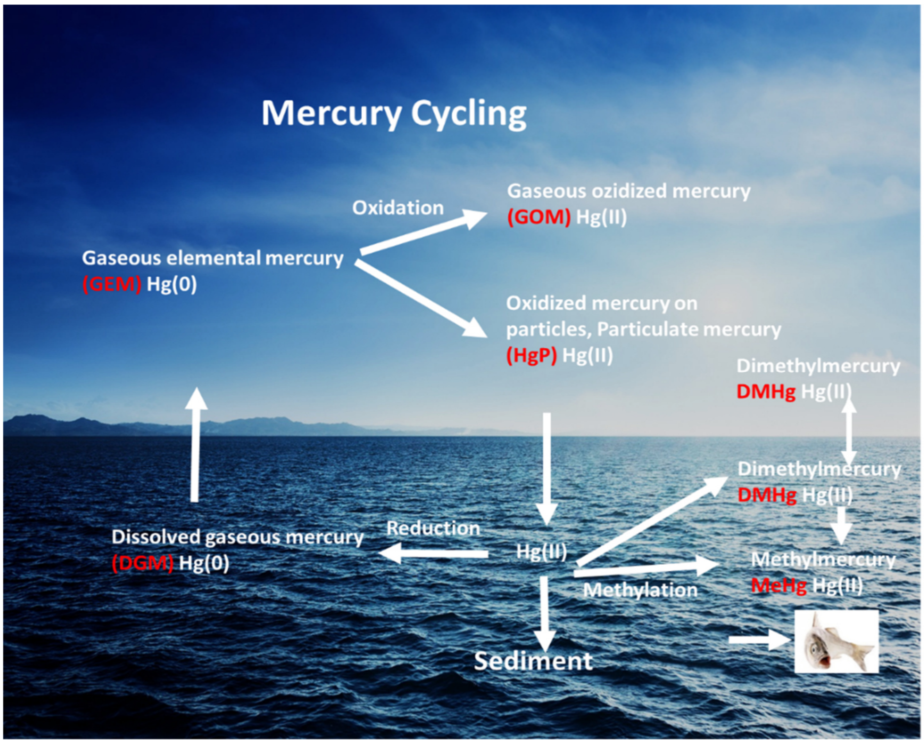

Figure 2.2: Atmospheric mercury depletion events (AMAP, 2011).

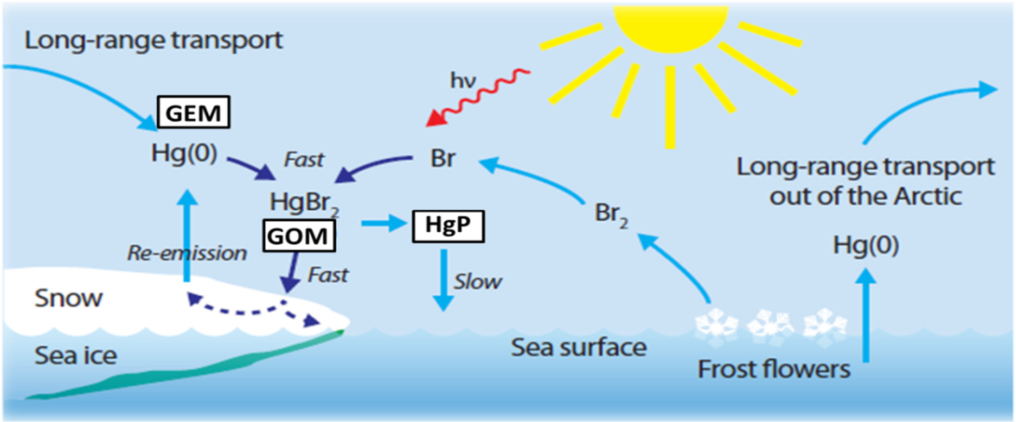

Figure 2.3: Time series for gaseous elemental mercury (six-hourly averaged data) concentrations at Alert, Nunavut, Canada from 1995 to 2008 (top) and time series of reactive gaseous mercury, particulate phase mercury and gaseous elemental mercury (three-hourly averaged data) concentrations from Alert 2002 to 2008 (bottom) (AMAP, 2011)

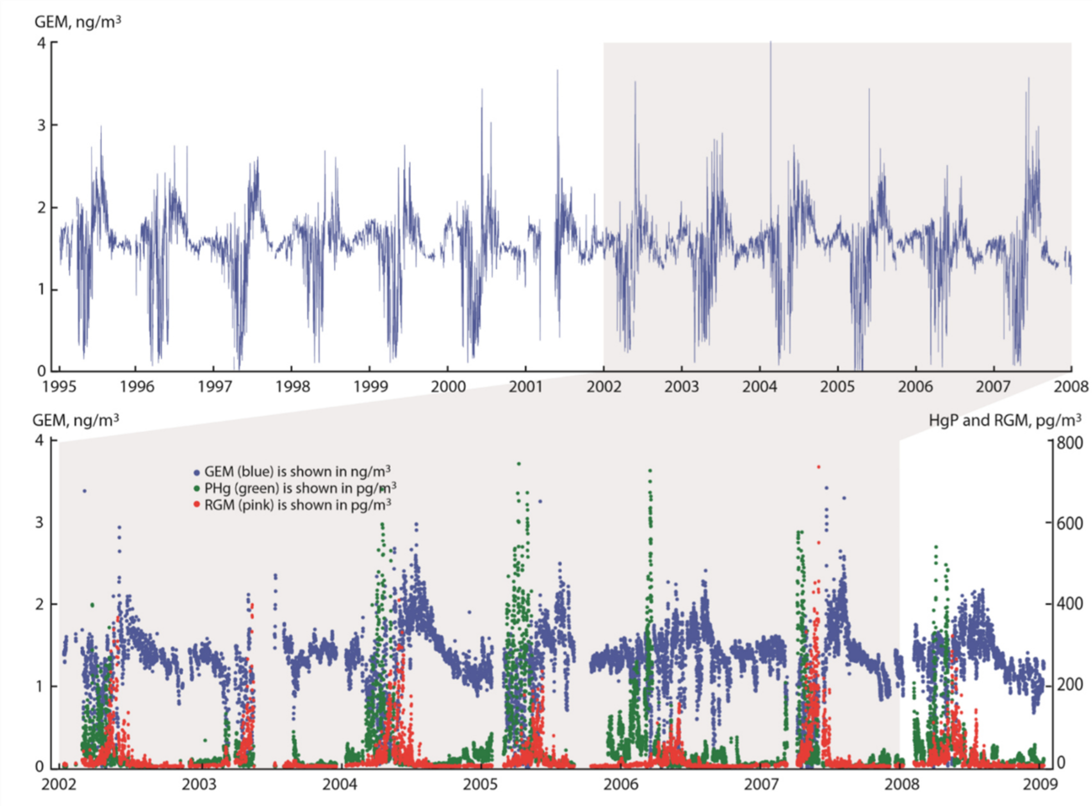

2.4.2 Lead (Pb)

Lead (Pb) can be transported by long-range atmospheric transport to Arctic from distant anthropogenic sources (AMAP, 1997). It is emitted from high-temperature process, such as metal smelting and coal burning (Alloway, 2013). Its concentration in Arctic aerosol varied with seasonal shift, which reaches to its peak in winter and decreases to its minimum in summer (AMAP, 1997). Pb binds with clay minerals, Fe and Al hydroxides as well as organic matter (Gray et al., 2005). Additionally, it also strongly binds with Ca carbonate particles or phosphate in soils. Pb level tends to increase with rising silicon content in silicate rocks. Pb is strongly absorbed and bound to organic matter in soils and hence have high concentration in organic rich surface soils (Meyers et al., 1992). The stable Pb-organic complexes may form in soil at high pH value. The Pb solubility may increase with rising acidity. Monodentate complexes can be formed by binding of Pb to humic matter in soils at pH 4 and above. Pb has strongest ability to bind with humic matter compares to other trace elements except for Hg and Cu; therefore, humic matter also play a key role in controlling Pb deposit and transport from surface soil to deeper layers. Pb predominantly exists with +2 oxidation state and forms inorganic salts, such as lead oxides and lead sulfides. Lead sulfides (PbS) are the major Pb minerals (Alloway, 2013). Also, Kaste et al (2006) showed the correlation between Pb and Fe that indicated the strong adsorption of Pb on Fe-oxides. Dörr and Münnich (1991) used Pb isotope (^{210}Pb) to trace Pb leaching and indicated that it mainly happened with organic matter release (Fleming et al, 1977).

The deposition of Pb in organic soils can come from different sources, however, atmospheric deposition is the most important one among these sources (Bazzano et al., 2016). The accumulation of Pb can affect biological activities of surface soils; for example, it may limit enzymatic activities and therefore increasing formation of materials which are incompletely decomposed in soils (Kabata-Pendias and Pendias, 2001).

2.4.3 Cadmium (Cd)

Cadmium (Cd) is a byproduct from production of Lead (United Nations Environment Programme 2010). In addition, P fertilizer, fossil fuel combustion and waste incineration are main sources of Cd (Alloway, 2013). The trace level of Cd has showed predominant toxicity because its bioavailability does not reduce in the long term (Voogt, 2017). Cd can be effectively taken by root and leaf system of plants and transported through food chain, it also accumulates in soil organisms (AMAP, 1997). pH and clay are considered as major factors to control Cd uptake (Alloway, 2013). In Arctic, the atmospheric deposition of Cd is attributed by long-range atmospheric transportation (AMAP, 1997) due to local and distant anthropogenic activities. The concentrations of Cd ranged from 0.1-1μg/g in soils (Alloway, 2013). Farrah and Pickering (1977) indicated that adsorption of Cd to clay has been the predominantly binding process; therefore, the increased Cd concentration may result from content of soil clay fraction. Cd levels also correlated with the contents of Fe and Mn due to binding of Cd to Fe and Mn (hydr)oxides (Voogt, 2017). It has been reported that Cd has affinity for S and Zn (Kabata-Pendias and Pendias, 2001). The higher level of Cd has been found in topsoils compared to soils of deep depth (Halbach et al., 2017).

Cd exists in soils with +2 oxidation state, and SOM, oxyhydroxides of Fe, Mn and Al are the major Cd adsorbents. The sorption is followed as shown in equation5 (Allow, 2013). pH inversely influences Cd sorption and sorption decreases with pH increase and vice versa. Additionally, pH affects Cd mobility in soils (Figure 2.4). The adsorption can control Cd concentration in soil solutions (Soon, 1981). In acidic soils, the organic matter controls Cd solubility (Kabata-Pendias and Pendias, 2001). Buekers et al (2008) proposed that Cd bind to SOM under pH 6.5 and bind to Fe-oxides above pH 6.5. Cd form minerals upon oxidation. Moreover, Cd may bind to dissolved organic matter (DOM) to form complexes in solutions, while these complexes increase Cd mobility (Alloway, 2013).

$$S\text{-}OH + Cd^{2+} \rightleftharpoons S\text{-}OCd^{+} + H^{+} \quad (5)$$

S-OH is the surface hydroxyl group.

Figure 2.4: Solubility of Cd^{2+} in soils as a function of soil pH. Equilibration with 15, 25, and 100 µg Cd per 2 g of soil (Kabata-Pendias and Pendias, 2001)**.**

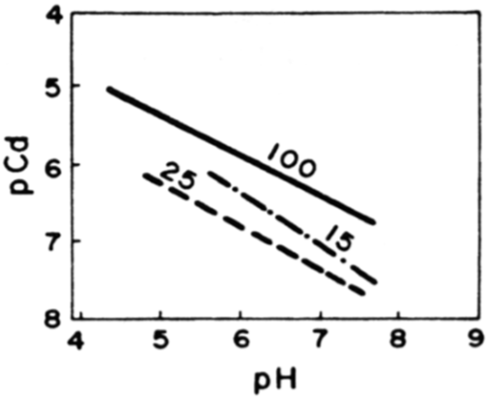

2.4.4 Cobalt (Co) and Chromium (Cr)

Cobalt (Co) can be released from weathering of rocks and leaching from soils to water due to its high mobility (Allow, 2013). Co is associated with silicates, organic matter and Mn-oxides in soils. pH is an important factor to control Co sorption and formation of Co complexes (Figure 2.5) (Kabata-Pendias and Pendias, 2001). Due to similar chemical properties, Co and Manganese (Mn) are strongly correlated in soils. The oxidation of Co^{2+} to Co^{3+} occurs by Mn-oxides from pH 4 to pH 7, which is described by equation 6. However, the oxidation lowers Co availability (Alloway, 2013).

$$2Co^{2+}_{(aq)} + 2MnO_{2(s)} + 3H_2O \rightleftharpoons 2CoOOH_{(s)} + Mn_2O_{3(s)} + 4H^+_{(aq)} \quad (6)$$

Chromium release in environment as a result of emission from large industrial use, such as metallurgical industry, electroplating and textile industry. Cr can be released in water by leaching from acidic soils (James et al., 1988). On the other hand, Cr can remain in soils by adsorption to Fe-oxides. Cr concentrations range from 1 to 3000µg/g in soils (Allow, 2013). However, low Cr concentrations are found in organic-rich soils (AMAP, 1997). As shown in equations 7 and 8, pH highly influence conversion between Cr^{3+} and Cr^{6+} (Alloway, 2013). Most stable form of Cr in soils is Cr^{3+} at acidic pH, and it generally precipitates completely at pH 5. While Cr^{6+} is unstable and mobile in both acid and alkaline soils (Figure 2.6) (Kabata-Pendias and Pendias, 2001). The common chemical form of Cr is $Cr(OH)_2^+$ which can bind to humic matters.

$$HCrO_4^- + 7H^+ 3e^- \rightleftharpoons Cr^{3+} + 4H_2O \quad (7)$$
$$CrO_4^{2-} + 4H_2O + 3e^- \rightleftharpoons Cr(OH)_3 + 5OH^- \quad (8)$$

Figure 2.5: Effects of pH on the sorption of Co by (a) Mn nodules and (b) goethite and effects of time on the sorption of Co by (c) birnessite (Kabata-Pendias and Pendias, 2001).

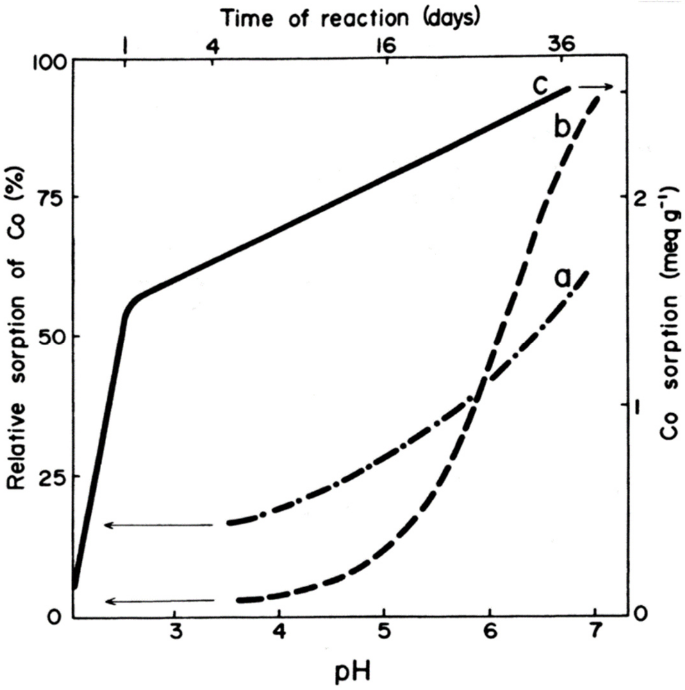

Figure 2.6: Solubility of trivalent and hexavalent Cr as a function of pH (Kabata-Pendias and Pendias, 2001).

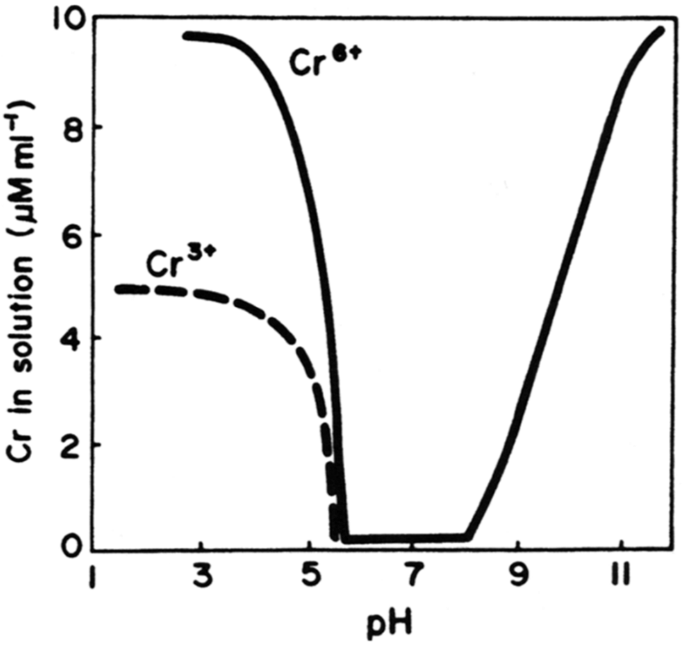

2.5 Impact of ongoing climate change on soil properties

2.5.1 Climate change

The global climate change is attributed to changes of greenhouse gas levels in the atmosphere (Brevik, 2013). According to Intergovernmental Panel on Climate Change (IPCC), the average global temperature increased between 1.8 and 4.0℃ during 1980-1999. The temperature has been observed for longest series since the first permanent weather station was established in Svalbard in 1911 (Førland et al., 2011). The positive trends of temperature were found in four seasons (Figure 8). Also, a sharp increase started in 2000 for all seasons (Figure 2.7). The future temperature in 2100 will be around 10℃ higher than in 2000 for spring, autumn and winter. For summer, the future temperature will be two times higher during latest 100 years (2000-2100) (Figure 8). The climate change can impact on soils. This is because the greenhouse gases are mainly based on carbon and nitrogen, whereas soils are part of C and N cycles.

2.5.2 Impact of climate change on soil properties

a. Soil organic matters

Carbon and nitrogen are important components of SOM; therefore, climate change can affect contents of SOM. Plant growth will rise by global warming with increasing level of CO_2 in atmosphere, which can promote to content of organic matter in soils. Conversely, the rising air temperature lead to consistently increased decomposition and thereby losing organic matter. According to a current study, loss of SOM through decomposition exceeded compared to level of SOM from obtained plant growth (Karmakar et al., 2016). As a result, climate change reduces the content of SOM in soils. The increasing level of CO_2 also increases the soil C:N ratio, nitrogen mineralization therefore reduces because decomposition in soil needs more nitrogen. Mineralization plays an essential role in supplying nitrogen to plants; in that case, this negatively affect plant growth due to lower level of available nitrogen to plants (Brevik, 2013) and thus reduce the production of SOM. Additionally, climate change alters the global precipitation, which also influences in SOM (Karmakar et al., 2016).

As the major component of soils, SOM plays a key role for soil quality through impact on soil structure, water holding capacity, soil stability and supply of nutrient. Consequently, climate change can also influence in these above through affecting SOM (Brevik, 2013). For example, decreased level of SOM results in reducing soil aggregate stability (Karmakar et al., 2016); the rising temperature leads to more evapotranspiration loss of water from soil (Farkas et al., 2008).

b. Soil microbes

There are direct and indirect effects on soil microbes due to climate change (Bardgett et al., 2008). Because climate change affects decomposition of organic matter, as a result, the rate of microbial activities will be accelerated and thus increasing the export of CO_2 to the atmosphere. In addition, climate change (Davidson et al., 2006; Jenkinson et al., 1991) can indirectly affect soil microbial communities and activities through impacts on plant growth. These effects are operated by various mechanisms (Bardgett et al., 2008). The most important mechanism is that increased atmospheric concentrations of CO_2 influences in soil microbes through increased plant photosynthesis and transfer of photosynthate carbon to roots, fungi and heterotrophic microbes (Johnson et al., 2005; Hogberg et al., 2006; Bardgett et al., 2005).

Figure 2.7: Temperature projectionsforSvalbard (Førland et al., 2011).

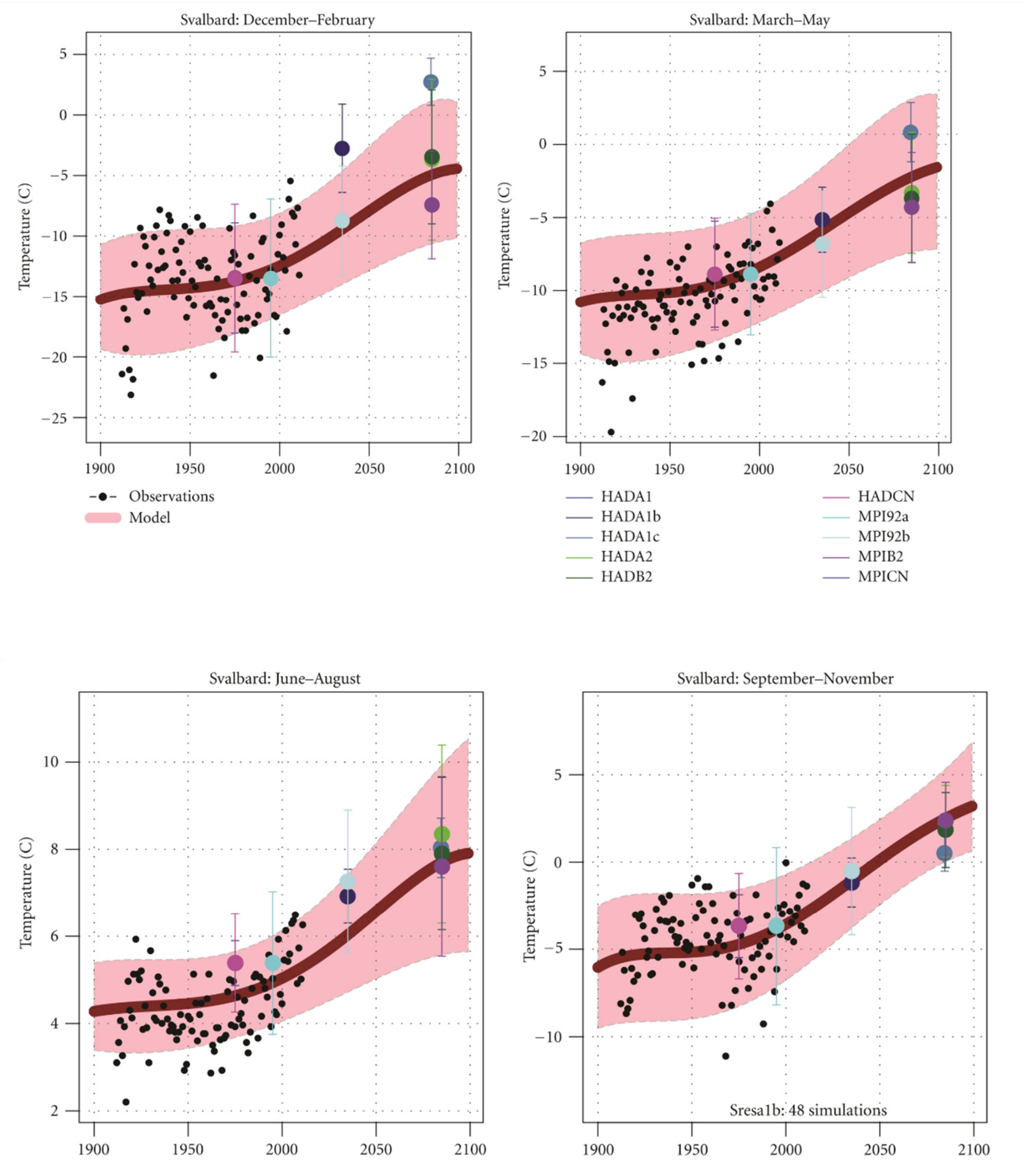

2.6 Inductively coupled plasma mass spectrometry (ICP-MS)

Inductively Coupled Plasma Mass Spectrometry (ICP-MS) is an analytical technology to be used for elemental determination. It was introduced in 1983 and quickly accepted by many laboratories. ICP-MS serves as quantitative and semi-quantitative instruments, it enables to analyze approximate 80 elements in few minutes for an unknown sample by using semi-quantitative software (Vanhaecke, 2001).

The samples are formed an aerosol of fine size droplets to enter the argon plasma. This plasma then releases electron to generate positively charged ions to pass through mass spectrometer which is capable to quickly scan the atomic mass. Only one mass-to-charge ratio ions can be allowed passing through mass spectrometer to get into detector. A measurable electronic signal is generated after the positively charged ions strike on the negatively active surface of detector. The ICP-MS provides the data through one of four ways, including semi-quantitative analysis, quantitative analysis, isotope dilution analysis and isotope ratio analysis. The software makes up the calibration curve to determine the concentration of elements by comparison between intensities of measured signals and standards (Thomas, 2008).

The high temperature ICP source is used to convert elemental atoms to ions, then these ions can be separated and determined by mass spectrometry. The components consist of ICP-MS include sample introduction system, ICP torch and radio frequency (RF) coil, interface, vacuum system, collision and reaction cell, ion optics, mass spectrometer, detector, as well as data handling and system controller. The system of sample introduction which is consisted by nebulizer and spray chamber is responsible for breaking samples into small droplets after samples enter instrument as liquid. The nebulizer creates an aerosol of droplet with fine size which then pass through spray chamber in order to enter the argon plasma. RF coil connects with a RF generator; therefore, energy is supplied to the RF coil from RF generator with the argon to generate the argon plasma. As argon plasma travels through ICP torch, it absorbs more energy and release electron to form charged ions (Figure 2.8). Interface which includes two or three cones transmits the ions from atmospheric pressure ICP ion source to the low pressure's region of mass spectrometer through intermediate vacuum region. The two cones sample the central portion of the ion beam from ICP torch, are respectively called Skimmer Cone and Sampler Cone (Figure 2.9). With two-cone design, there are only two steps to reduce pressure (Figure 2.10). While recently introduce a third cone is called Hyper-skimmer Cone into the interface. With three-cone design, it needs three-step reduction in pressure (Figure 2.10). However, this design eliminates the conventional ion lenses, improve ion transmission and long-term stability. The purpose of vacuum system is to remove gas molecules in the distance between the interface and the detector of ICP-MS by combination of turbomolecular pump and mechanical roughing pump as the main components of the vacuum system. Because ion cannot collide with gas molecules when they travel the distance from interface to the detector. The generation of ions from plasma results in interference in ICP-MS, while interference will degrade the detection limits. The collision or reaction cell which is arranged before mass spectrometer can remove interferences. Presently there are three operating mode: 1) standard mode is used in condition without interferences; 2) collision mode is used to remove minor interference; 3) reaction mode is used to remove large interference. There is also a cell called "universal cell" can be used as both collision cell and reaction cell. Ions can be separated by mass spectrometer by their different mass-to-charge ratio (m/z). The mass spectrometer can quickly switch to any m/z in order to allow ions with single m/z pass through to the detector; therefore, this is the sequential filter changes for each specific m/z at a time. The commonly used type of mass spectrometer is called quadrupole (Figure 2.11). "The quadrupole is capable of scanning at a rate > 5000 atomic mass units per second; this is the reason ICP-MS can determine so many different elements quickly". The purpose of detector is to counts ions existing the mass spectrometer and translate them to strike the active surface of the detector. The active surface of detector normally keeps high negative voltage, which attract positively charged ions to strike. A measurable electronic signal is generated after ions strike the active surface. The commonly used active surface of detector is discrete dynode type detector. The dynode has wider linear dynamic ranges which is important for ICP-MS to analyze nanoparticles between sub-ppt to high ppm (Thomas, 2008).

The popularity of ICP-MS is resulted from the advantages it possesses. It has detection limits for most elements as well as higher throughput. The ability to achieve isotopic analysis and superior detection. Because of high temperature of ICP source, ICP-MS enables to handle complicated matrix with minimum interferences (Thomas, 2008).

Presently, ICP-MS has been used in various fields. The primary use lies in medical field and environmental field. The samples for former are blood cells, plasma and serum. The latter includes water testing and soil analysis. In addition, ICP-MS is also widely used for geochemistry to detect different isotopes, especially for uranium and lead.

Figure 2.8: The ICP torch shows fate of the sample (PerkinElmer.Inc, 2004-2011).

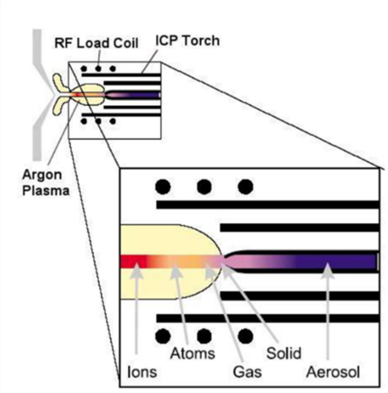

Figure 2.9: The interface region of an ICP-MS (PerkinElmer.Inc, 2004-2011).

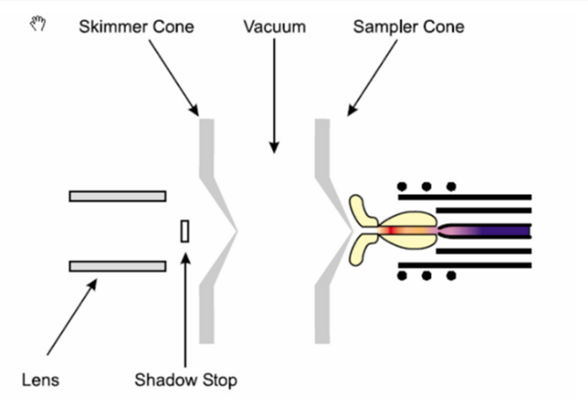

Figure 2.10: The two-cone design on the left shows a wide ion beam divergence resulting from a single, large pressure reduction. The three-cone design on the right shows a small ion beam divergence, resulting from two small pressure reductions (PerkinElmer.Inc, 2004-2011).

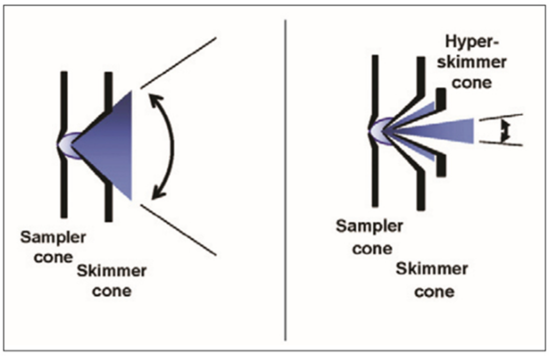

Figure 2.11: Schematic of quadrupole mass filter (PerkinElmer.Inc, 2004-2011).

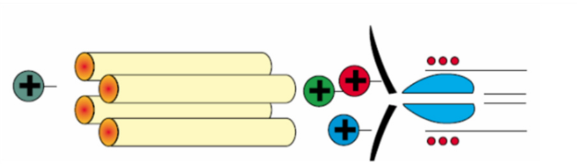

2.7 Statistical analysis

Principal component analysis (PCA) is a dimension-reduction method that can be used to reduce a large set of variables to a small number of factors that still contains most of information in the large set (Abdi and Williams, 2010). PCA was first introduced by Karl Pearson in 1901 (Pearson, 1901), however it was named later as PCA in 1930s (Hotelling, 1933). PCA is used to analyze exploratory data and make predictive models. The mathematical procedure that transforms a number of correlated variables into a smaller number of uncorrelated variables is called principal components. The first principal component accounts for as much of the variability as possible. In this study, PCA was used to study the profile of inorganic elements in organic soils and mineral soils, and the impact of pH on elemental leaching from Svalbard soils.

At first, a normalization step of the initial data was accomplished in order to standardize the range of initial variables to be equally contributed for analysis. This was done by using following formula.

$$Z = (\text{value} - \text{mean}) / \text{standard deviation}$$

The continuous steps include covariance matrix computation, which associated with all possible pairs of the initial variables to obtain positive pairs and negative pairs. The significance of principal components is identified after computing the eigenvectors and eigenvalues of covariance matrix. Then vector is featured in order to keep or discard some components. The last step is to reorient the data from the original axes of principal components (Abdi and Williams, 2010). Moreover, PCA also has limitations that must be taken into account when interpreting the output (Lever et al., 2017).

Chapter 3

Sampling

3.1 Sampling areas

Svalbard is an Arctic Archipelago (74º ~ 81º N, 10º ~ 25º E) with total area of 62700 km^2 and population of 2667 in 2016. It consists of four main islands Spitsbergen, Nordauslandet, Edgeoya and Barentsøya, and small islands (Jia et al., 2012). Among, Spitsbergen is the largest island in Svalbard (Singh et al., 2013) while Ny-Ålesund is a small settlement, which is located on the west coast of Spitsbergen in 78º54' N and 11º52'E (Gong et al., 2010; Byun et al., 2014; Van der Meij et al., 2016; Zhang et al., 2016) (Figure 3.1). Sixteen permanent research stations are set up here with all-year permanent population of 30 to 35, and total population increases to 120 in summer (Krawczyk et al., 2003). The common traffic tool is bicycle. Due to influence of Atlantic warm current, the average temperature in these areas is between -17℃ and -3.8℃ in January, and average 5℃ in July (Krawczyk et al., 2003). The mean annual precipitation can reach 400 mm, which mostly fall as snow from October to May (Williams et al., 2017). The River Bayelva is located on western Spitsbergen, which is situated about 3km from Ny-Ålesund. River is approximate 4km long and has a catchment area of 32km^2 (Zhu el al., 2016). The glacial Bayelva River originates from the two branches of Brøggerbreen, Austre and Vestre, and then discharges into Kongsfjord (Zhang et al., 2015; Zhu el al., 2016).

Ny-Ålesund and Bayelva catchments have silty clay sand gley soils, which are covered by a thin organic soil layer (Jia et al., 2012). Compared to other areas with the similar latitude, these regions are covered by more vegetation (van der Meij et al., 2016; Zhang et al., 2016), including 168 species of vascular plants, 373 species of bryophyte and 606 species of lichen, 705 fungi and 1100 algae at least (Jia et al., 2012). Approximately 50% of the Bayelva area are covered by sand and bare soil with vegetation (Boike et al. 2018). Lower sedimentary rocks mostly consist of sandstone and conglomerate with a small amount of shale and coal seams (Byun et al., 2014).

In Ny-Ålesund and Bayelva areas, the coal mine is the important sources of heavy metals release to environment (Kim et al., 2017). The coal mine was operated in 1916 by Kings Bay company and was closed down in summer 1963. In addition, there is also a small airport in East side of Bayelva. Consequently, local anthropogenic activities are possible sources of toxic element in soil and water.

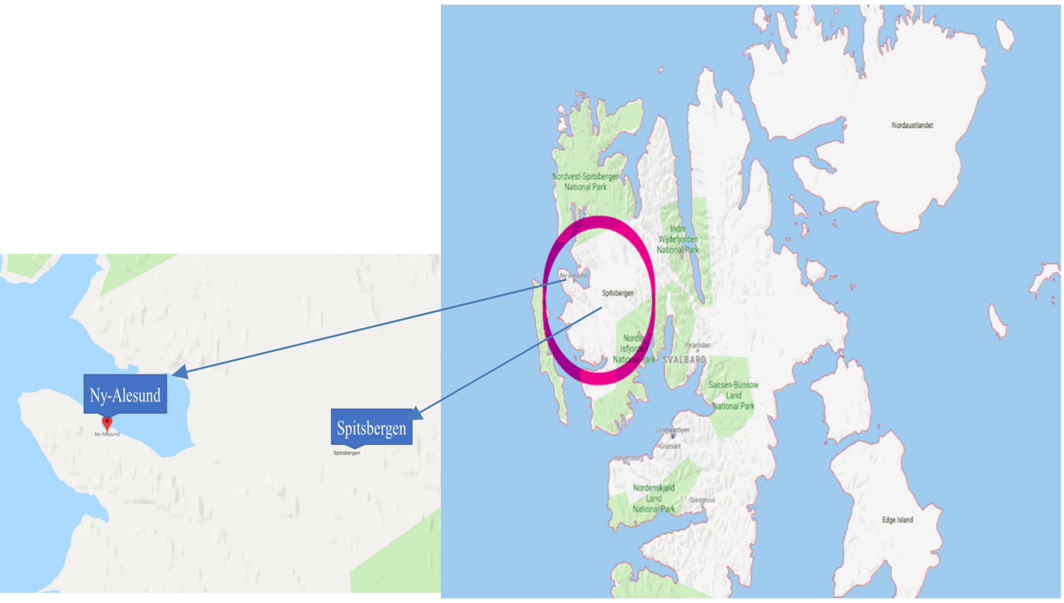

Figure 3.1: Map of Svalbard

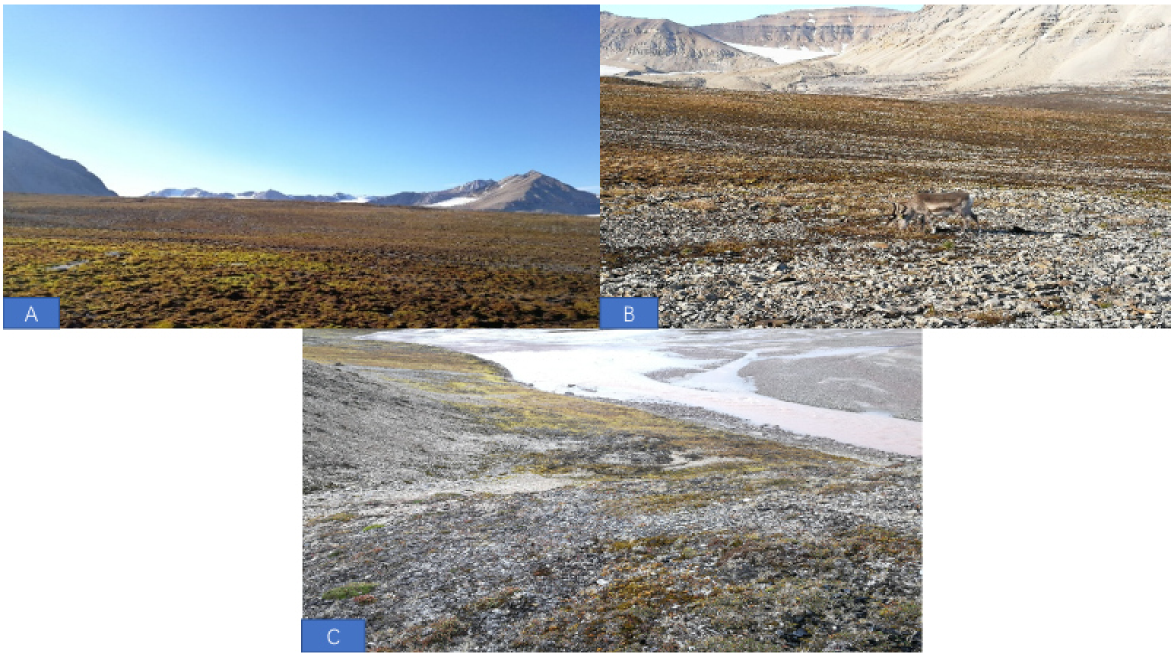

Figure 3.2: Sampling areas in west side / Bayelva (A), east side / Bayelve (B), airport area (C) (photos taken in August 2018)

3.2 Sampling method

Overall 29 organic and 25 mineral soil samples were collected from 5 sampling locations (airport area, west side, east side 1, east side 2 of Bayelva and Stuphalle) around Ny-Ålesund during 6th August to 16th August 2018 (Figure 3.1, 3.2). Figure 3.3, 3.4, 3.5 present 15 sampling sites (Table A1 and A2 of Appendix). The weather was sunny most of the days except for 14th August, when it was raining and windy. In total 26 organic and 24 mineral soil samples were collected from West side and East sides of Bayelva (Figure 16). All sampling sites of Bayelva were reached by foot. Airport is located on the East side of Bayelva. In addition, several mining activities took place in east side in past, however all mining activities were closed down in summer 1963. West side was devoid of human activities. In order to collect reference soil samples (relatively less contaminated), 3 organic and 1 mineral soil samples were collected from a remote area Stuphalle (reached by boat).

All sampling sites were at least 500m away from seashore. Sampling sites selected had full coverage of surface soil with vegetation. Selected sampling sites had approx. 0.5cm vegetation thickness. In general, total depth of the soil layers including both organic and mineral layers was approx. 30cm. Organic soil layers were approx. 3cm thick (Figure 3.6 A), while thickness of mineral layer was approx. 20cm (Figure 3.6 D). Organic and mineral soils were characterized by color, the color of former was dark (Figure 3.6 B).

Surface organic soil samples were collected by cutting squares of soil using normal stainless steel knife. Samples were then placed in paper bags. Mineral soil samples were taken separately using a plastic shovel in plastic vials depth of 30 cm where no influence of organic soil was apparent. Soil temperature was measured by using FANTAST thermometer (Figure 3.6 C).

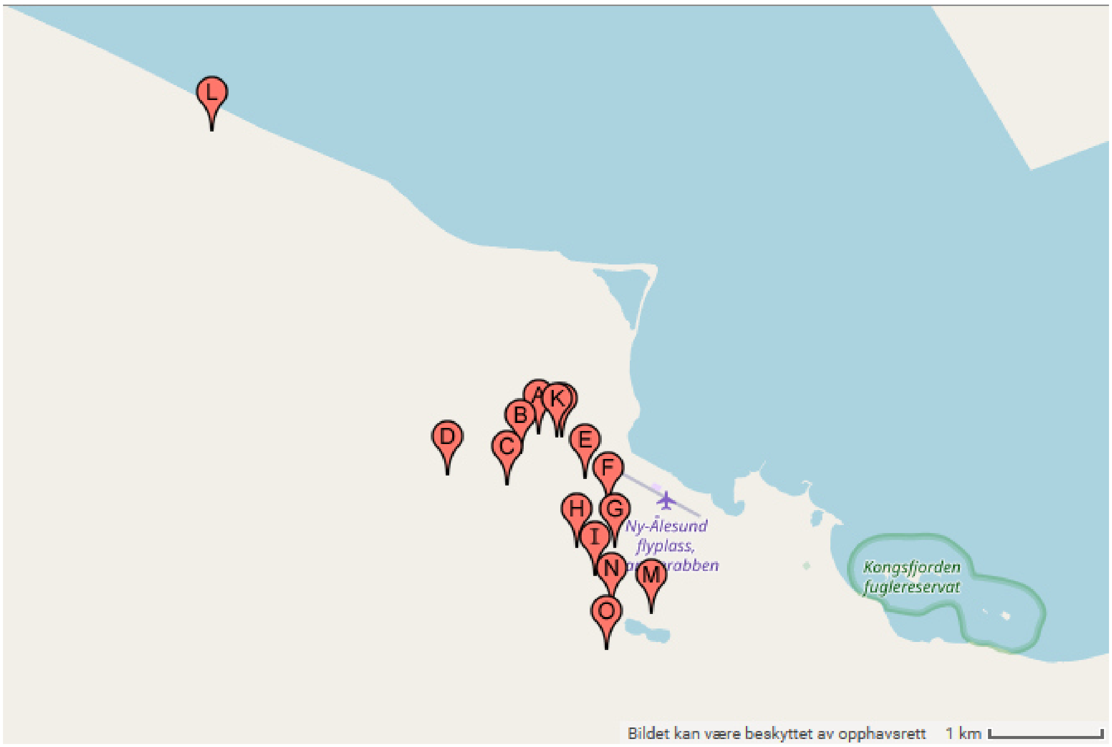

Figure 3.3: Map showing the sampling sites.

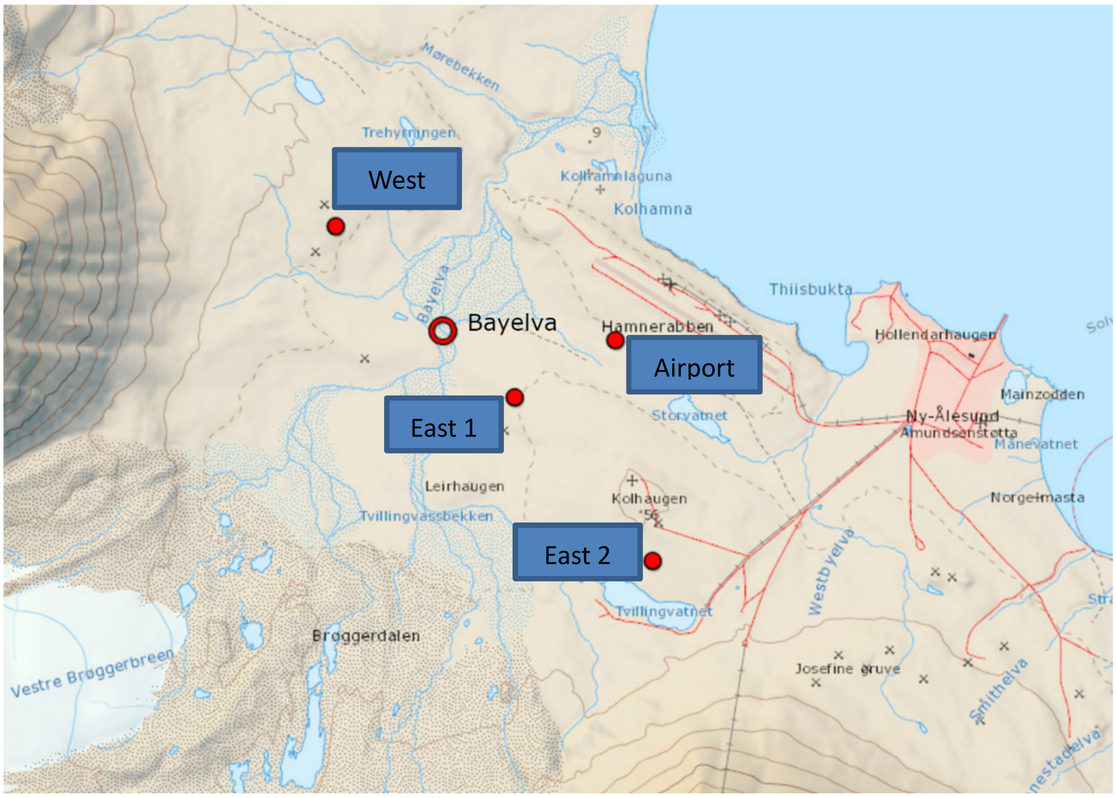

Figure 3.4: Map of sampling locations in Bayelva.

Figure 3.5: Map of sampling location in Stuphalle.

Figure 3.6: soil sampling: organic soil (A), organic soil samples with vegetable layer (B), soil temperature (C), mineral soil (D).

Chapter 4

Materials and methods

4.1 Pretreatment of organic soil samples

Soil samples were air dried for three weeks until the weight loss was less than 5%. Stones and thick roots were removed with clean forceps. The samples were homogenized in mortar. Homogenized samples were then transferred to plastic bags and were stored at room temperature.

4.2 The determination of SOM by Loss on Ignition (LOI)

Loss on Ignition (LOI) is a semi-quantitative method to determine the soil organic matter (SOM) (Bojko and Kabala, 2014; Mu.et. al., 2017). Approximately 3 to 4g soil samples were weighed in dried crucible. Soil samples were then dried in the oven (Termaks, type of TS 8056) for 1 hour at 105°C. Samples were then allowed to cool down to room temperature in a desiccator and were weighed with high accuracy again. These crucibles were then placed in furnace (Carbolite, type of ELF 11/6) and samples were combusted at 550°C for 3 hours. Samples were then allowed to cool down to room temperature and were weighed again.

LOI (%) was then calculated using the equation given below:

$$\text{LOI (\%)} = \frac{\text{Dried soil weight at 105°C} - \text{soil weight after ignition (550°C)}}{\text{Dried soil weight at 105°C}} \times 100$$

4.3 pH measurements

pH of soil samples was measured using a pH meter (Model 3510, JENWAY) at room temperature. Approx. 2.5g of each sample was transferred to 50 ml glass beaker, and 10ml water (18.2 MΩ, MilliQ) was added to this. Samples were then agitated for 1h. The pH meter was calibrated using buffer solutions of pH4 and pH7 before the measurements were taken.

4.4 Leaching test

Soil samples were mixed to produce 5 unique samples representing 5 location areas as given below, samples mixed together are given within parentheses

(1) West side/Bayelva (points A, B, C, D),
(2) East side 1/Bayelva (points G, H, I),
(3) East side 2/Bayelva (points M, N),
(4) Stuphalle (point L)
(5) Airport area (E, F, J, K)

The organic soil samples taken from sampling locations as describe above were mixed to produce five mixed organic soil samples. These five mixed samples were used to study elemental leaching from soils to water soluble form in different locations. Every mixed samples were made up by adding 20g of each organic soil samples (in total 100g by adding 20 g from 5 different soils in 1:1:1:1:1 (w/w) ratio).

10g mixed samples were weighed in clean beakers (100 ml) and to this ~30 ml Milli-Q water was added to this, pH was adjusted to 2, 7 and 10 with 2mol/L nitric acid and 1mol/L sodium hydroxide. After pH adjustment water level was adjusted to ~40 ml in each pH treatment. Glass beakers were covered by parafilm and soil-water mixtures were agitated for four weeks. Leachates were diluted by adding Milli-Q water up to the mark of 100 ml on beakers. Leachate were then removed using a syringe, the first two drops were discarded and leachate were then filtered through 0.45um filter (make and company). Approximately 0.1~0.2g of leachate was added to 15ml PP-vails (make and company) and then weight was adjusted to 10g with Milli-Q water. Diluted leachates were acidified with 1M nitric acid. Samples were then analyzed by ICP-MS to measure elemental composition of solutions. The data for pH 2 solutions in sample 1 (west side) was lost during analysis.

4.5 The elemental determination by inductively coupled plasma mass spectrometry (ICP-MS)

Elemental composition was determined by Thermo Scientific ELEMENT 2 high-resolution Inductively coupled plasma mass spectrometry (ICP-MS) (Halbach et al., 2017). The specification of the instrumentation was given in Table 2.

Approx. 300mg soil samples were weighed into perfluoroalkoxy (PFA, company name) tubes. Then 9mL of 50% (v/v) nitric acid was added and samples were digested in a high-pressure digestion unit UltraCLAVE. After digestion, samples were diluted to 107~112mL by water (18.2 MΩ, Milli-Q). Diluted samples were then transferred to 15ml PP-vials for ICP-MS analysis. Four blanks were treated by the same process. All results were corrected for blank values. The detection limits (DL) of ICP-MS analysis were given in Table A3 (Appendix). The instrumental detection limits (IDL) were resulted from the concentration yielding to 25% of relative standard deviation at three scans, while the blank detection limits (BDL) were calculated by three times the standard deviation (STD) of blanks.

Table 4.1: Specification for ICP-MS instrumentation and extraction.

Instrument	ICP-HR-MS Element 2 (Thermo Scientific)
Sample introduction system	Auto-sampler-SC2DX
Gas flow	Splitting of sample gas, 10% methane in Argon
Analysis resolution	Low (400)
	Medium (5500)
	High (10000)
Extraction	UltraCLAVE
	High pressure digestion unit

4.6 Statistical methods

4.6.1 Statistical analysis

Statistical analysis was carried out using IBM SPSS Statistics version 25. The significance level for all tests was set as $p < 0.05$. The data was tested for normality by Shapiro-Wilk test. Data did not always follow normal distribution, therefore parametric and non-parametric tests were used based on the normality of variables. Significant differences of SOM and elemental distribution in between different soil and sampling sites were performed with T-test (for normal distribution), or Mann-Whitney U-test (for non-normal distribution). The significant difference of elemental distribution and SOM in organic soil or mineral soil among five sampling locations (west side, east side 1, east side 2, stuphalle and airport area) were evaluated either by ANOVA (for normal distributed data) or Kruskal Wallis test (for non-normal distribution adjusted using the Bonferroni correction for pairwise comparison). The correlation analysis of variables was performed by Spearman's rank correlation.

4.6.2 Principal component analysis (PCA)

Given a matrix of observations, principal component analysis (PCA) performs an orthogonal linear transformation, that creates a new coordinate system while retaining as much as possible of the variation present in the data set (Lever et al., 2017). The transformed variables called principal components (PCs) are the new coordinates. The PCs are uncorrelated (mutually orthogonal) and are ordered such that the greatest variance is along the first coordinate (PC1), the second greatest variance along the second coordinate (PC2), and so on. It is typically used as a dimension-reduction routine in which the best summary of the data can be obtained using a limited number of PCs. Here, PCA was carried out using the R statistical software package. Prior to the analysis, the data was centered and scaled due to the large differences in elemental concentrations between trace elements and other elements. The results are summarised visually using biplots that combine both scores (plot of the observations) and loadings (plot of the variables) plots.

Chapter 5

Results

5.1 Soil properties

5.1.1 Soil organic matter (SOM)

SOM contents ranged from 15.19 to 82.96% for organic soils, and from 1.70 to 13.12% for mineral soils (Figure 19, Table 3). Overall, SOM contents were significantly higher (T-test, $t_{(23.503)} = 11.208$ at $p=0.038$) in organic soils (mean, 47.33 ± 16.56%) than in mineral soil (mean, 6.07 ± 4.76%). The levels of SOM determined by LOI and moisture content at 105°C for both organic and mineral soils in each sampling station are presented in Table A4 (Appendix).

Figure 5.1: Soil organic matter (SOM) content at organic soil and mineral soil

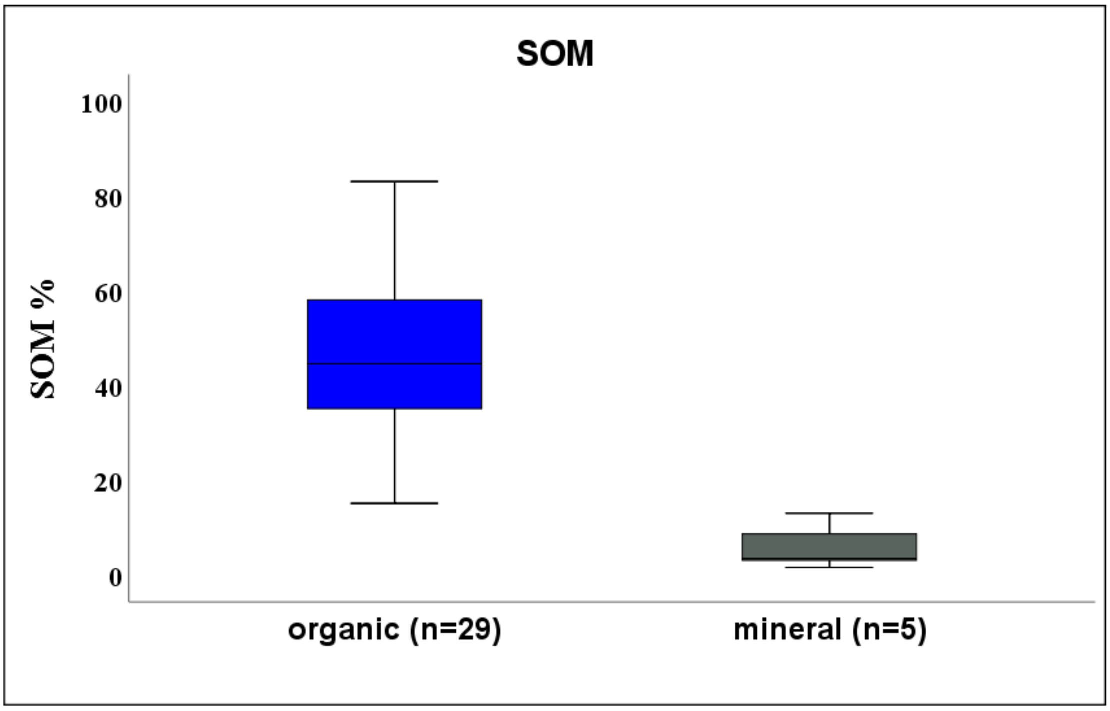

5.1.2 pH of soils

Soil pH was in the range of 4.98-7.55 for organic soils and from 5.42-8.91 for mineral soils (Table 3). Overall, pH values of organic soils (mean 6.495 ± 0.66) were significantly lower (T-test, $t_{(9.142)} = 1.693$ at $p=0.123$) than mineral soils (mean 7.22 ± 1.15).

5.2 Water leaching

Impact of 3 different pH levels (pH 2, 7 and 10) was tested on leaching of elements from Svalbard organic rich soils. Elemental concentrations (µg/L) for 5 samples from leaching experiment are presented in Table 5.1. Overall, 13 elements, namely Cd, Hg, Pb, Co, Ni, Cr, Se, U, Zn, Fe, Al, S were chosen for this study. The concentrations of Cd, Co, Ni, Cu, Zn, Fe, Al were highest in pH 2 leachates, while the concentrations of Cr, Hg, Pb, Se, U and S were greatest in pH 10 leachates. Additionally, the concentrations of Cd, Co, Cr, Ni, Cu, Zn, Fe and S were lowest in pH 7 leachates and their concentration curves formed V-shaped curves from pH 2 to pH 10 (Figure 5.2).

Impact of pH on elemental leaching in soils from different samples (locations)

The higher concentration of elements namely Cd, Co and Zn were measured in pH 2 leachates for all samples. Concentrations of Ni, Cr, Cu and Fe were higher in pH 2 leachates from sample 5 only; whereas, the concentration of Al increased in pH 2 leachates from sample 4 and sample 5. Only concentration of U increased in pH 10 leachates from all samples. In addition to U, the concentration of Al and S were higher in pH 10 leachates from sample 2 and 3 (Table 5.1). Moreover, higher concentrations of Cr, Cu and Fe were observed in pH 10 leachates in samples 2, 3, 4. Also, higher concentration of Hg, Pb Se and U were showed in pH 10 leachates in samples 3, 4, 5.

Impact of pH on elemental leaching in soils from west and two east locations

The concentration of elements Co (east 1: 91.636 µg/L; east 2: 37.264 µg/L), Fe (east 1: 1582.1 µg/L; east 2: 463.4 µg/L), Al (east 1: 2505 µg/L; east 2: 820.1 µg/L) were higher for east 1 than for east 2 in pH 2 leachates. Particularly for Ni, the higher concentration was measured in east part 1 (east 1: 87.92 µg/L; east 2: 16.54 µg/L).

When compared east sides with west sides, elemental concentrations in west part were lower compared to east sides in pH 7 leachates for most of elements. The concentrations of Co (east 1: 19.822 µg/l; east 2: 8.04 µg/L), Ni (east 1: 32.67 µg/L; east 2: 14.01 µg/L), Zn (east 1: 104.19 µg/L; east 2: 56.16 µg/L), Fe (east 1: 9461.5 µg/L; east 2: 7502.6 µg/L), Al (east 1: 7325.3 µg/L; east2: 5344.1 µg/L), S (east 1: 8449 µg/L; east 2: 5740 µg/L) were higher for east 1 than for east 2, while the contents of Cd, Pb, Cr, U and Cu were similar in two east parts in pH 7 leachates.

Except for Al, the concentrations of the rest of elements were higher for east part 2 compared to west and east 1, particularly for U (west: 0.9918 µg/L; east 1: 1.9236 µg/L; east 2: 59.1289 µg/L). To the contrary, Al had highest level in east part 1 (11195.2 µg/L) and similar level between west (6016.7 µg/L) and east part 2 (7631.5 µg/L).

Table 5.1: Elements concentration (µg/L) of water leaching with 3 pH values

E	pH	Mean conc. ± SD	Sample1	Sample 2	Sample 3	Sample 4	Sample 5
		µg/L	west (A,B,C,D)	east 1 (G,H,I)	east 2 (M,N)	stuphalle (L)	airport (F,K,J)
Cd	pH 2	13.82 ± 10.13	ND	6.832	3.923	19.238	25.284
	pH 7	0.560 ± 0.254	0.213	0.716	0.779	0.533	ND
	pH 10	1.61 ± 1.40	0.548	0.475	0.992	3.739	2.321
Hg	pH 2	0.605 ± 0.173	ND	0.549	0.390	0.691	0.788
	pH 7	0.932 ± 0.116	0.805	1.045	1.015	0.865	ND
	pH 10	1.22 ± 0.17	1.153	0.958	1.419	1.252	1.302
Pb	pH 2	10.99 ± 7.95	ND	5.670	3.326	20.506	14.472
	pH 7	23.96 ± 6.67	16.007	31.915	25.844	22.087	ND
	pH 10	32.86 ± 9.93	21.974	22.031	40.008	39.321	40.974
Co	pH 2	116518 ± 232816	ND	91.636	37.264	201.865	465741.952
	pH 7	11.27 ± 6.82	4.036	19.822	8.040	13.176	ND
	pH 10	26.40 ± 25.01	10.335	8.434	22.150	69.730	21.367
Ni	pH 2	55752 ± 111339	ND	87.92	16.54	142.04	222760.22
	pH 7	20.83 ± 8.44	15.63	32.67	14.01	21.01	ND
	pH 10	47.67 ± 45.58	17.90	21.17	30.10	127.53	41.63
Cr	pH 2	18.05 ± 30.04	ND	1.45	1.16	6.63	62.96
	pH 7	14.04 ± 3.74	9.72	18.42	15.44	12.59	ND
	pH 10	23.07 ± 17.03	12.75	14.19	22.46	52.69	13.27
Se	pH 2	15.11 ± 4.34	ND	13.7	9.8	17.3	19.7
	pH 7	23.3 ± 2.9	20.1	26.1	25.4	21.6	ND
	pH 10	30.4 ± 4.3	28.8	24.0	35.5	31.3	32.6
U	pH 2	0.142 ± 0.102	ND	0.0912	0.1077	0.0765	0.2943
	pH 7	1.65 ± 0.97	0.5611	2.1418	2.7291	1.1589	ND
	pH 10	29.51 ± 28.36	0.9918	1.9236	59.1289	57.1702	28.3488
Cu	pH 2	674 ± 1322	ND	9.53	6.73	22.73	2657.89
	pH 7	25.44 ± 8.27	15.91	31.51	21.20	33.15	ND
	pH 10	66.24 ± 57.24	25.79	20.43	55.50	162.45	67.05
Zn	pH 2	1795 ± 1378	ND	763.23	483.59	2679.84	3253.14
	pH 7	79.49 ± 22.21	66.05	104.19	56.16	91.55	ND
	pH 10	135 ± 73	71.23	75.01	104.66	230.05	195.00
Fe	pH 2	85061 ± 160740	ND	1582.1	463.4	12158.2	326041.7
	pH 7	7378 ± 1660	5414.7	9461.5	7502.6	7133.0	ND
	pH 10	13549 ± 12443	6544.4	7806.0	11441.6	35511.0	6443.9
Al	pH 2	14795 ± 16019	ND	2505.0	820.1	21662.5	34192.9
	pH 7	6200 ± 1096	5179.8	7325.3	5344.1	6952.1	ND
	pH 10	5882 ± 3803	6016.7	11195.2	7631.5	1714.9	2853.6
S	pH 2	8778 ± 6255	ND	4852	4517	7857	17887

	pH 7	6872 ± 1589	5288	8449	5740	8012	ND
	pH 10	19053 ± 19814	5707	5385	12582	53160	18432

Figure 5.2: Leached concentration (µg/L) of elements (Cd, Co, Cr, Cu, Fe, Ni, S, Zn) at pH 2, pH 7 and pH 10.

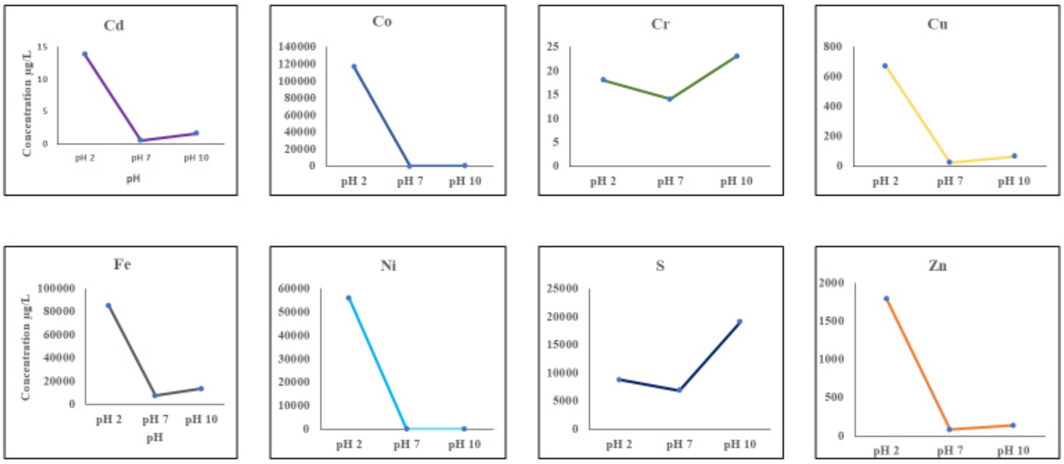

PCA was conducted to investigate the impact of pH on the leaching of elements from soil. The first 2 components explained 85.4% of the variance in the data. Three samples (samples 3, 4 and 5 collected from east 2, stuphalle and airport areas respectively) of pH 10 soil leachate from separated from the rest of samples on one side of the plot due to the high concentrations of trace elements namely Hg, Pb, Se and U. while one sample (sample no. 5 collected from airport area) of pH 2 leachate characterized by high concentration of Fe, Cu, Ni and Cr separated on the other side of plot. While one sample However, rest of the samples did not show any specific grouping in PCA analysis (Figure 5.3).

Figure 5.3: Principal component analysis for leaching tests.

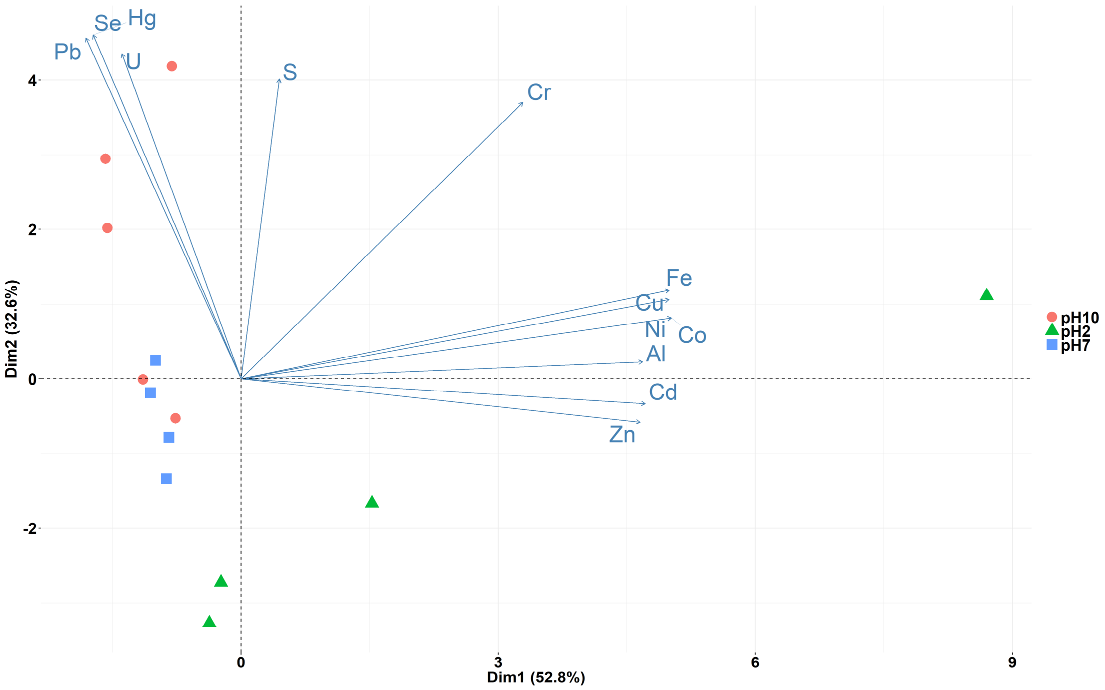

5.3 The composition of organic and mineral soil

5.3.1 Elemental composition of organic and mineral soil

Overall, 65 elements were analyzed in organic and mineral soils. In this thesis, 22 out of 65 elements, including 11 trace elements, namely cadmium (Cd), chromium (Cr), cobalt (Co), copper (Cu), lead (Pb), mercury (Hg), nickel (Ni), uranium (U) rubidium (Rb), selenium (Se) and zinc (Zn), and 11 macro elements, namely aluminum (Al), boron (B), calcium (Ca), iron (Fe), potassium (K), magnesium (Mg), manganese (Mn), sodium (Na), phosphorus (P), silicon (Si) and sulfur (S) are presented. Concentrations of elements are presented in Table 3. Except for Ca, Co, Fe, Mn and U, the concentrations of other elements between organic and mineral soil were significantly different ($p<0.05$) (Table 5.2, Figure 5.4).

5.3.2 Elemental distribution in organic and mineral soil

Among the trace elements concentrations of Cd ($t_{(31.68)}=6.291$ at $p=0.0001$), Hg ($U_{(51)}=6$ at $p=0.001$), Pb ($t_{(47.013)}=4.463$ at $p=0.036$), Se ($U_{(51)}=127$ at $p=0.0001$) and Zn ($U_{(51)}=174$ at $p=0.006$) were significantly greater in organic soils, whereas Al ($U_{(51)}=464$ at $p=0.006$), Cr ($U_{(51)}=443.5$ at $p=0.018$), Cu ($t_{(22.019)}=-9.426$ at $p=0.0001$), Ni ($t_{(23.707)}=-10.427$ at $p=0.0001$) and Rb ($U_{(51)}=471$ at $p=0.004$) were significantly higher in mineral soils (Table 3, Figure 19). Among macro/micro elements P ($U_{(51)}=606$ at $P=0.0001$) S ($U_{(51)}=8$ at $p=0.0001$) and Si ($t_{(43.34)}=4.955$ at $p=0.014$) were significantly higher in organic soils, while B($U_{(51)}=629$ at $p=0.0001$), K ($U_{(51)}=638$ at $p=0.0001$), Mg ($U_{(51)}=622$ at $p=0.0001$) and Na ($U_{(51)}=634$ at $p=0.0001$) were higher in mineral soils (Table 4, Figure 18). The levels of Hg in organic soil was four times greater compared to mineral soil, this was followed by S (3.2 times) and Cd (3.2 time) (Table 5.3).

Table 5.2: Elemental concentrations (µg/g) in organic soil (n=29) and mineral soil (n=22). (range, median, mean and standard deviation (SD)). Significance levels are presented with *, ** and * for p<0.05, <0.01 and <0.001 respectively.**

Element		Range	Median	Mean ± SD
pH**	organic	4.98-7.55	6.59	6.495 ± 0.66
	mineral	5.42-8.91	7.35	7.22 ± 1.15
SOM***	organic	15.19-82.96	44.61	47.33 ± 16.56
	mineral	1.70-13.12	3.58	6.07 ± 4.76
Concentrations of trace elements (µg/g)				
Cd***	organic	0.081-1.528	0.435	0.511 ± 0.285
	mineral	0.037-0.301	0.149	0.16 ± 0.07
Co	organic	0.88-9.44	5.17	5.01 ± 1.85
	mineral	4.51-11.83	7.74	7.84 ± 2.05
Cr*	organic	4.8-79.2	33.7	32.4 ± 16.5
	mineral	22.8-128.6	40	45.7 ± 23.7
Cu***	organic	4.6-13.7	9.7	9.7 ± 1.9
	mineral	4.7-18.8	10.2	10.6 ± 3.7
Hg***	organic	0.039-0.341	0.123	0.132 ± 0.072
	mineral	0.008-0.067	0.028	0.027 ± 0.013
Ni***	organic	2.7-23.7	13.4	13.2 ± 4.9
	mineral	9.9-32.2	16.5	17.5 ± 5.4
Pb*	organic	9.3-28.3	14.5	15.3 ± 4.1
	mineral	5.8-17.0	11	10.9 ± 2.5
Rb**	organic	5.4-64.8	34.7	35.7 ± 15.3
	mineral	26.6-106.6	48.6	49.9 ± 18.1
Se***	organic	0.32-1.84	0.7	0.76 ± 0.34
	mineral	0.12-0.95	0.36	0.42 ± 0.23
Zn	organic	35.9-112.3	61.7	65.0 ± 17.1
	mineral	30.5-86.5	50.6	52.5 ± 13.2
U	organic	0.46-5.15	1.38	1.69 ± 1.15
	mineral	0.82-4.09	1.45	1.70 ± 0.92
Concentrations of micro and macro elements (mg/g)				
Al**	organic	3.5-40.6	20.9	20.7 ± 8.9
	mineral	14.2-62.4	26.8	28.1 ± 10.5
B***	organic	0.013-0.049	0.025	0.027 ± 0.008
	mineral	0.014-0.069	0.021	0.025 ± 0.013
Ca	organic	4.9-28.8	13.4	14.7 ± 6.7
	mineral	1.5-69.4	3.6	9.8 ± 16.2
Fe	organic	2.8-28.3	14	14.8 ± 6.1
	mineral	13.4-35.9	22.5	23.3 ± 4.7
K***	organic	1.6-11.6	6.2	6.2 ± 2.4
	mineral	4.3-18	8.1	8.4 ± 3.0
Mg***	organic	1.7-18.2	4.5	4.7 ± 2.7

	mineral	2.7-28	4.3	6.6 ± 6.1
Mn	organic	0.075-0.467	0.288	0.266 ± 0.104
	mineral	0.186-0.781	0.389	0.411 ± 0.144
Na***	organic	0.172-0.851	0.388	0.402 ± 0.149
	mineral	0.205-1.1	0.414	0.474 ± 0.205
P***	organic	0.425-1.2	0.737	0.767 ± 0.2
	mineral	0.315-1.1	0.44	0.495 ± 0.214
S***	organic	0.761-2.23	1.6	1.6 ± 0.355
	mineral	0.162-1.02	0.405	0.483 ± 0.249
Si*	organic	0.995-2.8	1.7	1.7 ± 0.385
	mineral	0.837-1.8	1.3	1.3 ± 0.196

Figure 5.4: Distribution profile of elements between organic soil (blue) and mineral (grey) soils. Number of samples is 29 and 22 for organic and mineral soils respectively.

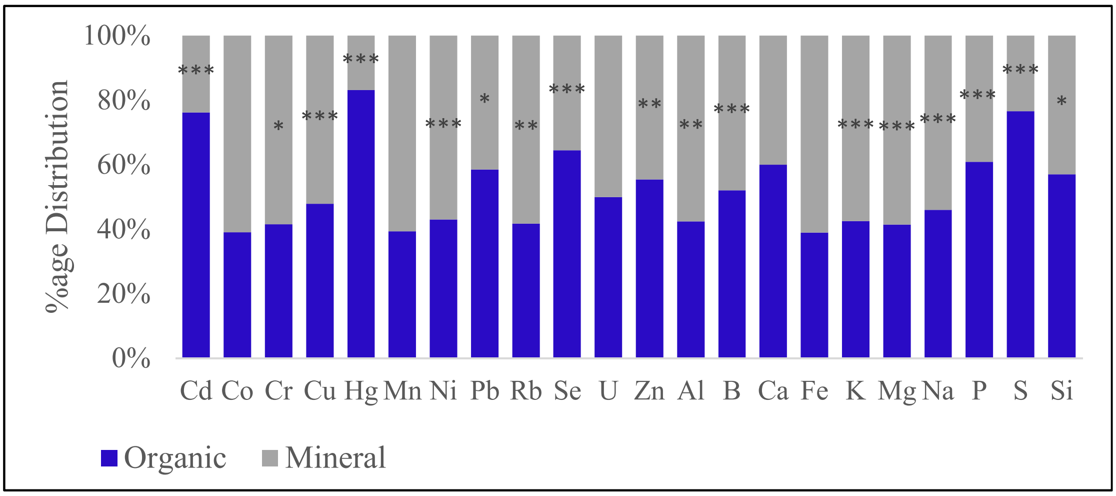

Table 5.3: Ratio of elemental concentrations in the organic soil (n=29) and mineral soil (n=22).

Trace elements	Ratio	Other elements	Ratio
Cd	3.19	Al	0.73
Co	0.64	B	1.08
Cr	0.71	Ca	1.50
Cu	0.92	Fe	0.64
Hg	4.89	K	0.74
Mn	0.65	Mg	0.71
Ni	0.75	Na	0.85
Pb	1.40	P	1.55
Rb	0.72	S	3.25
Se	1.81	Si	1.32
U	1.00		
Zn	1.24		

5.4 Comparison of elemental profile in soils between west and east side

In order to study the impact of local activities in the studied area, elemental concentrations were compared between west side (points A, B, C, D) and east side (E, F, G, H, I, J, M, N) of Bayelva. West side is generally devoid of local pollution sources, whereas Airport and shut down mine were located in east side; therefore, the east side was more impacted with the anthropogenic activities. The mean concentration of 22 elements in organic and mineral soils from both west side and east side are presented in Table 5.4. Concentrations of most of elements except for Cd ($t_{(8.522)}$=1.734 at p=0.02), Se ($t_{(8.3)}$=1.192 at p=0.021) and P ($t_{(19.714)}$=-1.283 at p=0.008) were almost similar in organic soils collected from east and west side of Bayelva (Table 5). For mineral soils, Concentrations of Se ($t_{(14.738)}$=-0.297 at p=0.01), S ($t_{(14.875)}$=-1.867 at p=0.005) and P ($t_{(13.619)}$=-1.675 at p=0.033) were significantly higher in mineral soils from west side. Concentration of all other elements studied here did not show any significant differences between two sites (Table 5.4).

5.5 Comparison of five sampling locations

5.5.1 SOM

Organic content and elemental profile of five sampling locations namely west side/Bayelva (points A, B, C, D), east side 1/Bayelva (points G, H, I), east side 2/Bayelva (points M, N), Stuphalle (point L) and airport area (E, F, J, K) were compared (Figure 5.5, Table A5). Highest SOM contents were measured in organic soils from Stuphalle (70.67 ± 16.30). Whereas, lowest organic contents were measured in organic soils from west side (38.90 ± 13.06), however these differences were not statistically significant.

5.5.2 Comparison of elemental profile among different sampling sites

The mean concentrations of 12 selected elements (Cd, Hg, Al, Fe, Si, S, Mn, Cr, Rb, Pb, Co, Se) in organic and mineral soils from five sampling locations, are presented in Table 6. Boxplots in Figure 21 (A-E) featured profile of Cd, Hg, Pb, Co and Cr in both organic and mineral soils for 5 sampling locations. The mean concentrations of Cd, Hg, Pb were higher in organic soils than in mineral soil in all sampling locations. The significantly higher proportion of Cd was observed in organic soils compared to underlying mineral soils in east side 1 ($t_{(6.297)}$=4.813 at p=0.001) and west ($t_{(5.358)}$=2.936 at p=0.024) sides (Figure 23). In organic soils significantly higher concentration of Hg was observed from airport area (T-test, $t_{(7.081)}$=3.084 at p=0.013), while significantly higher concentration of S was noted in west side (T-test, $t_{(5.825)}$=6.582 at p=0.05). In addition, the concentrations of Si were significantly higher in west side ($t_{(6.567)}$=3.353 at p=0.02) and airport area ($U_{(14)}$=4.00 at p=0.008) in organic soils. In contrast concentrations of Co, Cr were higher in mineral soils. In east side 2, the concentration of Cr in organic and mineral soils was significantly different ($t_{(3.024)}=-0.257$ at p=0.018) (Table 5.5, Figure 5.6, Figure 5.7). These results were similar to as presented Table 5.2.

Apart from Co ($F_{(4)}=2.966$ at p=0.042) and Pb ($H_{(4)}=9.784$ at p=0.044) elemental concentrations among different sites were not significantly different. (Table 5.5, Figure 5.6).

Table 5.4: The elemental of organic soil elements in West side (n=8) and East side (n=15) and of mineral soil elements in West side (n=7) and East side (n=12). Significance levels are presented with *, ** and * for p<0.05, <0.01 and <0.001 respectively.**

	Organic soils		**Mineral soils**	
	West side	**East side**	**West side**	**East side**
Concentrations of trace elements (µg/g)				
Cd	* 0.698 ± 0.44	0.415 ± 0.20	0.195 ± 0.074	0.127 ± 0.059
Co	5.71 ± 2.06	5.36 ± 1.42	7.96 ± 1.44	7.59 ± 2.14
Cr	35.6 ± 15.9	36.3 ± 17.0	43.95 ± 7.34	51.60 ± 31.03
Cu	10.1 ± 1.43	10.3 ± 1.47	31.05 ± 9.17	36.28 ± 9.86
Hg	0.097 ± 0.03	0.126 ± 0.07	0.027 ± 0.009	0.03 ± 0.016
Ni	15.3 ± 3.84	13.9 ± 4.52	55.86 ± 14.75	52.63 ± 17.99
Pb	17.4 ± 3.13	15.1 ± 4.68	11.12 ± 1.57	11.81 ± 2.41
Rb	38.2 ± 14.6	39.4 ± 13.5	47.68 ± 8.49	56.48 ± 21.57
Se	* 0.87 ± 0.46	0.67 ± 0.19	**0.411 ± 0.093	0.436 ± 0.275
U	1.85 ± 1.13	1.84 ± 1.34	1.54 ± 0.45	1.68 ± 0.97
Zn	73.1 ± 15.0	60.1 ± 18.7	56.94 ± 8.23	51.16 ± 15.19
Concentrations of micro and macro elements (mg/g)				
Al	21.66 ± 8.8	23.29 ± 7.9	27.16 ± 4.6	31.62 ± 12.65
B	0.026 ± 0.007	0.029 ± 0.008	0.068 ± 0.021	0.084 ± 0.05
Ca	15.18 ± 7.21	11.83 ± 4.75	25.78 ± 44.36	21.86 ± 25.91
Fe	16.33 ± 7.07	15.95 ± 4.87	23.23 ± 2.26	24.47 ± 5.46
K	6.69 ± 2.2	6.75 ± 2.05	23.68 ± 5.06	28.26 ± 10.64
Mg	6.24 ± 4.86	4.33 ± 0.65	22.95 ± 16.97	27.77 ± 6.92
Mn	0.269 ± 0.097	0.28 ± 0.102	0.377 ± 0.067	0.379 ± 0.147
Na	0.401 ± 0.143	0.452 ± 0.152	1.42 ± 0.429	1.56 ± 0.738
P	**0.708 ± 0.089	0.795 ± 0.234	*1.235 ± 0.211	1.629 ± 0.767
S	1.408 ± 0.356	1.628 ± 0.372	**0.379 ± 0.093	0.537 ± 0.267
Si	1.69 ± 0.274	1.556 ± 0.322	1.272 ± 0.146	1.284 ± 0.245

Figure 5.5: Soil organic matter (SOM) (%) and moisture content (MC) (%) at 105 °C of surface soil in five sampling locations. Letters show significant differences (same letter means no significant difference).

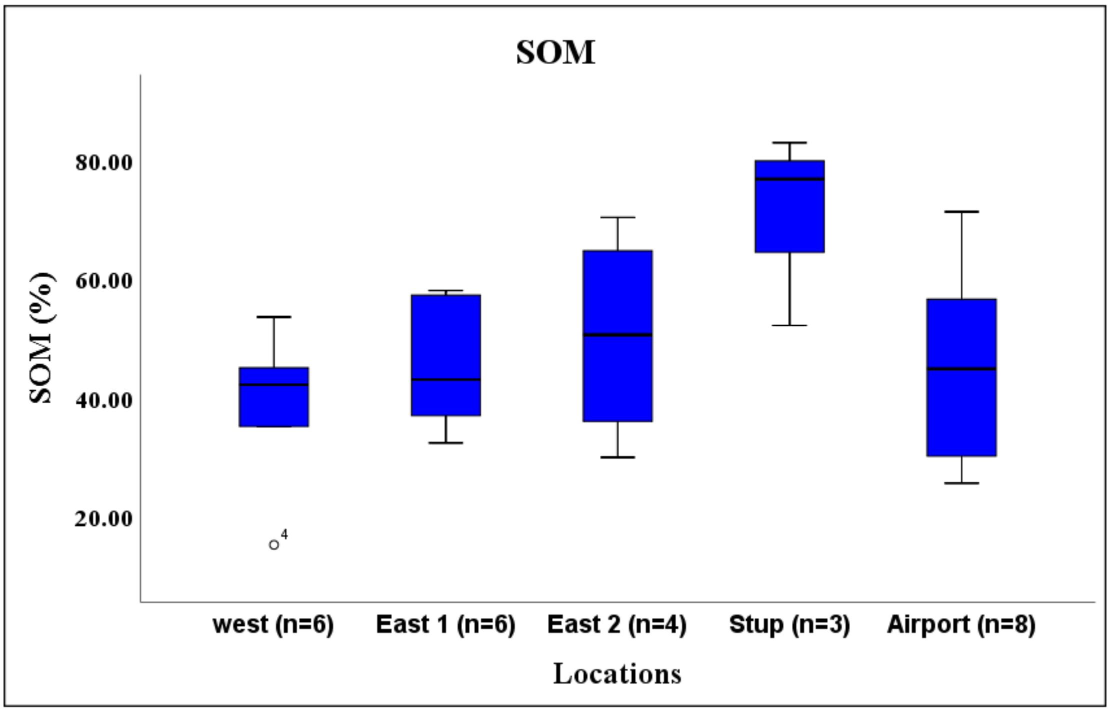

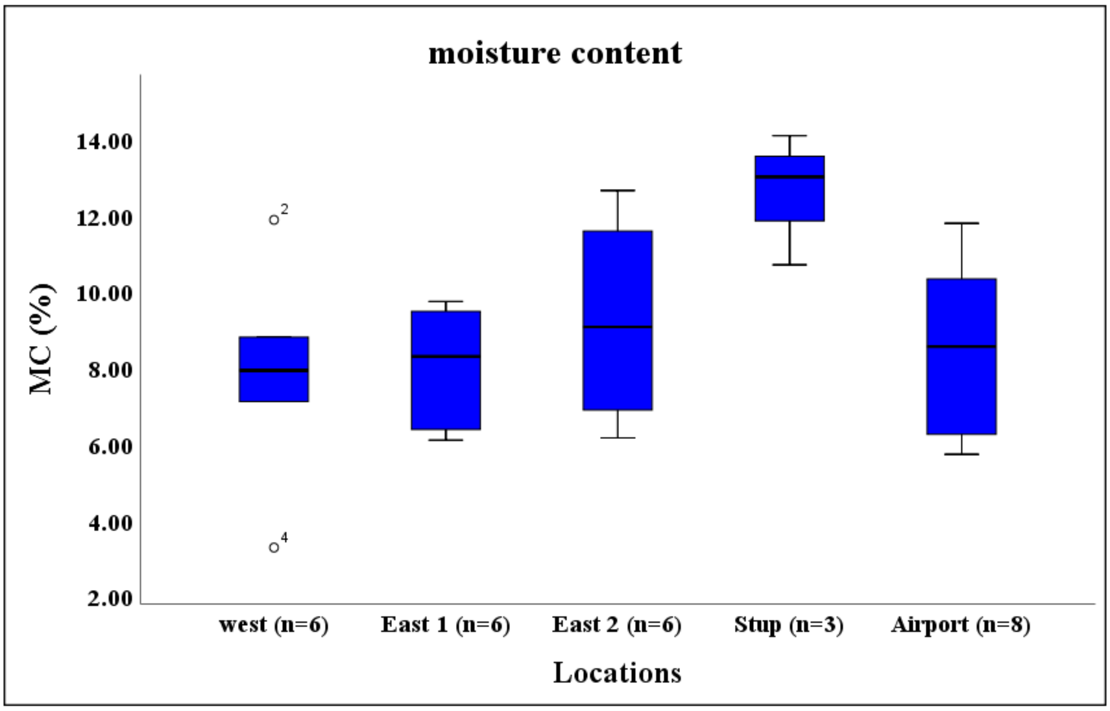

Table 5.5: Concentrations (µg/g) of 12 elements in organic soil and mineral soil in five sampling sites. (mean and standard deviation (SD)). Letters show significant differences (same letter means no significant difference).

		West side	East side 1	East side 2	Stuphalle	Airport area
Concentrations of trace elements (µg/g)						
Cd	Organic	0.59 ± 0.33	0.47 ± 0.17	0.50 ± 0.25	0.48 ± 0.25	0.38 ± 0.19
	Mineral	0.18 ± 0.06	0.11 ± 0.06	0.18 ± 0.04	0.14	0.13 ± 0.06
Co	Organic	6.04 ± 2.12 ^{a}	5.67 ± 1.53 ^{ab}	4.27 ± 1.59 ^{ab}	2.29 ± 1.62 ^{b}	5.04 ± 1.46 ^{ab}
	Mineral	8.05 ± 1.55	7.41 ± 1.96	6.62 ± 2.06	11.16	7.68 ± 2.57
Cr	Organic	34.8 ± 14.6	41.9 ± 24.3	30.9 ± 14.2	17 ± 17.5	28.4 ± 9.8
	Mineral	42.4 ± 6.7	68.6 ± 43.5	32.7 ± 0.7	34.5	39.4 ± 11.9
Hg	Organic	0.10 ± 0.03	0.16 ± 0.08	0.14 ± 0.07	0.15 ± 0.02	0.14 ± 0.11
	Mineral	0.03 ± 0.01	0.04 ± 0.02	0.03 ± 0.01	0.01	0.02 ± 0.01
Mn	Organic	284 ± 94	328 ± 125	220 ± 93	144 ± 77	268 ± 91
	Mineral	385 ± 69	365 ± 111	317 ± 116	570	496 ± 215
Se	Organic	0.85 ± 0.52	0.64 ± 0.18	0.82 ± 0.22	0.56 ± 0.41	0.67 ± 0.17
	Mineral	0.41 ± 0.10	0.49 ± 0.30	0.64 ± 0.24	0.18	0.34 ± 0.23
Pb	Organic	16.8 ± 3.5 ^{a}	15.8 ± 3.6 ^{ab}	17.8 ± 7.0 ^{ab}	11.8 ± 2.1 ^{b}	12.5 ± 2.2 ^{b}
	Mineral	11.2 ± 1.7	13.0 ± 3.0	10.6 ± 1.2	8.5	9.7 ± 3.0
Rb	Organic	38.8 ± 13.8	41.2 ± 18.5	34.2 ± 12.9	19.7 ± 21.5	34.3 ± 12.3
	Mineral	46.4 ± 8.6	69.1 ± 28.9	44.1 ± 8.3	39.7	44.3 ± 11.6
Concentrations of micro and macro elements (mg/g)						
Al	Organic	22.6± 8.8	24.9± 10.7	21.1 ± 8.8	12.3 ± 13.0	18.9± 6.6
	Mineral	27.2 ± 5.0	39.0 ± 17.4	24.4 ± 1.3	25.2	23.9 ± 7.2
Fe	Organic	17.3 ± 7.0	15.6 ± 5.5	13.0± 5.4	9.1 ± 8.6	15.4 ± 5.4
	Mineral	23.4 ± 2.4	26.3 ± 7.1	21.1 ± 5.3	23.4	22.2 ± 5.0
S	Organic	1.4 ± 0.347	1.8 ± 0.216	1.9 ± 0.361	1.4 ± 0.175	1.5 ± 0.428
	Mineral	0.385 ± 0.1	0.561 ± 0.279	0.715 ± 0.35	0.162	0.505 ± 0.267
Si	Organic	1.7 ± 0.321	1.5 ± 0.399	1.5 ± 0.358	2.1 ± 0.653	1.8 ± 0.334
	Mineral	1.2 ± 0.129	1.3 ± 0.255	1.3 ± 0.257	1.4	1.3 ± 0.234

Figure 5.6: Boxplots of the elemental distribution in organic (blue) and mineral (grey) soil in five sampling locations (A-E). Elemental profile in mineral soil in Stuphalle was neglected due to limited data points (n=1).

A

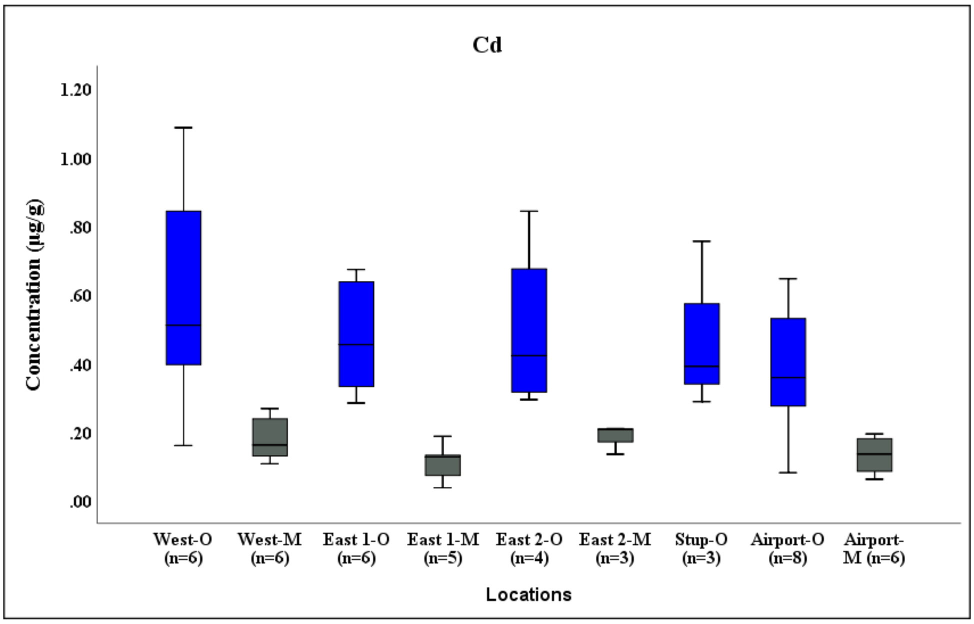

B

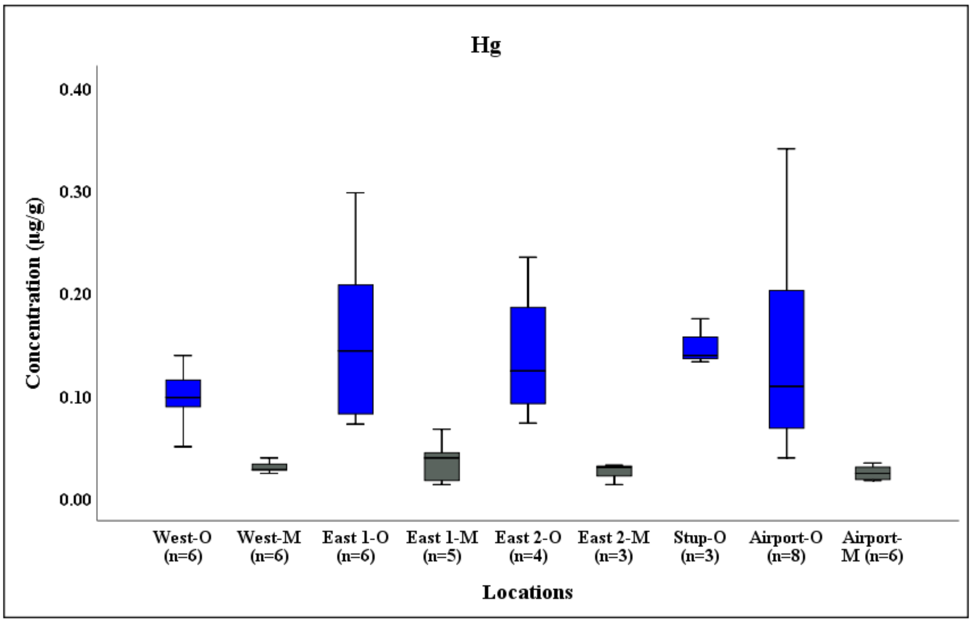

C

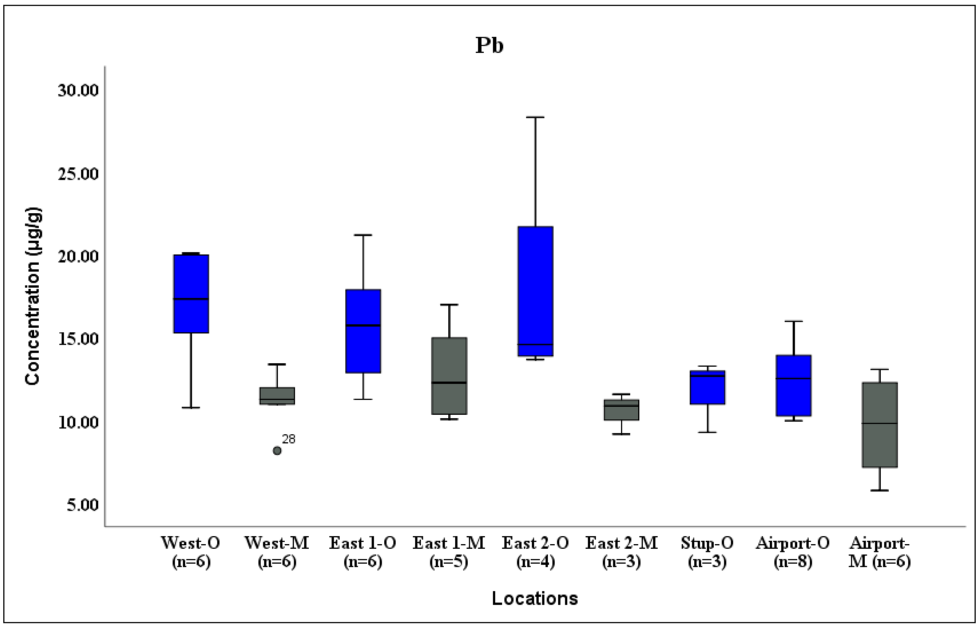
Pb
30.00
25.00
20.00
15.00
10.00
5.00
Concentration (µg/g)
28
West-O (n=6)
West-M (n=6)
East 1-O (n=6)
East 1-M (n=5)
East 2-O (n=4)
East 2-M (n=3)
Stup-O (n=3)
Airport-O (n=8)
Airport-M (n=6)
Locations

D

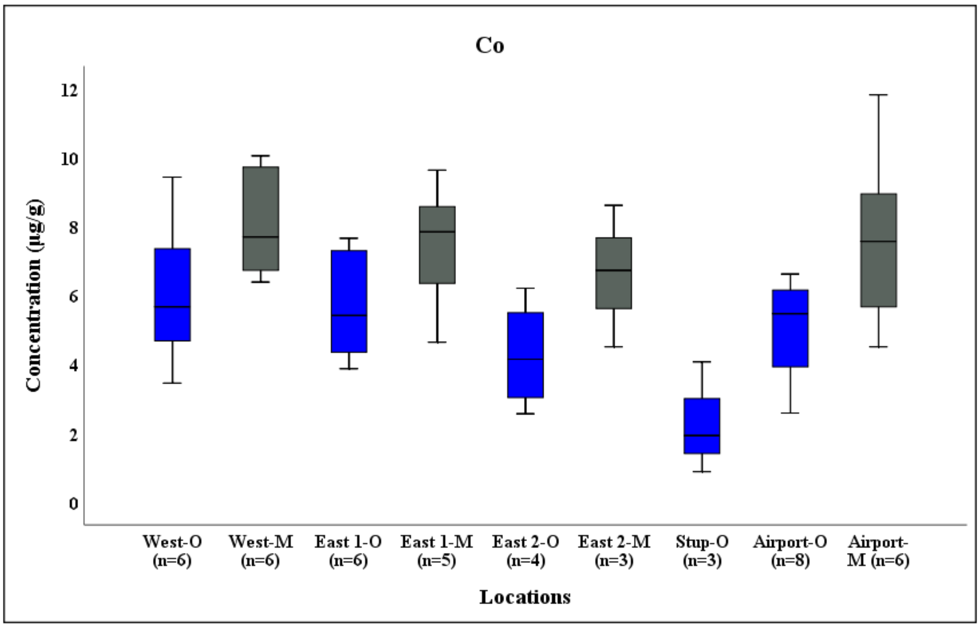
Co
12
10
8
6
4
2
0
Concentration (µg/g)
West-O (n=6)
West-M (n=6)
East 1-O (n=6)
East 1-M (n=5)
East 2-O (n=4)
East 2-M (n=3)
Stup-O (n=3)
Airport-O (n=8)
Airport-M (n=6)
Locations

E

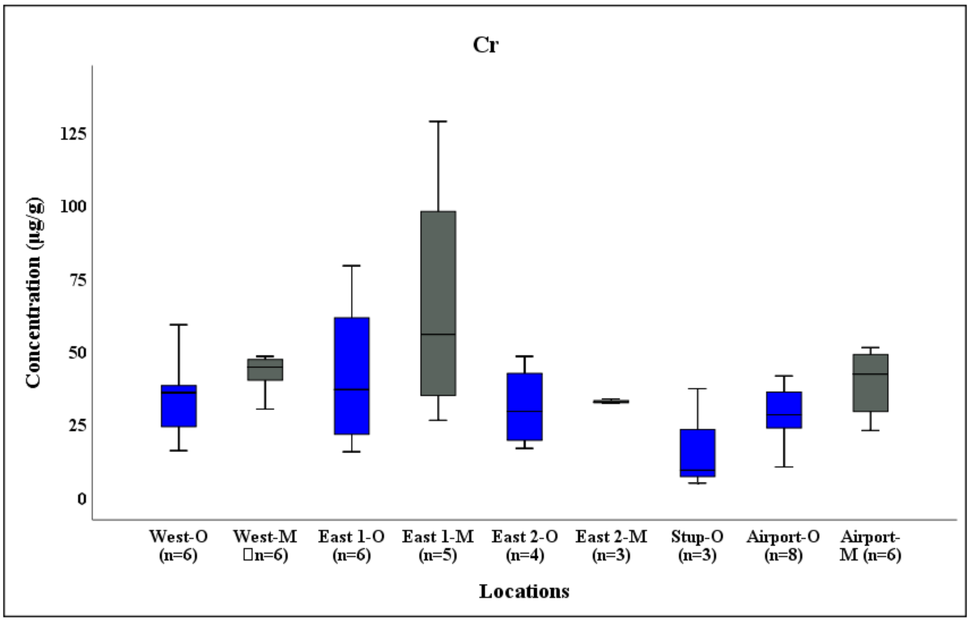

Figure 5.7: Distribution of 12 elements between organic soil (blue) and mineral soil (grey) in five sampling sites. Significance levels are presented with *, ** and * for p<0.05, <0.01 and <0.001 respectively.**

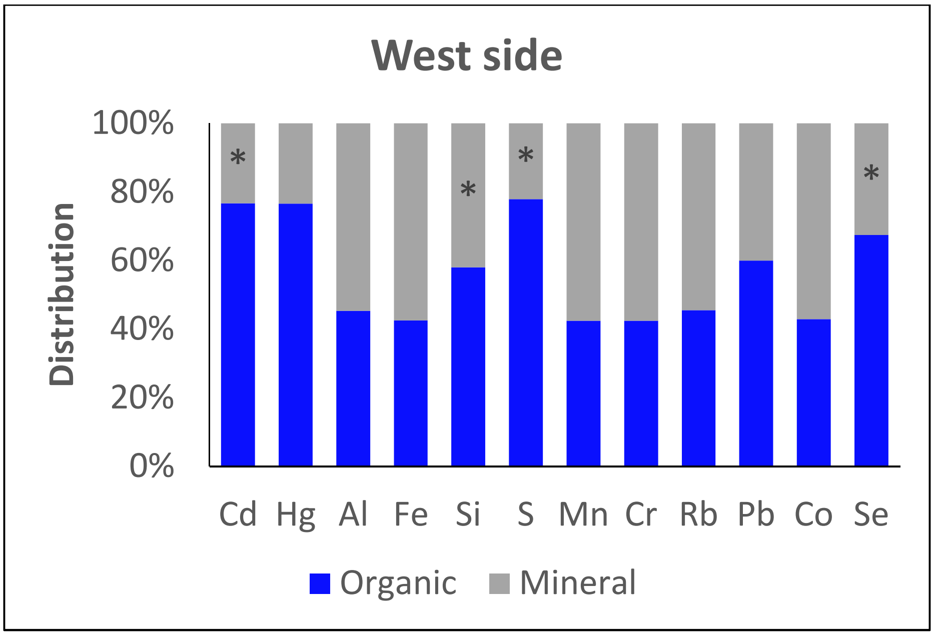

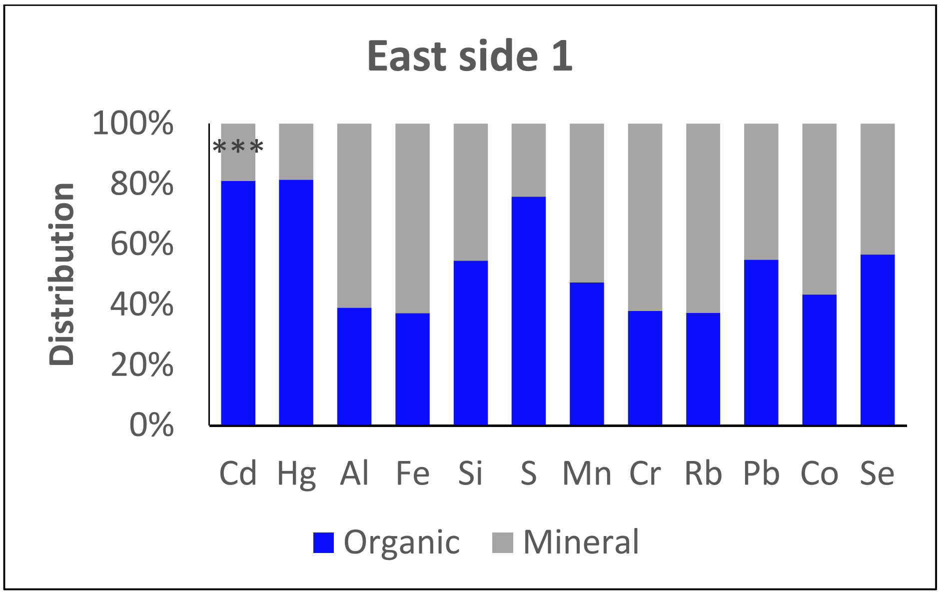
East side 1
Distribution
100%
80%
60%
40%
20%
0%
***
Cd
Hg
Al
Fe
Si
S
Mn
Cr
Rb
Pb
Co
Se
Organic
Mineral

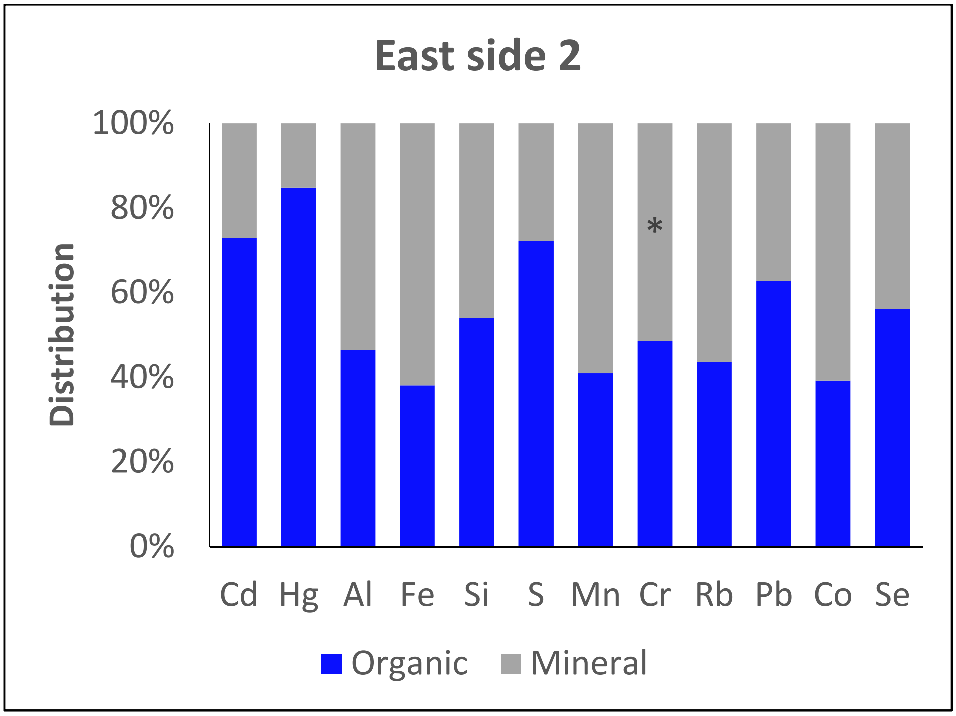
East side 2
Distribution
100%
80%
60%
40%
20%
0%
*
Cd
Hg
Al
Fe
Si
S
Mn
Cr
Rb
Pb
Co
Se
Organic
Mineral

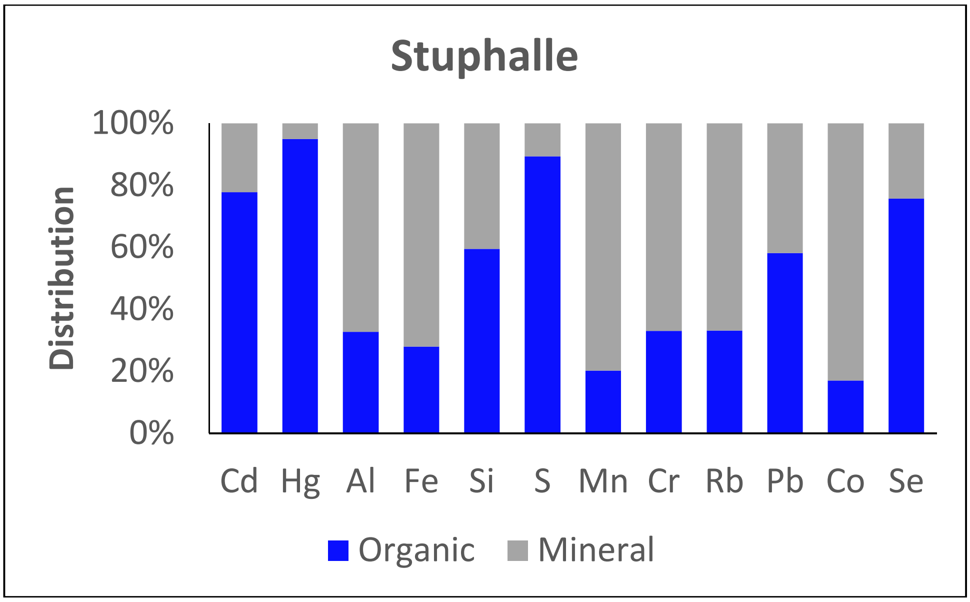
Stuphalle
Distribution
100%
80%
60%
40%
20%
0%
Cd
Hg
Al
Fe
Si
S
Mn
Cr
Rb
Pb
Co
Se
Organic
Mineral

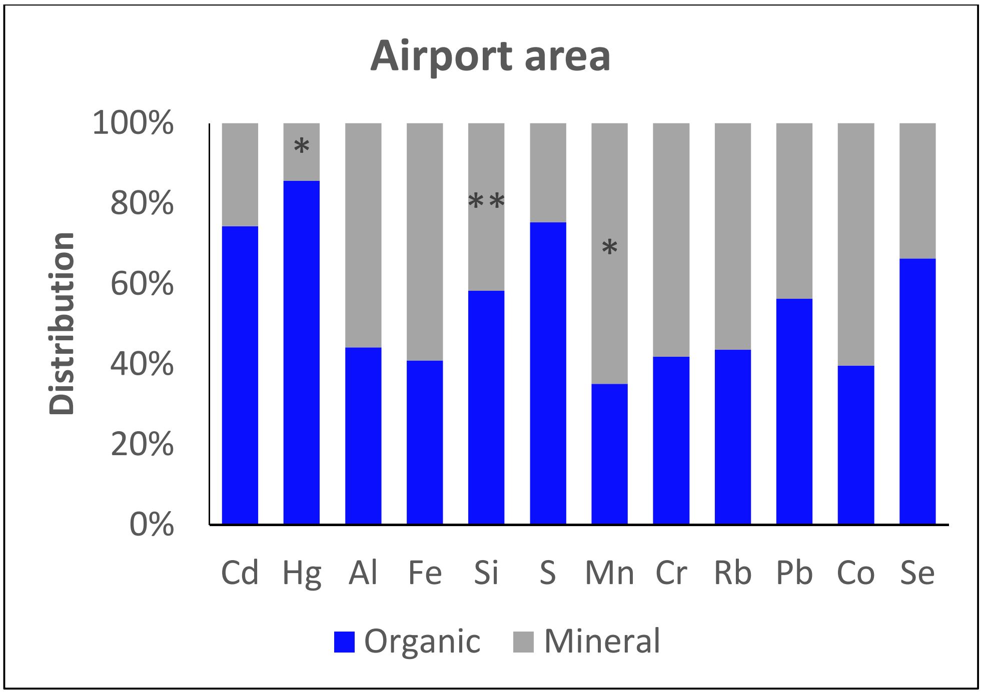
Airport area
Distribution
100%
80%
60%
40%
20%
0%
*
**
*
Cd
Hg
Al
Fe
Si
S
Mn
Cr
Rb
Pb
Co
Se
Organic
Mineral

5.6 Correlations

The relationship between different elements and SOM levels was explored using Spearman correlation analysis (Table 5.6). SOM positively correlated with Cd (ρ=0.623 at $p < 0.01$), Hg (ρ=0.847 at $p < 0.01$), Si (ρ=0.528 at $p < 0.01$), S (ρ=0.744 at $p < 0.01$), Ca (ρ=0.646 at $p < 0.01$) and inversely correlated related with other elements except for Pb, Se, P and U (Table 8). There was a negative correlation between pH and Hg (ρ=0.744 at $p < 0.01$), Mg (ρ=0.351 at $p < 0.05$), S (ρ=0.066 at $p < 0.05$).

Concentrations of most of elements correlated with each other (Table 5.6). A strong correlation was observed between Cd, Hg and S (Cd-Hg, ρ=0.725 at $p < 0.01$; Cd-S, ρ=0.805 at $p < 0.01$; Hg-S, ρ=0.915 at $p < 0.01$); in addition, S was negatively corelated with Ni (ρ=-0.812 at $p < 0.01$), Mg (ρ=-0.817 at $p < 0.01$), K (ρ=-0.802 at $p < 0.01$). Furthermore, Al, Fe, K and Cr, Co, Cu, Ni, Rb have significantly positive association with each other (Table A6)

5.7 Principal components analysis (PCA)

PCA was performed to compare the elemental profile of organic and mineral soil samples collected from Ny-Ålesund, Svalbard (Figure 5.8).

The first 2 PCs explain almost 69.3% of the variance in the data. In the plots the points have been coloured to indicate the different groupings of organic and mineral soils.

PC1 (Dim1) explained 54.8% while PC2 (Dim2) explained 14.5% of total variances. Organic soil samples separated from mineral soil samples on one side of the plot due to high concentration of Pb, Zn, Se, Hg, Cd and S. While mineral soils were characterized with high concentrations of Cr, Al, Rb, P, B, Na, Fe, Cu, K and separated on the other side of the plot.

The loadings were showed for 21elements as arrows. The angle between two arrows was a measure of the correlation between variables. The angles between Cd, Hg and S were small, Pb, Se and Zn were also showed small angles with each other. However, these elements had large angles with elements Cr, Al, Rb, B, Na, Fe, K, P and Cu. In the right side, the arrows of Cr, Al and Rb were closed.

Figure 5.8: Principal components analysis for organic and mineral soils.

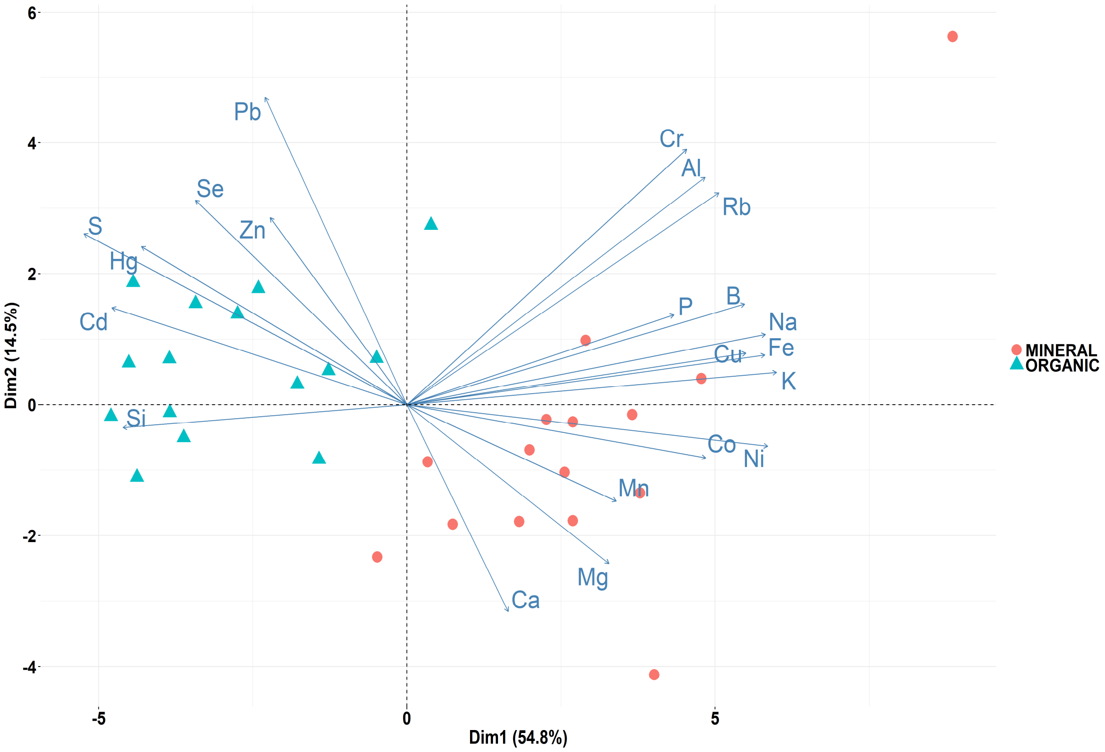

Table 5.6: The correlation between elements, SOM and pH (N=51).

	Cd	Hg	Al	Fe	Si	S	Mn	Cr	Rb	Pb	Co	Se	B	Na	Mg	P	Ca	Cu	K	Ni	pH	SOM
Cd		**	**	**	**	**	**	**	**	**	**	**	**	**	**	**	**	**	**	**		**
Hg	.725		*	**	**	**	**	*	**	**	**	**	**	**	**	**		**	**	**	**	**
Al	-.56	-.356		**	**	**	**	**	**		**		**	**	**	**	**	**	**	**		**
Fe	-.751	-.673	.85		**	**	**	**	**		**	**	**	**	**	**	**	**	**	**		**
Si	.489	.406	-.551	-.516		**	**	**	**		**		**	**	**	**	*	**	**	**		**
S	.805	.915	-.46	-.753	0.406		**	**	**	**	**	**	**	**	**	**		**	**	**	*	**
Mn	-.425	-.404	.494	.702	-.418	-.471		**	**		**		**	**	**	**	**	**	**	**		**
Cr	-.46	-.277	.931	.776	-.578	-.366	.486		**		**		**	**	**	**	**	**	**	**		**
Rb	-.55	-.409	.956	.865	-.515	-.476	.499	.923			**		**	**	**	**	**	**	**	**		**
Pb	.488	.613	.222	-.095	.081	.553	-.029	.272	.174			**										
Co	-.609	-.631	.75	.936	-.45	-.71	.817	.699	.764	-.049		**	**	**	**	**	**	**	**	**		**
Se	.526	.615	-.118	-.405	.006	.702	-.236	-.056	-.142	.527	-.418		*	**	**			**	**	**		
B	-.636	-.659	.663	.724	-.684	-.64	.486	.636	.649	-.18	.628	-.308		**	**	**		**	**	**		**
Na	-.772	-.724	.767	.875	-.67	-.771	.673	.686	.747	-.217	.814	-.423	.879		**	**	*	**	**	**		**
Mg	-.662	-.837	.637	.804	-.528	-.817	.514	.565	.691	-.266	.748	-.419	.841	.859		**		**	**	**	*	**
P	-.531	-.462	.424	.561	-.555	-.424	.61	.441	.478	-.235	.502	-.216	.773	.752	.617			**	**	**		
Ca	.426	.114	-.435	-.505	.34	.205	-.403	-.479	-.429	-.023	-.457	.115	-.095	-.315	-.05	-.182		*				**
Cu	-.737	-.734	.679	.837	-.616	-.749	.65	.596	.699	-.202	.785	-.393	.829	.933	.836	.768	-.302		**	**		**
Ag	-.548	-.447	.561	.588	-.615	-.385	.416	.565	.616	-.063	.478	-.105	.715	.704	.626	.745	-.203	.728	**	**		*
K	-.766	-.774	.771	.893	-.667	-.802	.625	.716	.789	-.226	.813	-.406	.898	.968	.919	.739	-.267	.938		**		**
Ni	-.715	-.778	.719	.883	-.649	-.812	.681	.68	.736	-.253	.845	-.432	.876	.953	.911	.736	-.255	.916	.971			**
U	.059	-.054	.148	.012	-.3	.078	-.13	.206	.154	.239	-.075	.435	.274	.03	.143	.061	.103	.115	.116	.037		
pH	-.133	-.514	.057	.155	.066	-.377	-.146	.008	.073	-.225	.079	-.284	.221	.072	.351	-.189	.039	.145	.173	.129		
SOM	.623	.847	-.711	-.875	.528	.744	-.516	-.693	-.724	.203	-.859	.319	-.468	-.778	-.798	-.219	.646	-.744	-.855	-.809	-.206	

(-1)-(-0.75)	(-0.75)-(-0.5)	(-0.5)-(-0.25)	(-0.25)-0	0-0.25	0.25-0.5	0.5-0.75	0.75-1

Chapter 6

Discussion

6.1 General characteristics of Svalbard soils

6.1.1 SOM

In this study, the SOM content ranged from 15.19 to 82.96% (mean 47.33 ± 16.56%, median 44.61%) for organic soils and from 1.7 to 13.12% (mean 6.07 ± 4.76%, median 3.58%) for mineral soils.

The content of SOM in surface soils from the samples of this study (2018) was lower compared to samples of 2015 (Table A7). Climate change might be the important reason to affect the content of SOM in soils after 3 years. As mentioned in section 3.5.2, the rising air temperature lead to consistently increased decomposition and therefore reducing the content of SOM (Karmakar et al., 2016). According to Halbach (2016), thin organic layers are involved in cryosols and mixed with underlying mineral soils; moreover, the sparse vegetation cover and low microbial activity also lead to lower SOM content. In thesis of Huber (2017), the mean content of SOM in surface soil was 22.5% due to analysis for combination of vegetation layer with soil samples. Furthermore, the SOM content in surface soil of this study (2018) was also lower than in natural soils in mainland, Norway (Nygård et al., 2012).

For comparison of SOM contents in surface soils with five sampling locations, Stuphalle (bird areas) had the highest level (70.67 ± 16.30%), while west side had the lowest (38.90 ± 13.06%). For the whole east side (east side 1, ast side 2 and airport area), the SOM contents in organic soils were similar. Also, according to Halbach (2016), The variation of SOM contents in different sampling locations might be attributed to various size of organic layers and associated with different vegetation cover (Halbach et al., 2017). In mineral soils, the SOM content was highest in airport areas and lowest in bird areas.

6.1.2 The comparison of trace elemental levels in surface soils with soils from Svalbard and mainland, Norway

The comparisons of mean elemental concentrations of organic soils and mineral soils from Bayelva, Svalbard between 2015 (Halbach, 2016) and 2018 are presented (Table A8 and A9). The mean elemental concentrations were similar in organic soils between sampling of 2015 and 2018 except for elements Cr. The level of Cr from samples taken in 2018 was approx.1.6 times higher than in 2015. For mineral soils, the mean concentrations of all elements were similar in sampling of 2018 compared to samples taken in 2015. The difference in organic soils could be due to local variations (Halbach, 2016).

Elemental concentrations measured in organic rich soils were comparable with the earlier studies where organic soils from Svalbard (Huber, 2017; Halbach, 2016; Marquès et al., 2017; Damhaug, 2014; Hao et al., 2013). The comparison of the elemental concentrations with previous studies is shown in Table 13. There were some notable differences of trace elemental concentration such as Cd concentration was highest and Cu concentration was lowest compared to other studies.

For Cd, its mean concentration (0.02 µg/g) was much lower in samples of 2012 (Hao et al., 2013); conversely, these samples had the highest mean concentration of Hg. The samples in that study were collected around the Huanghe station in Ny- Ålesund during the summer of

2012. The lowest mean concentration of Hg (0.08 µg/g) was found in samples were taken from Bayelva and Adventdalen in 2016 (Huber, 2017). It has been evidenced that trace elements Cd, Hg, Pb and Zn were typical representatives of elements transported long distances in the air (Stainnes and Friedland, 2006). These elements could effectively accumulate in surface soils. Also, they could strongly bind to soil organic matters and can be taken by plants (Berthelsen, 1995). However, several factors such as atmospheric deposition from natural and anthropogenic sources, binding capacity to soil organic substances, plant uptake as well as transport by root could affect accumulation of elements in surface soils (Stainnes and Friedland, 2005). Therefore, the variation of elemental concentration might result from different sampling locations (Ny- Ålesund, Bayelva, Adventdalen and Pyramiden), where had various condition of soil properties and vegetation. Moreover, the distant anthropogenic sources might impact on air deposition in Svalbard, because the emission of elements from originating might be changed in different year.

The concentration of Cr (mean 7.86 µg/g) and Ni (mean 7.46 µg/g) sampled from Norway mainland in 1995 were lower compared to samples from Svalbard (Nygård et al., 2012). In this study, the concentration of Cr was four times greater than of mainland and the concentration of Ni was approximate two times higher than of mainland (Table 6.1). This might be because of geological difference between Svalbard and Norway mainland (Halbach et al.,2017). Moreover, the concentration of Pb from samples of mainland was three times higher than samples from this study (Table 6.1). Additionally, the concentration range of Cd, Pb and Se from sampling of mainland, Norway were presented in Steinnes & Lierhagen (2018), where the concentration of these three trace elements (Cd, Pb, Se) decreased from south to north of mainland. In south of mainland, the concentration of Cd, Pb, Se were ranged from 0.12-5.71 µg/g, 7.6-1260 µg/g and 0.20-3.3 µg/g; while the concentration of these trace elements (Cd, Pb, Se) were ranged from 0.05-1.19 µg/g, 3.8-50.9 µg/g and 0.07-1.67 µg/g in north of mainland (Steinnes & Lierhagen, 2018). In this study, the concentration range of Cd, Pb and Se were 0.081-1.528 µg/g, 9,3-28.3 µg/g and 0.32-1.64 µg/g; therefore, the concentration of these elements (Cd, Pb, Se) were closed to elemental concentration in north of mainland.

The elemental concentrations Svalbard soils (Table 6.2, A10) were under the recommended levels for clean soils therefore these concentrations represent background levels only (Hansen & Danielsberg, 2009).

Table 6.1: The concentrations of trace elements in Svalbard and Norway mainland.

	Svalbard						**Norway mainland**
Sampling time	**2018**[a]	**2016**[b]	**2015**[c]	**2014**[d]	**2013**[e]	**2012**[f]	**1995**[g]
	Mean concentrations (µg/g)						
Cd	0.511	0.356	0.363	0.23	0.479	0.02	0.57
Cr	32.4	26.7	27.7	19.5	ND	40.57	7.86
Cu	9.7	12.7	12.5	20.8	13.9	18.31	11.6
Hg	0.132	0.08	0.11	0.09	0.109	0.28	ND
Ni	13.2	15.6	17.8	25.1	9.46	15.47	7.46
Pb	15.3	10.3	8.77	16.3	14.1	9.0	46.4
Zn	65	63.6	63.4	76.2	68.6	78.85	62.4

a. Samples were taken around Bayelva regions in August, 2018 (this study).

b. Samples were taken from Bayelva and Adventdalen during the summer 2016 (Huber, 2017).
c. Samples were taken from Adventdalen during the summer of 2015 (Halbach, 2016).
d. Samples were taken from Pyramiden in 2014 (Marquès et al., 2017).
e. Samples were taken from Ny- Ålesund in 2013 (Damhaug, 2014).
f. Samples were taken from Ny-Ålesund in 2012 (Hao et al., 2013)
g. Samples were taken from Norway mainland (Nygård et al., 2012).

Table 6.2: Classification of condition for contaminated sites (Hansen and Danielsberg, 2009)

	Status class					Svalbard	
	Very good	Good	Moderate	Poor	Very Poor	Organic	Mineral
Pb	< 60	60-100	100-300	300-700	700-2500	9.3-28.3	5.8-17
Cd	< 1.5	1.5-10	10-15	15-30	30-1000	0.081-1.528	0.037-0.301
Hg	< 1	1-2	2-4	4-10	10-1000	0.039-0.341	0.008-0.067
Cu	< 100	100-200	200-1000	1000-8500	8500-25000	4.6-13.7	4.7-18.8
Zn	< 200	200-500	500-1000	1000-5000	5000-25000	35.9-112.3	30.5-86.5
Cr	< 50	50-200	200-500	500-2800	2800-25000	4.8-79.2	22.8-128.6
Ni	< 60	60-135	135-200	200-1200	1200-2500	2.7-23.7	9.9-32.2

6.2 Spatial variations

There are different anthropogenic conditions between west and east side of Bayelva. East side included airport and shutdown coal mine, while west side was devoid of human activities. However, the distant sources from Arctic may be the important reason to result in variation of elemental accumulation in soils. For example, Cd and Se showed significantly higher abundance in organic soils in west side, which evidenced these two elements came from long-range atmospheric transport rather than local sources (Halbach et al., 2017).

For comparison of five sampling locations, the differences of elemental concentrations in mineral soil are mainly attributed by diversity of geology (Table A11). Additionally, the differences in some minerals and local variations may also importantly result in spatial variation of elemental accumulation (Table A11) (Ottesen et al., 2010). In Svalbard, geology of the area is highly variable (Elvevold et al., 2007). The geology in both west side and east side 2 were formed in period of Paleocene which was lasted from 66 to 56 million years ago. East side 1 and airport area had similar geological conditions that formed in Permian, this period was lasted from 289 to 251 million years ago. Stuphalle was a remote region also belong to bird area, the geology there was formed from late Carboniferous to early Permian (Elvevold et al., 2007). As a result, these locations have different ages and different kinds of rocks and minerals. Clastic sedimentary rocks are mainly in west side and east side 2, while east side 1 and airport area mainly limestone (organic sedimentary rocks) and some types of clastic sedimentary rocks, such as siliceous shale and sandstone (Ottesen et al., 2010). Carbonate rocks as clastic sedimentary rocks are abundant in Stuphalle (Ottesen et al., 2010). In mineral soils, higher concentration of trace elements Co (11.16 µg/g), Mn (570 µg/g) were found in Stuphalle; while the concentration of Cr (68.6 ± 43.5) was predominantly higher in east side 1.The differences in the elemental concentrations in these areas can be potentially attributed to soil geology.

The significant differences were found for elements Co and Pb in organic soils between west side and Stuphalle (bird area). Compared to other locations, the highest concentrations of these two elements (Co and Pb) were measured in west side. As mentioned by Ottesen (2010), Co is naturally associated with Pb in copper-cobalt sulphide ores. Reinders were present in the east and west sampling sites, therefore high concentrations of Co in organic soils in the west side could be affected by animal activities. According to Halbach et al (2017), the main reason to result in difference of Pb accumulation was local anthropogenic sources. Because there is airport in Ny-Ålesund. Fang et al (2014) also found higher concentration of Pb in sampling sites closed to airport compared to different sampling sites in other studies.

6.3 The sources of trace elements

The elements which significantly accumulated in mineral soils mainly come from soil parent material. The deposition of elements Co, Cr, Mn and Ni as well as Al and Fe were implied as results of crustal contribution and rock weathering (Singh et al., 2013). The levels of Cr and Ni in surface soils of Svalbard was higher than of Norway mainland (Cr 7.86 ug/g; Ni 7.46 ug/g) (Nygård et al., 2012). This difference was also indicated in paper of Halbach et al in 2017. The author support that the local geological condition might result in these concentrations in Svalbard. According to rotated component matrix for surface soil samples, the factor one (f1) which involved elements Al, Cr, Cu, Fe, Ni mostly reflected the influence of underlying mineral soil and bedrock (Halbach et al., 2017); these elements also negatively associated with SOM and element S. It is coincident with this study (2018). In the section 6.5, the test of Spearman's rank correlation evidenced that the elements Al, Fe, Cr, Cu, Ni had significantly positive association with each other and negative correlation with SOM. Moreover, the elements K, Co and Rb also positively related with these elements and negatively correlated with SOM; therefore, it might evidence that the source of elements Al, Fe, K, Cr, Co, Cu, Ni and Rb was natural geology.

Conversely, the elements Cd, Hg, Pb, Se, Zn negatively correlated with Al, Fe, Cr, Cu, Ni and positively related with SOM. Also, these elements (Cd, Hg, Pb, Se, Zn) were higher abundance in organic soils. It might illustrate that they come from air deposition (Halbach et al., 2017) due to local anthropogenic activities, such as airport. Additionally, the strong influence of long-range atmospheric transport on these elements (Cd, Hg, Pb, Se, Zn) had been supported by previous studies (Berg et al., 1995; Steinns and Friedland, 2006; Halbach et al., 2017). Therefore, the sources of these elements could involve origin in long distance from Arctic. According to Durnford et al (2010), Asia was considered as the dominant source of Hg in four seasons, generated most long-range transport events. North America, Russia and Europe were also important origin. Moreover, the test of Spearman's rank correlation showed the strong correlation between Cd, Hg and S. The chemical association of Hg and S resulted from atmospheric deposition was conducted by factor analysis (Halbach et al., 2017). Therefore, the trace elements Cd and Hg may bind to S for deposition.

Although Hg is the element experiences long-range atmospheric transport, it is not associated with same factors as Cd, Pb and Zn (Halbach et al., 2017). This is attributed that mercury is transported by its gaseous elemental form in the atmosphere (Berg et al., 1995; Berg and steinnes, 1997; Halbach et al., 2017). Then, Hg can be transported by its oxidation (Hg (II)) to soil layers through wet or dry deposition and AMDEs from atmosphere. Additionally, snow has been considered as key media between atmosphere and landscape, thus melting snow and glaciers could be the second sources of mercury deposited in soils. While AMDEs is the most important pathway for contribution of deposited mercury in snow.

Låg and Steinnes (1978) presented that Se accumulates in organic soil layers was contributed by airborne supply. Se originated from three types of sources, including marine sources, natural terrestrial sources (e.g. plant decomposition and volcanic activity) and anthropogenic sources. Se could be released from coal burning and metallurgical processes also experienced long-range atmospheric transportation to reach Svalbard.

6.4 Water leaching

In nature, the trace elements can be released from soils. However, pH is the most important factor to control these processes because pH value can affect mobility and chemical speciation of trace elements (Dijkstra et al., 2014). The purpose of leaching test is to identify the effects of different pH values on release of trace elements from soil.

In this study, the concentrations of Cd, Co, Ni, Cu, Zn, Fe, Al were higher in pH 2 leachates, while the concentrations of S and Cr, Hg, Pb, Se, U were greater in pH 10 leachates. Additionally, the concentrations of Cd, Co, Cr, Ni, Cu, Zn, Fe and S were lowest in pH 7 leachates. Among, the concentrations of elements Cd, Co, Cr, Cu, Ni, Zn and Fe, S decreased with increasing pH from 2 to 7 and increased again from pH 7 to 10; only element Al decreased with increasing pH value from 2 to 10. Conversely, the elements Hg, Pb, Se and U increased with raising pH value. Figure 5.3 featured that increasing in pH value significantly promoted leaching of elements Pb, Se, Hg and U from soils. These trends were partly consistent with the findings of Pédrot et al (2009) where increased in concentration of Cr, Fe, Pb, U and decreased in concentration of Al, Co, Ni, Zn with raising pH value from 4 to 7.2 was observed. The trends of Cr and Fe were inverse compared to this study.

Dijkstra et al (2014) reported “V-shaped” leaching curves reflecting a strong pH dependence of the leached concentration of trace elements. The concentration of leached trace elements (Ni, Cu, Zn, Cd, Pb) reduced with rising pH value from high concentration at pH 2 to reach the lowest points at neutral pH value, then increased again from neutral pH to alkaline pH values. In this study, the concentration of leached elements Cd, Cr, Co, Cu, Fe, Ni, S and Zn formed “V-shaped” leaching curves at pH values from 2 to 10.

The elemental speciation which was strongly dependent on pH explained V-shaped leaching. Metals generally presented in soils with dissolved free metal ions at pH 2, which promoted to metal release. Metal tended to cation sorption with rising pH values and bound to hydroxide minerals and organic matter; as a result, leaching concentrations decreased. At alkaline pH, metals bound to Dissolved organic matters (DOMs) and thereby their concentrations increased in leachates.

Cd existed in soils with +2 oxidation state. Its solubility highly depended on pH value. Cd mainly existed as free cation (e.g. Cd^{2+}) below pH 5 (Alloway 2013); therefore, Cd was most mobile in acidic soils. SOM, oxyhydroxides of Fe, Mn as well as Al were the major Cd adsorbents at low to neutral pH conditions (Kabata-Pendias & Pendias, 2001). Cd majorly bound to SOM below pH 6.5, while Fe-oxides was shifted to be important above pH 6.5; $CdCO_3$ and $Cd_3(PO_4)_2$ might control Cd mobility in soils above pH 7.5 (Kabata-Pendias & Pendias, 2001). However, the sorption reduced with increased pH values from neutral to high pH conditions, and thus Cd might bind on dissolved organic carbon (DOC) to form complexes for leaching at high alkaline pH values. these complexes increased Cd mobility (Alloway 2013).

Komonweeraket et al (2015) indicated that Cr leached with amphoteric conditions, in which the leached concentrations were minimum at neutral pH and maximum at acidic and basic pH values. This could probably because dissolved (hydr)oxides strongly affected mobility of these elements, which was highly coincident with Dijkstra et al (2004). Most stable form of Cr was Cr^{3+} at acid pH, while Cr^{6+} was easily mobilized at both acid and alkaline pH (Kabata-Pendias & Pendias, 2001). $Cr(OH)_3$ was formed from pH 5 to pH 7; therefore, Cr stably existed in soils as insoluble $Cr(OH)_3$ at neutral pH conditions, or with form of $Cr(OH)_2^+$ bind to organic matters (Alloway, 2013). While these complexes were easier to dissolve at acidic or basic pH conditions (Alloway, 2013).

Pédrot et al (2009) mentioned that leached Co and Zn concentrations increased with decreased pH value because of their dissolved state at acidic pH. The oxidation of Co^{2+} to Co^{3+} was occurred by role of Mn-oxides from pH 4 to pH 7; Co could be leached with free metal iron from soils to solution with pH at 2.

Moreover, the leached concentration of elements U increased with raising pH values due to their binding relation with anionic ligands, plus this binding was favored at high pH conditions.

Hg had strong tendency to form complexes with Cl^- ($HgCl_2$), OH^- ($Hg(OH)_2$) and S^{2-} (HgS), this adsorptive behavior could affect solubility of Hg (Schuster, 1991). HgS has very low solubility. The high solubility of Hg could be occurred by binding of Hg(II) to OH^- and Cl^- (Schuster, 1991). Hg(II) might mainly formed $HgCl_2$ from pH 3 to 5, while the predominant species might be $Hg(OH)_2$ from pH 6 to 8 (Figure 6.1). In the highly alkaline soil, Hg existed as soluble form of HgS_2^{2-} (Alloway, 2013). As indicated by Steinnes, S., the mobility of Hg decreased below pH 3 and above pH 12 (Alloway, 2013). Increased acidity enhanced the sorption of Hg to humic matters, which decreased Hg leaching. This might also explain the increasing concentration of Hg in soil leachates from pH 2 to pH 10 for this study.

Figure 6.1: Predicted speciation of Hg as influenced by pH (Schuster, 1991).

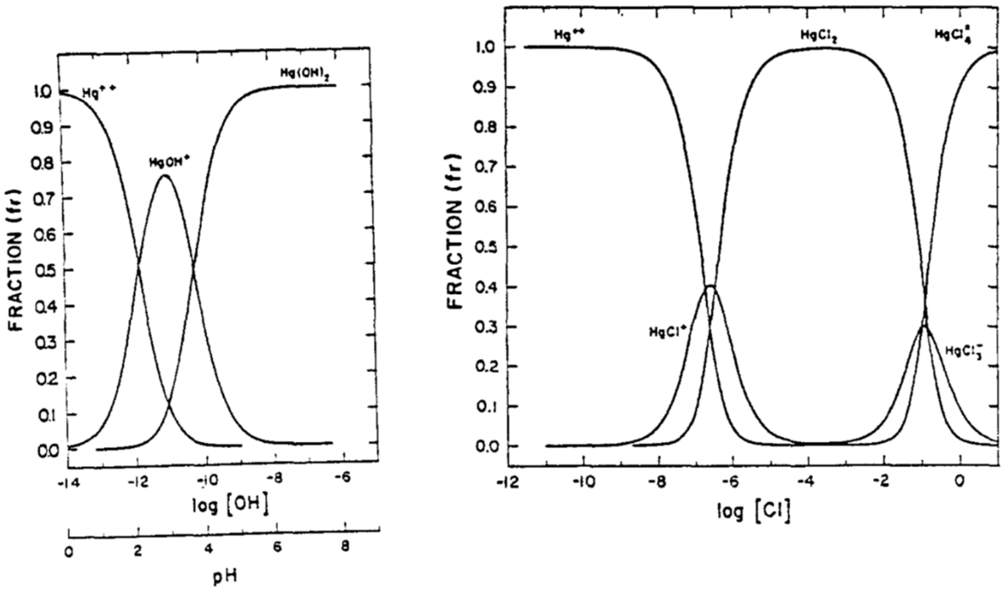

The section 2.4.2 mentioned that stable Pb-organic complexes might form in soil at high pH value and Pb solubility might increase with rising acidity (Alloway, 2013). In addition, Pb absorbed to humic matters at pH 4 and above (Alloway, 2013). Therefore, Pb might be less soluble at neutral pH value. Both Dijkstra et al (2004) and Martín-Torre (2015) reported that DOC positively influenced in release of Pb at basic pH value. Moreover, these two papers evidenced that the leaching of Pb followed "V-Shaped" curves. Whereas in this study, we did not find Pb concentration follow V-shape curves; it increased with increasing pH value from pH 2 to pH 7. This might because the different soil conditions with unpredicted bind for complexes, and thus further researches were needed in future.

6.5 Potential impact of pH on concentrations of trace elements in Svalbard soils in future as a consequence of ongoing global warming

The air temperature in Svalbard were increasing between 2010 and 2018 was displayed (Figure 6.2, Table A12). The trend of CO_2 increased coincides with temperature rise (Figure 6.3, Table A12). According to levels of selected trace elements in Svalbard from 2012 to 2018 (Table 6.1), which did not reflect any effects of global warming on trace elemental accumulation in surface soil. However, as introduced in section 3.5, the increasing level of CO_2 in atmosphere could promote to content of SOM in soils, whereas trace elements would bind on SOM to accumulate in soils. Conversely, the rising air temperature could reduce the content of SOM through increasing decomposition or altering global precipitation (Karmakar et al., 2016).

Climate change has also prolonged snow-free period (Halbach et al., 2017). Snow and glacier were recognized as “key reservoirs” of elements, they were also second source to release elements to soil through their melting; therefore, climate change might indirectly lead to increased levels of trace elements in soils. The effects of climate change on mercury had been supported by literatures (Dommergue et al., 2010). The input of mercury in soils increased by longer snow-free period. In the other hand, climate change also resulted in thawing permafrost, which contributed to release of mercury from soils. The increased decomposition of SOM contributed to production of DOM, which strongly influenced in release of Hg from soils (Dommergue et al., 2010; AMAP, 2011; Fisher et al., 2013).

Furthermore, the chemical reaction of sulfur and nitrogen could result in generation of sulfuric and nitric acids that mixed with precipitation and formed acid rain. The pH level of acid rain was 5.2 or below, while the normal pH of rain was approximate 5.6 (Bradford, 2018). Norwegian Polar Institute reported that the emission from Europe and Russia added to the deposition of acid rain in Svalbard. Additionally, acid rain could increase acidity of soil, which might promote to elements (Cd, Co, Ni, Cu, Zn) leaching from soils with decreasing pH value. Moreover, the leaching of mercury was also showed increased level from acidic to neutral pH conditions in the leaching tests in this study. Therefore, the harmful effects may occur if increased leaching will happen in nature, because mercury can biomagnify through food chain and thereby may reaching toxic level in high trophic level species (Alloway, 2013).

For future studies, the selected range of pH value should be large, such as range of pH 0-14. The high numbers of samples should be collected for better analysis. Additionally, the lager spatial variation should be chosen for sample collection due to different chemical composition of soils in large areas.

Figure 6.2: Temperature of Svalbard between 2010 and 2018 [Environmental monitoring of Svalbard and Jan Mayen (MOSJ)].

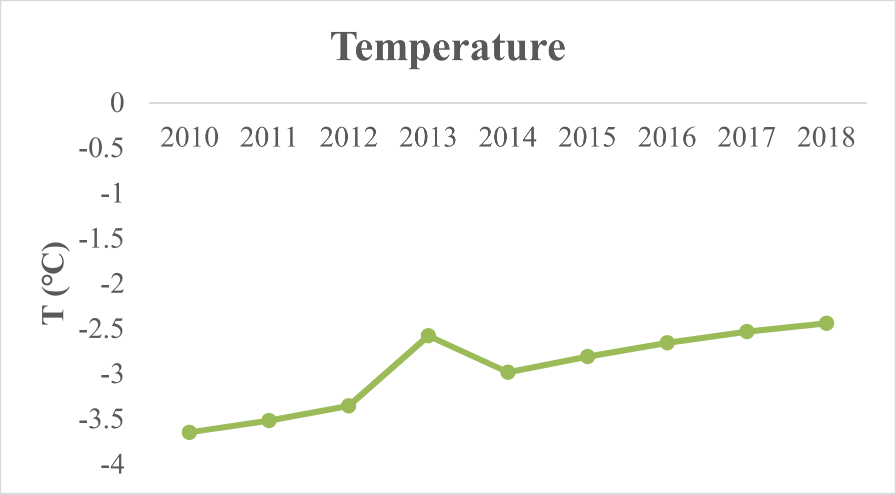

Figure 6.3: The content of CO2 in atmosphere between 2010 and 2017 [Environmental monitoring of Svalbard and Jan Mayen (MOSJ)].

.

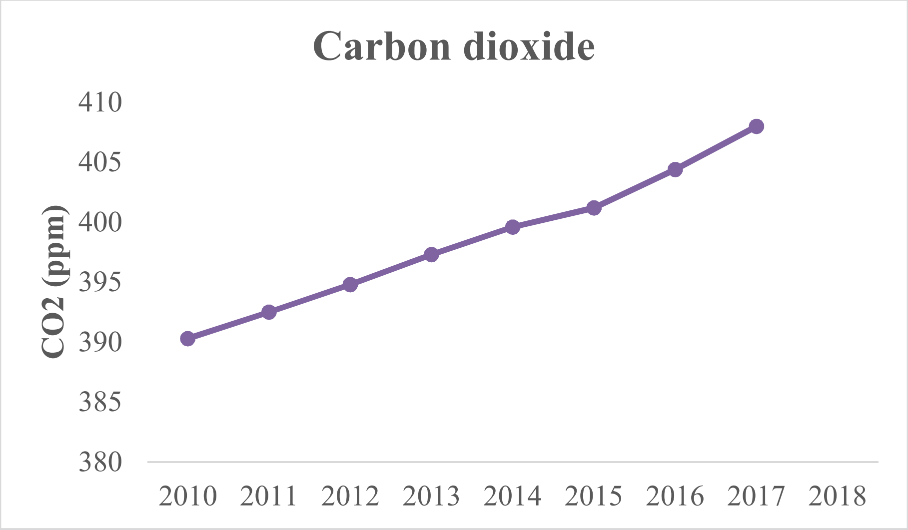

Chapter 7

Conclusion

The impact of pH on leaching of elements from soils was tested. The highest concentrations of Cd, Co, Cu, Ni, Al, Fe were found in pH 2 leachates, while the concentrations of S and Cr, Hg, Se, U were greatest in pH 10 leachates. The concentrations of Cd, Co, Cr, Cu, Ni, Zn, Fe and S were lowest in pH 7 leachates. In addition, the concentrations of elements Cd, Co, Ni, Zn and Fe decreased with increasing pH from 2 to 7 and increased again from pH 7 to 10; only element Al decreased with increasing pH value from 2 to 10. Conversely, the element Hg, Se, Pb, U increased with raising pH value.

SOM contents were significantly higher in organic soils (47.33 ± 16.56%) compared to mineral soils (6.07 ± 4.76%). Conversely, pH value of organic soils (6.495 ± 0.66) were significantly lower than mineral soils (7.22 ± 1.15).

The levels of 11 trace elements (Cd, Cr, Co, Cu, Hg, Ni, Pb, Rb, Se, U, Zn) and 11 macro and micro elements (Al, B, Ca, Fe, K, Mg, Mn, Na, P, Si, S) for samples from both organic soils and mineral soils were investigated. The concentrations of Cd, Hg, Pb, Se and Zn were significantly higher in organic soils, whereas concentrations of Cr, Cu, Ni and Rb were significantly higher in mineral soils.

The comparison of west and east of Bayelva showed there was not predominant difference for concentrations of most elements except for elements Cd, Se and P. Additionally, the concentrations of elements Se, S and P were significantly higher in mineral soils of west side.

In organic soils of five sampling locations, the significantly higher concentration of Hg and S was found in west side and airport area, respectively. Moreover, the significant higher concentration of Si was found in both west side and airport area.

SOM positively correlated with Cd, Hg, Ca, S, Si and negatively related with Al, Fe, Mn, Cr, Cu, Ni, Rb, Co, Na, Mg, K, B. Cd, Hg and S had strongly positive correlation with each other. Al, Fe, K and Co, Cr, Cu Ni, Rb had significantly positive association with each other.

Reference

Abdi, H., Williams, L.J., 2010. Principal component analysis. Wiley interdisciplinary reviews: computational statistics 2 (4), 433-459.

Alloway, B.J., 2013. Heavy metals in soils. Third edition. Springer Dordrecht Heidelberg New York London.

AMAP, 2011. AMAP Assessment 2011: mercury in the Arctic, Arctic Monitoring and Assessment Programme (AMAP).

AMAP, 2005. AMAP Assessment 2002: Heavy metals in the Arctic. Arctic Monitoring and Assessment Programme (AMAP).

AMAP, 2002. AMAP Assessment 2002: Heavy metals in the Arctic, Arctic Monitoring and Assessment Programme (AMAP).

AMAP 1997. Heavy metals and persistent organic pollutants in sediments and fish from lakes in Northern and Arctic regions of Norway. Utflrende institusjon Akvaplan-niva.

Bazzano, A., Ardini, F., Grotti, M., Malandrino, M., Giacomino, A., Abollino, O., Cappelltti, D., Becagli, S., Traversi, R., Udisti, R., 2016. Elemental and lead isotopic composition of atmospheric particulate measured in the Arctic region (Ny-Ålesund, Svalbard Island). Rend. Fis. Acc. Lincei 27, 73-84.

Bazzano, A., Ardini, F., Becagli, S., Traversi, R., Udisti, R., Cappelltti, D., Grotti, M., 2015. Source assessment of atmospheric lead measured at Ny-Ålesund, Svalbard. Atmos Environ 113, 20-26.

Bazzano, A., Rivaro, P., Soggia, F., Ardini, F., Grotti, M., 2014. Anthropogenic and natural sources of particulate trace elements in the coastal marine environment of Kongsfjorden, Svalbard. Mar Chem 163, 28-35.

Bawker, M.A., 2007. Biological soil crust rehabilitation in theory and practice: an underexploited opportunity. Restoration ecology 15, 13-23.

Bardgett, R.D., Freeman, C., Ostle, N.J., 2008. Microbial contributions to climate change through carbon cycle feedbacks. ISME J. 2, 805-814.

Bardgett, R.D., Bowman, W.D., Kaufmann, R., Schmidt, S.K., 2005. A temporal approach to linking aboveground and belowground ecology. Trends Ecol. Evol. 20, 634-641.

Bettina, W., Burkhard, B., Jayne, B., 2016. Biological soil crusts: an organizing principle in drylands. Springer.

Beldowski, J., Miotk, M., Zaborska, A., Pempkowiak, J., 2015. Distribution of sedimentary mercury off Svalbard, European Arctic. Chemosphere 122, 190-198.

Belnap, J., 2003. Biological soil crusts: structure, function and management. Springer.

Berg, T., Steinnes, E., 1997. Recent trends in atmospheric deposition of trace elements in Norway as evident from the 1995 moss survey. Sci. Total Environ. 208, 197-206.

Berg, T., Røyset, O., Steinnes, E., Vadset, M., 1995. Atmospheric trace element deposition: principal component analysis of ICP-MS data from Moss samples. Environ. Pollut. 88, 67-77.

Berthelsen, B.O., Steinnes, E., Solberg, W., Jingsen, L., 1995. Heavy metal concentrations in plants in relation to atmospheric heavy metal deposition. J. Environ. Qual. 24, 1018-1026.

Boike, J., Juszak, I., Large, S., Chadburn, S., Burke, E., Overduin, P.P., Roth, K., Ippisch, O., Bornemann, N., Stern, L., Gouttevin, I., Hauber, E., Westermann, S., 2018. A 20-year record (1998-2017) of permafrost, active layer and meteorological conditions at a high Arctic permafrost research site (Bayelvam, Spitsbergen). Earth Syst. Sci. Data 10, 335-390.

Bockheim, J.G., 2015. Cryopedology. Progress in soil science. Springer Dordrecht Heidelberg New York London.

Bojko, O., Kabala, C., 2014. Loss-on-ignition as an estimate of total organic carbon in mountain soils. Polish journal of soil science 2 (2), 71-79.

Bockheim, J.G., Mazhitova, G., Kimble, J.M., Tarnocai, C., 2006. Controversies on the genesis and classification of permafrost-affected soils. Geoderma 137, 33-39.

Bollhöfer, A., Rosman, K.J.R., 2002; The temporal stability in lead isotopic signatures at selected sites in the southern and northern hemispheres. Geochimica et cosmochimica acta 66 (8), 1375-1386.

Bradford, A., 2018. Acid rain: causes, effects and solutions. Live science. https://www.livescience.com/63065-acid-rain.html.

Brevik, E.C., 2013. The potential impact of climate change on soil properties and processes and corresponding influence on food security. Agriculture 3, 398-417.

Buekers, J., Degryse, F., Maes, A., Smolders, E., 2008. Modelling the effects of ageing on Cd, Zn, Ni and Cu solubility in soils using an assemblage model. European journal of soil science 59, 1160-1170.

Byun, Y.H., Yoon, H.K., Kim, Y.S., Hong, S.S., Lee, J.S., 2014. Active layer characterization by instrumented dynamic cone penetrometer in Ny- Ålesund, Svalbard. Cold regions science and technology 104-105, 45-53.

Chételat, J., Amyot, M., Arp, P., Blais, J.M., Depew, D., Emmerton, C.A., Evans, M., Gamberg, M., Gantner, N., Girard, C., Graydon, J., Kirk, J., Lean, D., Lehnherr, I., Muir, D., Nasr, M., Poulain, A.J., Power, M., Roach, P., Stern, G., Swanson, H., Velden, S.V.D., 2015. Mercury in freshwater ecosystems of the Canadian Arctic: recent advances on its cycling and fate. Science of the total environment 509-510, 41-66.

Cole, A.S., Steffen, A., Pfaffhuber, K.A., Berg, T., Pilote, M., Poissant, L., Tordon, R., Hung, H., 2013. Ten-year trends of atmospheric mercury in the high Arctic compared to Canadian sub-Arctic and mid-latitude sites. Atoms. Chem. Phys. 13, 1535-1545.

Damhaug, M.E.F., 2014. Studie av kvikksølv, svovel og naturlig organisk materiale i jord i Ny-Ålesund, Svalbard. Master i realfag. Norges teknisk-naturvitenskapelige universitet.

Davidson, E.A., Post, W.M., Hennessy, K., 2006. Temperature sensitivity of soil carbon decomposition and feedbacks to climate change. Nature 440, 165-173.

Dijkstra, J.J., Meeussen, J.L., Comans, A.J., 2004. Leaching of heavy metals from contaminated soils: an experimental and modeling study. Environ. Sci. Technol. 38, 4390-4395.

Dörr, H., Münnich, K.O., 1991. Lead and cesium transport in European forest soils. Water, air, and soil pollution 57-58, 809-818.

Douglas, T.A., Loseto, L.L., Macdonald, R.W., Outridge, P., Dommergue, A., Poulain, A., Amyot, M., Barkay, T., Berg, T., Chételat, J., Constant, P., Evans, M., Ferrari, C., Gantner, N., Johnson, M.S., Kirk, J., Kroer, N., Larose, C., Lean, D., Nielsen, T.G., Poissant, L., Rognerud, S., Skov, H., Sørensen, S., Wang, F., Wilson, S., Zdanowicz, C.M., 2012. The fate of mercury in Arctic terrestrial and aquatic ecosystem, a review. Environ. Chem. 9, 321-355.

Douglas, T.A., Amyot, M., Barkay, T., Berg, T., Chetelat, J., Constant, P., Dommergue, A., Evans, M., Ferrari, C., Gantner, N., Johnson, M., Kirk, J., Kroer, N., Larose, C., Lean, D., Loseto, L., Macdonald, R., Muir, D., Nielsen, T.G., Outridge, P., Poulain, A., Poissant, L., Rognerud, S., Skov, H., Sorensen, S., Wang, F., Zdanowicz, C., 2011. Chapter 3, what is the fate of mercury entering the Arctic environment? in AMAP Assessment 2011, 45-65.

Dounford, D., Dastoor, A., Figueras-Nieto, D., Ryjkov, A., 2010. Long range transport of mercury to the Arctic and cross Canada. Atmospheric chemistry and physics discussions 10 (2), 4673-4717.

Douglas, T.A., Sturm, M., Simpson, W., Blum, J., Alvarez-Aviles, L., Keeler, G., Perovich, D., Biswas, A., Johnson, K., 2008. The influence of snow and ice crystal formation and accumulation on mercury deposition to the Arctic. Environ. Sci. Technol. 42, 1542.

Dommergue, A., Larose, C., Clarisse, O., Foucher, D., Hintelmann, H., Schneider, D., Ferrari, C., 2010. Deposition of mercury species in the Ny-Ålesund area (79ºN) and their transfer during snowmelt. Environ. Sci. Technol. 44, 901-907.

Durnford, D., Dastoor, A., Figueras-Nieto, D., Ryjkov, A., 2010. Long range transport of mercury to the Arctic and across Canada. Atoms. Chem. Phys. 10, 6063-6086.

Durnford, D., Dastoor, A., 2011. The behavior of mercury in the cryosphere: a review of what we know from observations. J. Geophys. Res. 116, D06305.

Durnford, D.A., Dastoor, A., Steen, A.O., Berg, T., Ryzhkov, A., Figueras, D., Hole, L.R., Pfaffhuber, K.A., Hung, H., 2012. How relevant is the deposition of mercury onto snowpacks? – Part 1: a statistical study on the impact of environmental factors. Atoms. Chem. Phys. 12, 9221-9249.

Edwards, A.C., Scalenghe, R., Freppaz, M., 2007. Changes in the seasonal snow cover of alpine regions and its effect on soil processes: a review. Quaternary international 162-163, 172-181.

Elvevold, S., Dallmann, W., Blomeier, D., 2007. Geology of Svalbard. Norsk Polarinstitutt.

Fang, G.C., Chiang, H.C., Chen, Y.C., Xiao, Y.F., Zhuang, Y.J., 2014. Particulates and metallic elements monitoring at two sampling sites (Harbor, Airport) in Taiwan. Environmental forensics 15, 296–305.

Farkas, C., Hagyó, A., Horváth, E., Várallyay, G., 2008. A chernozem soil water regime response to predict climate change scenarios. Soil water research 3, 558-567.

Faïn, X., Ferrari, C.P., Dommergue, A., Albert, M., Battle, M., Arnaud, L., Barnola, J.M., Cairns, W., Barbante, C., Boutron, C., 2008. Mercury in the snow and firn at Summit Station, Central Greenland, and implications for the study of past atmospheric mercury levels. Atoms. Chem. Phys. 8, 3441-3457.

Farrah, H., Pickering, W.F., 1977. Influence of clay solute interactions on aqueous heavy metal ion levels. Water, air and soil pollution 8 (2), 189-197.

Fisher, J.A., Jacob, D.J., Soerensen, A.L., Amos, H.M., Steffen, A., Sunderland, E.M., 2012. Riverine source of Arctic ocean mercury inferred from atmospheric observations. Nature geoscience 5 (7), 499.

Fleming, G.A., Parle, P.J., 1977. Heavy metal in soils, herbage and vegetation from an industrialized area west of Dublin-city. Irish journal of agricultural research 16, 35-48.

Førland, E.J., Benestad, R., Hanssen-Bauer, I., Haugen, J.E., Skaugen, T.E., 2011. Temperature and precipitation development at Svalbard 1900-2100. Advanced in meteorology, 1-14.

Flanner, M.G., Zender, C.S., Hess, P.G., Mahowald, N.M., Painter, T.H., Ramanathan, V., Rasch, P.J., 2008. Spring warming and reduced snow cover from carbonaceous particles. Atmos. Chem. Phys. Discuss. 8, 19819-19859.

Gangloff, S., Stille, P., Schmitt, A.D., Chabaux, F., 2016. Factors controlling the chemical composition of colloidal and dissolved fractions in soil solutions and the mobility of trace elements in soils. Geochimica et cosmochimica Acta 189, 37-57.

Gamberg, M., Chételat, J., Poulain, A.J., Zdanowicz, C., Zheng, J., 2015. Mercury in the Canadian Arctic terrestrial environment: an update. Sci. Total Environ 509-510, 28-40.

Gauchard, P.A., Aspmo, K., Temme, C., Steffen, A., Ferrari, C., Berg, T., Ström, J., Kaleschke, L., Dommergue, A., Bahlmann, E., Magand, O., Planchon, F., Ebinghaus, R., Banic, C., Nagorski, S., Baussand, P., Boutron, C., 2005. Study of the origin of atmospheric mercury depletion events recorded in Ny-Ålesund, Svalbard, spring 2003. Atmospheric environment 39, 7620-7632.

Gilmour, J.T., Miller, M.S., 1973. Fate of a mercuric-mercurous chloride fungicide added to turfgrass. Journal of environmental quality 2, 145-148.

Gong, H., Ryu, J., Jung, H.J., Chung, H., Ahn, K.H., Ro, C.U., 2010. Single-particle characterization of summertime Arctic aerosols collected at Ny-Ålesund, Svalbard. Environ. Sci. Techmol. 44, 234802353.

Grybos, M., Davranche, M., Gruau, G., Petitjean, P., 2007. Is trace metal release in wetland soils controlled by organic matter mobility or Fe-oxyhydroxides reduction? Journal of colloid and interface science 314, 490-501.

Halbach, K., Mikkelsen, Ø., Berg, T., Steinnes, E., 2017. The presence of mercury and other trace metals in surface soils in the Norwegian Arctic. Chemosphere 188, 567-574.

Halbach, K., 2016. Study of mercury and selected trace elements in soil in the Norwegian Arcitc, Svalbard. Master thesis, Norwegian university of science and technology.

Hao, Z.L., Wang, F., Yang, H.Z., 2013. Baseline values for heavy metals in soils on Ny-Ålesund, Spitsbergen Island, Arctic: the extent of anthropogenic pollution. Advanced materials research 779-780, 1260-1265.

Hansen, H. J., Danielsberg, A. 2009. Condition classes for contaminated soil, TA-2553/2009: Norwegian Pollution Control Authority.

Henkner, J., Scholten, T., Kühn, P., 2016. Soil organic carbon stocks in permafrost-affected soils in West Greenland. Geoderma 282, 147-159.

Hogberg, P., Read, D.J., 2006. Towards a more plant physiological perspective on soil ecology. Trends Ecol. Evol. 21, 548-554.

Hotelling, H., 1933. Analysis of a complex of statistical variables into principal components. Journal of educational psychology 24, 417-441 and 498-520.

Huber, C.E, 2017. Study of long range transported pollutants in Arctic soil. Master thesis, Norwegian university of science and technology.

James, B.R., Bartlett, R.J., 1988. Mobility and bioavailability of chromium in soil. In Nriagu, J.O., Nieboer, E., Chromium in natural and human environments, 265-305. New York: Wiley Interscience.

Jenkinson, D.S., Adams, D.E., Wild, A., 1991. Model estimates of CO2 emissions from soil in response to global warming. Nature 351, 304-306.

Jia, N., Sun, L., He, X., You, K., Zhou, X., Long, N., 2012. Distribution and impacts of factors of antimony in topsoils and moss in Ny-Ålesund, Arctic. Environmental pollution 171, 72-77.

Johnson, D., Krsek, M., Weillington, E.M.H., Stott, A.W., Cole, L., 2005. Soil invertebrates disrupt carbon flow through fungal networks. Science 309, 1047.

Johansson, K., Lindqvist, O., Timm, B., 1988. National Swedish Environment Protection Board, report 3470.

Karmakar, R., Das, I., Dutta, D., Rakshit, A., 2016. Potential effects of climate change on soil properties: a review. Science International, 65-73.

Kaste, J.M., Bostick, B.C., Friedland, A.J., Schroth, A.W., Siccama, T.G., 2006. Fate and speciation of gasoline-derived lead in organic horizons of the northeastern USA. Soil science society of America journal 70, 1688-1698.

Kabata-Pendias, A., Pendias, H., 2001. Trace elements in soils and plants. Third edition. CRC Press London New York.

Kim, G., Yoon, Y.J., Kim, H.A., Cho, H.J., Park, K., 2017. Elemental composition of Arctic soils and aerosols in Ny- Ålesund measured using laser-induced breakdown spectroscopy. Spectrochimica Acta part B 134, 17-24.

Kozak, K., Polkowska, Z., Stachnik, Ł., Luks, B., Chmiel, S., Ruman, M., Lech, D., Kozioł, K., Tsakovski, S., Simeonov, V., 2016. Arctic catchment as a sensitive indicator of the environmental changes: distribution and migration of metals (Svalbard). Int. J. Environ. Sci. Technol.

Komonweeraket, K., Cetinb, B., Aydilekc, A.H., Bensona, C.H., Edila, T.B., 2015. Effects of pH on the leaching mechanisms of elements from fly ash mixed soils. Fuel 140, 788-802.

Krawczyk, W.E., Lefanconnier, B., Pettersson, L.E., 2003. Chemical denudation rates in the

Bayelva catchment, Svalbard, in the fall of 2000. Physics and chemistry of the earth 28, 1257-1271.

Låg, J., Steinnes, E., 1978. Regional distribution of mercury in humus layers of Norwegian forest soils. Acta Agric. Scand. 28, 393-396.

Låg, J., Steinnes, E., 1978. Regional distribution of selenium and arsenic in humus layers of Norwegian forest soils. Geoderma 20, 3-14.

Larose, C., Dommergue, A., Angelis, M.D., Cossa, D., Averty, B., Marusczak, N., Soumis, N., Schneider, D., Ferrari, C., 2010. Springtime changes in snow chemistry lead to new insights into mercury methylation in the Arctic. Geochimica et Cosmochimica Acta 74, 6263-6275.

Lever, J., Krzywinski, M., Altman, N., 2017. Principal component analysis. Nature methods 14, 641-642.

Li, C.S., Cornett, J., Ungar, K., 2003. Long-term decrease of cadmium concentrations in the Canadian Arctic air. Geophysical research letters 30, 1256.

Marquès, M., Sierra, J., Drotikova, T., Mari, M., Nadal, M., Domingo, J.L., 2017. Concentrations of polycyclic aromatic hydrocarbons and trace elements in Arctic soils: a case-study in Svalbard. Environmental research 159, 202-211.

Marijin van der Meij, W., Temme, A.J.A.M., de Kleijn, C.M.F.J.J., Reimann, T., Heuvelink, G.B.M., Zwoliński, Z., Rachlewicz, G., Rymer, K., Sommer, M., 2016. Arctic soil development on a series of marine terraces on central Spitsbergen, Svalbard: a combined geochronology, fieldwork and modelling approach. Soil 2, 221-240.

Martín-Torre, M.C., Payán, M.C., Verbinnen, B., Coz, A., Ruiz, G., Vandecasteele, C., Viguri, J.R., 2015. Metal release from contaminated estuarine sediment under pH changes in the marine environment. Arch Environ Contam Toxicol 68, 577-587.

McGuire, A.D., Anderson, L.G., Christensen, T.R., Dallimore, S., Guo, L., Hayes, D.J., Heimann, M., Lorenson, T.D., Macdonald, R.W., Roulet, N., 2009. Sensitivity of the carbon cycle in the Arctic to climate change. Ecological monographs 79(4), 523–555.

Meyers, P.A., Pratt, L.M., Nagy, B., 1992. Introduction to geochemistry of metalliferous black shales. Chemical geology, 99 vii-xi.

Mu, Y., Saffarzadeh, A., Shimaoka, T., 2017. Influence of ignition process on mineral phase transformation in municipal solid waste incineration fly ash: implications for estimating Loss-on-ignition (LOI). Waste management 59, 222-228.

Nygård, T., Steinnes, E., Røyset, O., 2012. Distribution of 32 elements in organic surface soils: contributions from atmospheric transport of pollutants and natural sources. Water Air Soil Pollut 223, 699-713.

Obrist, D., Agnan, Y., Jiskra, M., Olson, C.L., Colegrove, D.P., Hueber, J., Moore, C.W., Sonke, E., Helmig, D., 2017. Tundra uptake of atmospheric elemental mercury drives Arctic mercury pollution. Nature 547, 201-204.

Osterkamp, T.E., 2001. Sub-sea permafrost. Encyclopedia of ocean science, 2902-2919.

Ottesen, R.T., Bogen, J., Finne, T.E., 2010. Geochemical atlas of Norway. Norges geologiske undersøkelse (NGU).

Pacyna, J.M., Ottar, B., 1985. Long-range transport of trace elements to Ny-Ålesund, Spitsbergen. Atmospheric environment 19, 857-867.

Pédrot, M., Dia, A., Davranche, M., 2009. Double pH control on humic substance-borne trace elements distribution in soil waters as inferred from ultrafiltration. Journal of colloid and interface science 339, 390–403.

PerkinElmer. The 30-minute guide to ICP-MS. ICP-Mass Spectrometry.

Pearson, K., 1901. On lines and planes of closest fit to systems of points in space. Philosophical magazine 2 (11), 559-572.

Pignatello, J.J., 1998. Soil organic matter as a nanoporous sorbent of organic pollutants. Advances in colloid and interface science 76-77, 445-467.

Poirier, V., Roumet, C., Munson, A.D., 2018. The root of the matter: linking root traits and soil organic matter stabilization processes. Soil biology and biochemistry 120, 246-259.

Reid, L., Mackay, D., 2008. Local and distant residence times of contaminants in multi-compartment models. Part II: application to assessing environmental mobility and long-range atmospheric transport. Environmental pollution 156, 1182-1189.

Schroeder, W.H., Beauchamp, S., Edwards, G., Poissant, L., Rasmussen, P., Tordon, R., Dias, G., Kemp, J., Heyst, B.V., Banic, C.M., 2005. Gaseous mercury emissions from natural sources in Canadian landscapes. Journal of geophysical research 110, D18302.

Schroeder, W.H., Anlauf, K.G., Barrie, L., Lu, J.Y., Steffen, A., 1998. Arctic spring time depletion of mercury. Nature 394, 331-332.

Schuster, E., 1991. The behavior of mercury in the soil with special emphasis on complexation and adsorption processes – a review of the literature. Water, air, and soil pollution 56, 667-680.

Sharp, M., Skidmore, M., Nienow, P., 2002. Seasonal and spatial variations in the chemistry of a high Arctic supraglacial snow cover. Journal of glaciology 48, 149-158.

Singh, S.M., Sharma, J., Sakhalkar, P.G., Upadhyay, A.K., Naik, S., Pedneker, S.M., Ravindra, R., 2013. Atmospheric deposition studies of heavy metals in Arctic by comparative analysis of lichens and cryoconite. Environ. Monit. Assess 185, 1367-1376.

Skyllberg, U., Xia, K., Bloom, P.R., Nater, E.A., Bleam, W.F., 2000. Binding of mercury (II) to reduced sulfur in soil organic matter along upland-peat soil transects. Journal of environmental quality 29, 855-865.

Søndergaard, J., Rigét, F., 2012. Mercury transport in a low-Arctic river in Kobbefjord, West Greenland (64° N). Water Air Soil Pollut 223, 4333-4342.

Soon, Y.K., 1981. Fungitoxicity of metal ions. Nature (London) 184, 475, 1959.

Steinnes, E., Lierhagen, S., 2018. Geographical distribution of trace elements in natural surface soils: Atmospheric influence from natural and anthropogenic sources. Applied geochemistry 88, 2-9.

Steinnes, E., Friedland, A.J., 2006. Metal contamination of natural surface soils from long-range atmospheric transport: existing and missing knowledge. Environ. Rev. 14, 169–186.

Steffen, A., Bottenheim, J., Cole, A., Douglas, T.A., Ebinghaus, R., Friess, U., Netcheva, S., Nghiem, S., Sihler, H., Staebler, R., 2013. Atmospheric mercury over sea ice during the OASIS-2009 campaign. Atmos. Chem. Phys. 13, 7007-7021.

Steffen, A., Douglas, T., Amyot, M., Ariya, P., Aspmo, K., Berg, T., Bottenheim, J., Brooks, S., Cobbett, F., 2008. A synthesis of atmospheric mercury depletion event chemistry in the atmosphere and snow. Atmos. Chem. Phys. 8, 1445-1482.

Szymanski, W., Skiba, S., Wojtuń, B., 2013. Distribution, genesis and properties of Arctic soils: a case study from the Fuglebekken catchment, Spitsbergen. Pol. Polar Res. 34, 289-304.

Szymanski, W., Siwek, J., Wascińska, J., Wojtuń, B., 2016. Texture and geochemistry of surface horizons of Arctic soils from a non-glaciated catchment, SW Spisbergen. Polish po;ar research 37, 361-377.

Szymański, W., 2017. Chemistry and spectroscopic properties of surface horizons of Arctic soils under different types of tundra vegetation – a case study from the Fuglebergsletta coastal plain (SW Spitsbergen). Catena 156, 325-337.

Thomas, R., 2008. Practical guide to ICP-MS: a tutorial for beginners; CRC Press 2008.

Vanhaecke, F., 2002. ICP-MS. Alternative means for the elimination of interferences. Anal. Bioanal. Chem. 372, 20-21.

Vidar, H., 1998. Svalbard: nature and history. Oslo: Norwegian polar institute.

Voogt, P.D., 2017. Review of environmental contamination and toxicology. Springer, Switzerland.

Wang, T., Camps-Arbestain, M., Hedley, C., 2016. Factors influencing the molecular composition of soil organic matter in New Zealand grasslands. Agriculture, ecosystem and environment 232, 290-301.

Wedepohl, K.H., 1995. The composition of the continental crust. Geochim. Cosmochim. Acta. 58A, 959-960.

Wild, B., Schnecker, J., Alves, R.J.E., Barsukov, P., Bárta, J., Capek, P., Gentsch, N., Gittel, A., Guggenberger, G., Lashchinskiy, N., Mikutta, R., Rusalimova, O., Santrucková, H., Shibistova, O., Urich, T., Watzka, M., Zrazhevskaya, G., Richter, A., 2014. Input of easily available organic C and N stimulates microbial decomposition of soil organic matter in arctic permafrost soil. Soil biology & biochemistry 75, 143-151.

Willianms, L., Borchhardt, H., Colesie, C., Baum, C., Buchmann, K.K., Rippin, M., Becker, B., Karsten, U., Büdel, B., 2017. Biological soil crust of Arctic Svalbard and of Livingston Island, Antarctica. Polar Biol 40, 399-411.

Zaborska, A., Beszczyńska-Möller, A., Wodarska-Kowalczuk, M., 2017. History of heavy metal accumulation in the Svalbard area: distribution, origin and transport pathway. Environmental pollution 231, 437-450.

Ziółek, M., Bartmiński, P., Stach, A., 2017. The influence of seabirds on the concentration of selected heavy metals in organic soil on the Bellsund coast, western Spitsbergen. Arctic, Antarctic, and Alpine Research 49, 507–520.

Zhang, T., Wang, N.F., Liu, H.Y., Zhang, Y.Q., Yu, L.Y., 2016. Soil pH is a key determinant of soil fungal community composition in the Ny- Ålesund region, Svalbard (high Arctic). Front. Microbiol. 7 (227), 1-10.

Zhu, Z.Y., Wu, Y., Liu, S.M., Wenger, F., Hu, J., Zhang, J., Zhang, R.F., 2016. Organic carbon flux and particulate organic matter composition in Arctic valley glaciers: examples from the Bayelva and adjacent Kongsfjorden. Biogeoscience 13, 975-987.

Appendix

A1: GPS data of sampling location.

Location	Organic sample	Mineral sample	Water sample	ºN	ºE
A	1	1		78.93250°N	11.82446°E
B	2,3	2,3	1	78.93083°N	11.81694°E
C	4,5	4,5	2	78.92833°N	11.81167°E
D	6	6		78.92917°N	11.78724°E
E	7,8,9	7,8	3	78.92889°N	11.84389°E
F	10,11	9,10	4	78.92667°N	11.85334°E
G	12,13	11,12	5,6,7	78.92333°N	11.85638°E
H	14,15	13,14	8,9	78.92333°N	11.84027°E
I	16,17	15,16		78.92111°N	11.84776°E
J	18,19	17,18		78.93222°N	11.83417°E
K	20	19		78.93222°N	11.83248°E
L	21,22,23	20	22,23	78.95667°N	11.68936°E
M	24,25	21,22	18,36,37	78.91803°N	11.87117°E
N	26,27	23,24	19,38,39	78.91859°N	11.85500°E
X	28,29	25		78.92328°N	11.79397°E

A2: GPS for sampling sites.

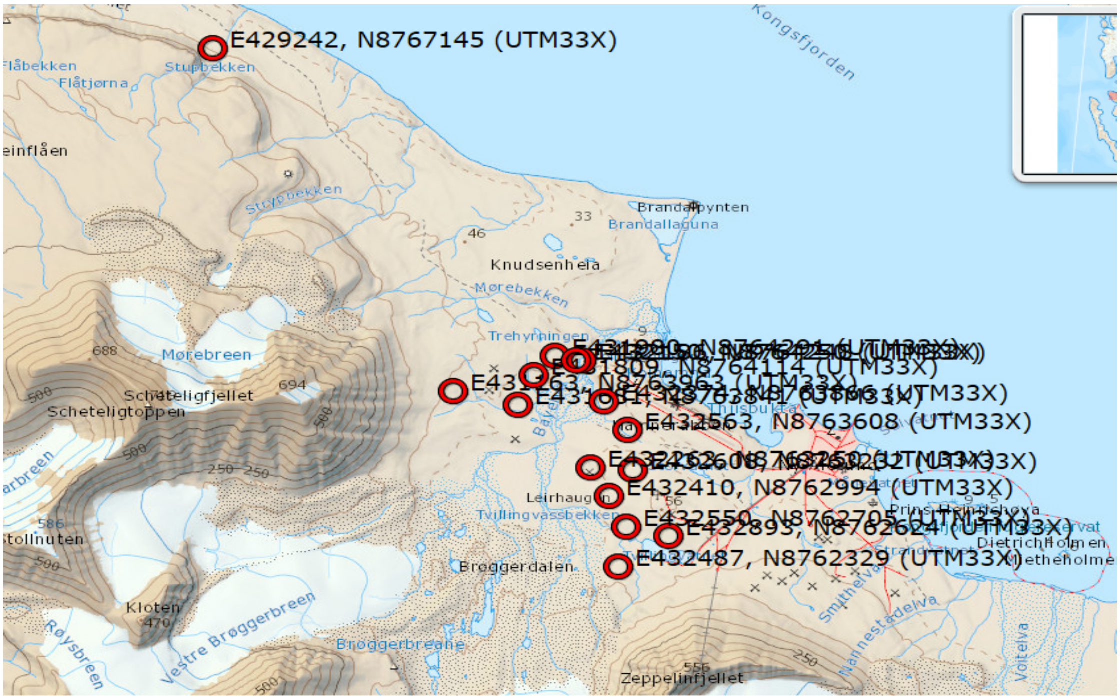

A3: Detection limits of ICP-MS analysis for 65 elements. Resolution is given as Lr (low), Mr (medium) and Hr (high).

Sign	Isotope	Element	Resolution	IDL (ug/g)	BDL
Al	27	Aluminium	Mr	0.576	2
Sb	121	Antimony	Mr	0.00576	0.082
As	75	Arsenic	Hr	0.072	
Ba	137	Barium	Mr	0.03744	
Be	9	Beryllium	Mr	0.02304	
Bi	209	Bismuth	Lr	0.00288	
B	11	Boron	Lr	0.144	
Br	81	Brom	Hr	8.64	
Cd	111/114	Cadmium	Lr	0.00576	
Cd	111/114	Cadmium	Mr	0.0288	
Ca	44	Calcium	Mr	5.76	
Ce	140	Cerium	Lr	0.000576	
Cs	133	Cesium	Lr	0.00144	
Cl	35	Chlorine	Mr	288	
Cr	53	Chromium	Mr	0.0576	
Co	59	Cobalt	Mr	0.01152	
Cu	63/65	Cupper	Mr	0.0864	
Dy	163	Dysprosium	Lr	0.002304	
Er	166	Erbium	Lr	0.000864	
Eu	153	Europium	Lr	0.002304	
Gd	155	Gadolinium	Mr	0.0576	
Ga	69	Gallium	Mr	0.02016	
Ge	72	Germanium	Hr	0.0576	
Au	197	Gold	Lr	0.000576	
Hf	178	Hafnium	Lr	0.00288	
Ho	165	Hollium	Lr	0.000576	
In	115	Indium	Lr	0.00144	
Fe	56	Iron	Mr	0.0576	42
Ir	193	Iridium	Lr	0.00144	
La	139	Lantan	Mr	0.00576	
Pb	208	Lead	Lr	0.00576	
Li	7	Lithium	Mr	0.0864	
Lu	175	Lutetium	Lr	0.000576	
Mg	25	Magnesium	Mr	1.44	
Mn	55	Manganese	Mr	0.01728	
Hg	202	Mercury	Lr	0.00576	0.002
Mo	98	Molybdenum	Mr	0.0576	0.48
Nd	146	Neodymium	Lr	0.000576	
Ni	60	Nikkel-60	Mr	0.0432	
Nb	93	Niob	Hr	0.072	0.89
P	31	Phosphor	Mr	1.152	4
K	39	Potassium	Mr	2.88	
Pr	141	Praseodymium	Lr	0.000864	
Re	185	Rhenium	Hr	0.1152	

Rb	85	Rubidium	Mr	0.03456	
Sm	147	Samarium	Lr	0.00144	
Sc	45	Scandium	Mr	0.01152	
Se	78	Selenium	Hr	0.432	
Si	29	Silisium	Mr	28.8	
Ag	109	Silver	Mr	0.0576	
Na	23	Sodium	Mr	28.8	
Sr	88	Strontium	Mr	0.072	
S	34	Sulphur	Mr	57.6	
Tb	159	Terbium	Lr	0.000576	
Tl	205	Thallium	Lr	0.00072	
Th	232	Thorium	Lr	0.00144	
Tm	169	Thulium	Lr	0.00144	
Sn	118	Tin	Lr	0.00288	0.809
Ti	47	Titanium	Mr	0.0576	297
U	238	Uranium	Lr	0.00072	
V	51	Vanadium	Mr	0.00864	1.7
W	182	Wolfram	Lr	0.00288	0.267
Yb	172	Ytterbium	Lr	0.001152	
Zn	67	Zink-67	Mr	0.1152	
Zr	90	Zirkonium	Hr	0.072	

A 4: Soil organic matter (SOM) and Moisture content (MC) at 105 °C of surface and mineral soil.

Sampling station	SOM (%)	MC (%)	Sampling station	SOM (%)	MC (%)
Organic soil					
1	45.05	8.80	16	32.36	6.10
2	53.59	11.88	17	44.61	8.70
3	41.69	8.13	18	48.12	9.17
4	15.19	3.28	19	71.34	11.79
5	42.71	7.73	20	65.11	11.49
6	35.16	7.11	21	82.96	14.09
7	43.17	7.99	22	52.18	10.70
8	25.59	5.73	23	76.87	13.01
9	29.53	6.15	24	29.94	6.16
10	30.80	6.35	25	59.13	10.52
11	46.58	9.12	26	42.10	7.62
12	36.97	6.38	27	70.37	12.65
13	41.55	7.89	28	65.69	12.44
14	58.05	9.74	29	28.85	5.16
15	57.29	9.48			
Minerla soil					
3	8.78	1.91	20	1.70	0.22
16	3.19	0.98	23	3.58	0.93
19	13.12	3.27			

A 5: Soil organic matter (SOM) and moisture content (MC) at 105 °C of surface soil in five sampling locations. Letters show significant differences (same letter means no siginificant difference).

Sampling location	n	SOM (%)	MC (%)
west side[a]	6	38.90 ± 13.06	7.82 ± 2.78
east side 1[ab]	6	45.14 ± 10.56	8.05 ± 1.55
east side 2[ab]	4	50.38 ± 17.91	9.23 ± 2.91
Stuphalle[b]	3	70.67 ± 16.30	12.60 ± 1.73
airport area[ab]	8	45.03 ± 16.61	8.48 ± 2.35

A 6: The correlations between elements Cr, Co, Cu, Ni, Rb and Al, Fe, K.

	Cr	Co	Cu	Ni	Rb	Al	Fe	K
Cr		0.699	0.596	0.68	0.923	0.931	0.776	0.716
Co	**		0.785	0.845	0.764	0.75	0.936	0.813
Cu	**	**		0.916	0.699	0.679	0.837	0.938
Ni	**	**	**		0.736	0.719	0.883	0.971
Rb	**	**	**	**		0.956	0.865	0.789
Al	**	**	**	**	**		0.85	0.771
Fe	**	**	**	**	**	**		0.893
K	**	**	**	**	**	**	**	

A 7: The comparison of SOM in surface soil between 2018 and 2015.

2018		**2015**	
Location	**SOM (%)**	**Location**	**SOM (%)**
West / Bayelva	38.90 ± 13.06	Bayelva A	56.8 ± 16.9
East 1 / Bayelva	45.14 ± 10.56	Bayelva B	52.4 ± 4.1
East 2 / Bayelva	50.38 ± 17.91		
Airport area	45.03 ± 16.61		

A 8: The comparison of mean elemental concentrations in organic soils from Bayelva between 2015 and 2018.

Sampling year Location	2018	2015
	Bayelva, Svalbard	
	Mean ± SD (µg/g)	
Cd	0.511± 0.285	0.571 ± 0.18
Cr	32.4 ± 16.5	19.9 ± 9.4
Cu	9.7 ± 1.9	10.5 ± 3.6
Hg	0.132 ± 0.072	0.122 ± 0.043
Mn	266 ± 104	230 ± 1238
Ni	13.2 ± 4.9	12.9 ± 5.9
Pb	15.3 ± 4.1	14.3 ± 4.5
Zn	65 ± 17.1	73.2 ± 14.9

A 9: The comparison of mean elemental concentration in mineral soils from Bayelva between 2015 and 2018.

Sampling year Location	2018	2015
	Bayelva, Svalbard	
	Mean concentrations (µg/g)	
Cd	0.16 ± 0.07	0.134 ± 0.049
Cr	45.7 ± 23.7	41.6 ± 11.7
Cu	10.6 ± 3.7	15.1 ± 6.4
Hg	0.027 ± 0.013	0.0294 ± 0.0156
Mn	411 ± 144	433 ± 137
Ni	17.5 ± 5.4	22.4 ± 7.9
Pb	10.9 ± 2.5	12.8 ± 4.3
Zn	52.5 ± 13.2	56.6 ± 14.4

A 10: Condition classes for contaminated soil (Hansen and Danielsberg, 2009)

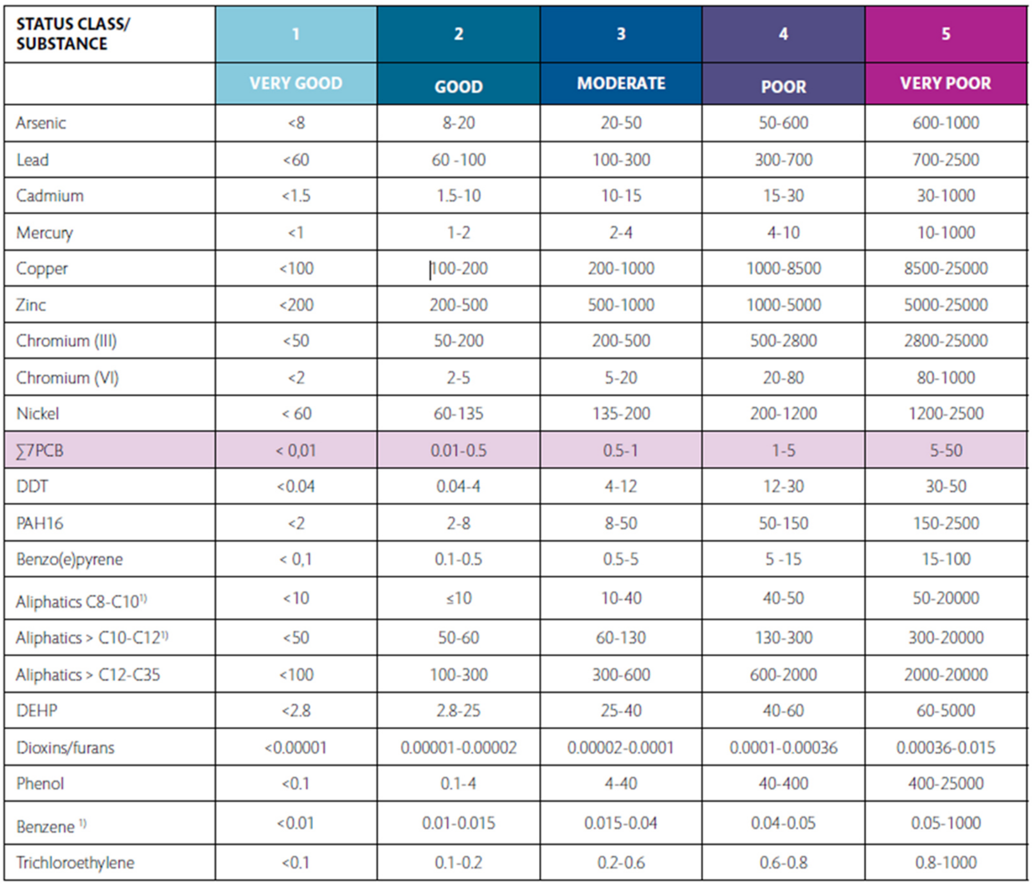

STATUS CLASS/ SUBSTANCE	1	2	3	4	5
	VERY GOOD	GOOD	MODERATE	POOR	VERY POOR
Arsenic	<8	8-20	20-50	50-600	600-1000
Lead	<60	60 -100	100-300	300-700	700-2500
Cadmium	<1.5	1.5-10	10-15	15-30	30-1000
Mercury	<1	1-2	2-4	4-10	10-1000
Copper	<100	100-200	200-1000	1000-8500	8500-25000
Zinc	<200	200-500	500-1000	1000-5000	5000-25000
Chromium (III)	<50	50-200	200-500	500-2800	2800-25000
Chromium (VI)	<2	2-5	5-20	20-80	80-1000
Nickel	< 60	60-135	135-200	200-1200	1200-2500
∑7PCB	< 0,01	0.01-0.5	0.5-1	1-5	5-50
DDT	<0.04	0.04-4	4-12	12-30	30-50
PAH16	<2	2-8	8-50	50-150	150-2500
Benzo(e)pyrene	< 0,1	0.1-0.5	0.5-5	5 -15	15-100
Aliphatics C8-C10 1)	<10	≤10	10-40	40-50	50-20000
Aliphatics > C10-C12 1)	<50	50-60	60-130	130-300	300-20000
Aliphatics > C12-C35	<100	100-300	300-600	600-2000	2000-20000
DEHP	<2.8	2.8-25	25-40	40-60	60-5000
Dioxins/furans	<0.00001	0.00001-0.00002	0.00002-0.0001	0.0001-0.00036	0.00036-0.015
Phenol	<0.1	0.1-4	4-40	40-400	400-25000
Benzene 1)	<0.01	0.01-0.015	0.015-0.04	0.04-0.05	0.05-1000
Trichloroethylene	<0.1	0.1-0.2	0.2-0.6	0.6-0.8	0.8-1000

A 11: Geological conditions of five sampling locations.

West side

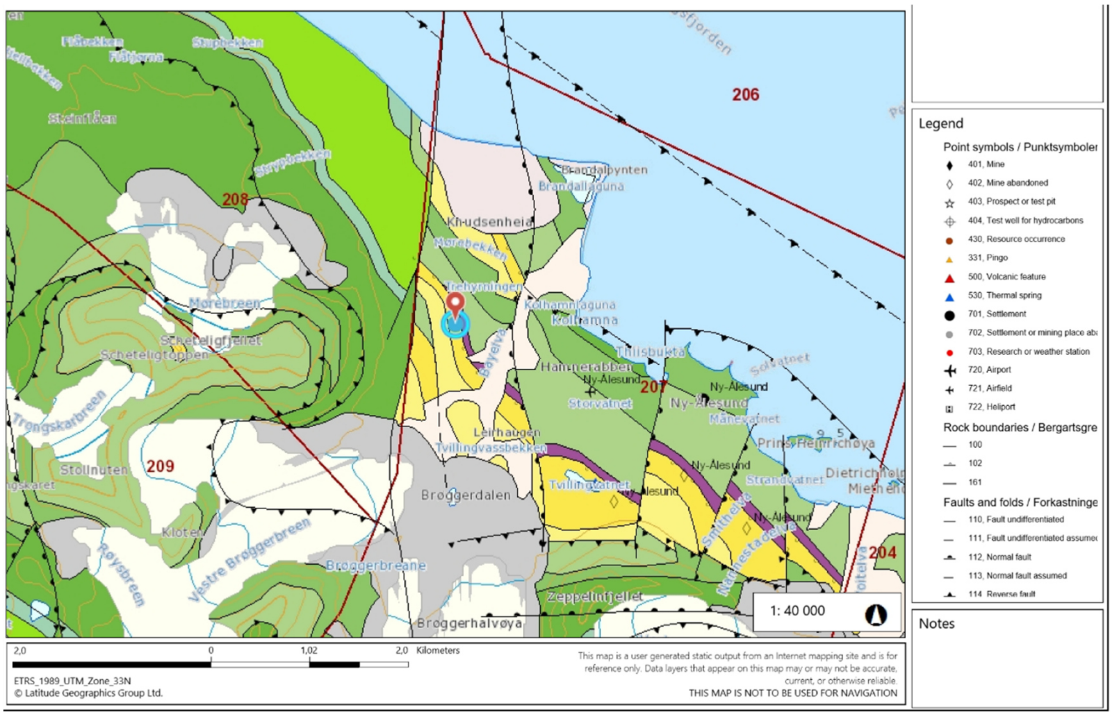

East side 1

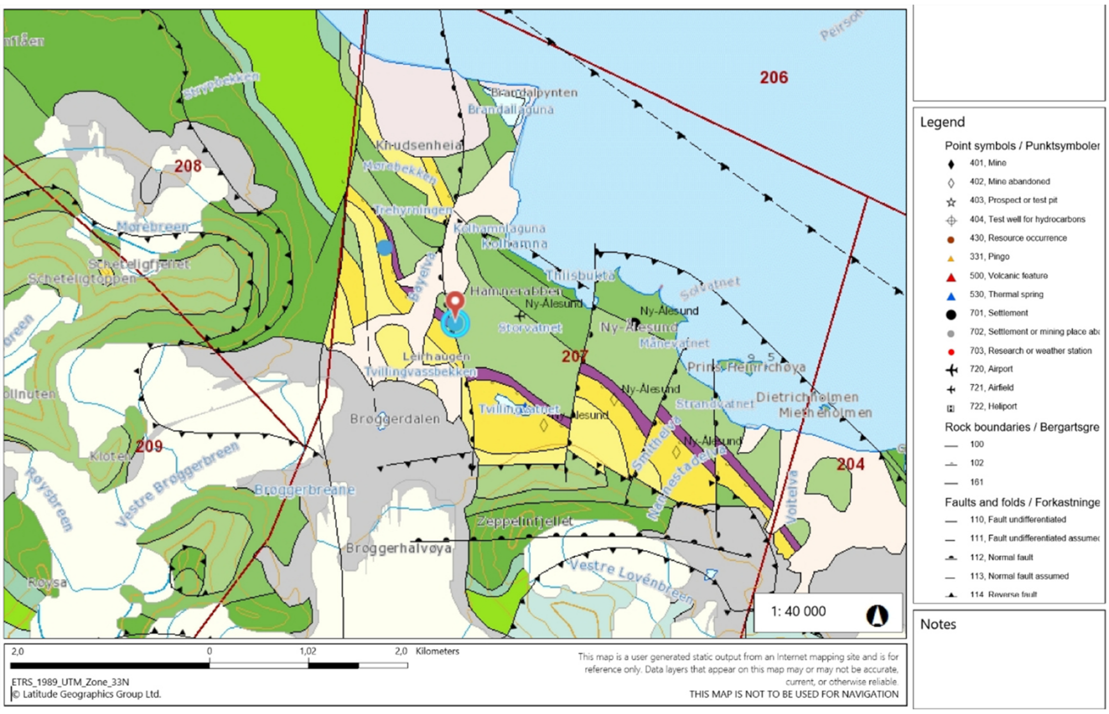

East side 2

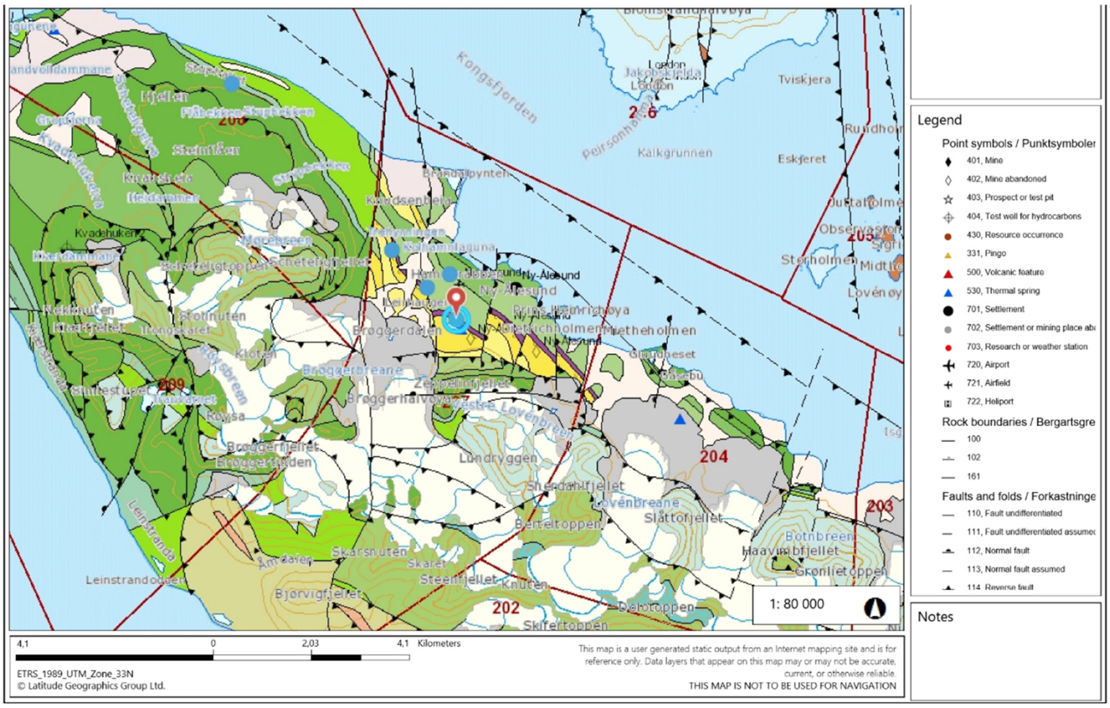

Stuphalle (bird area)

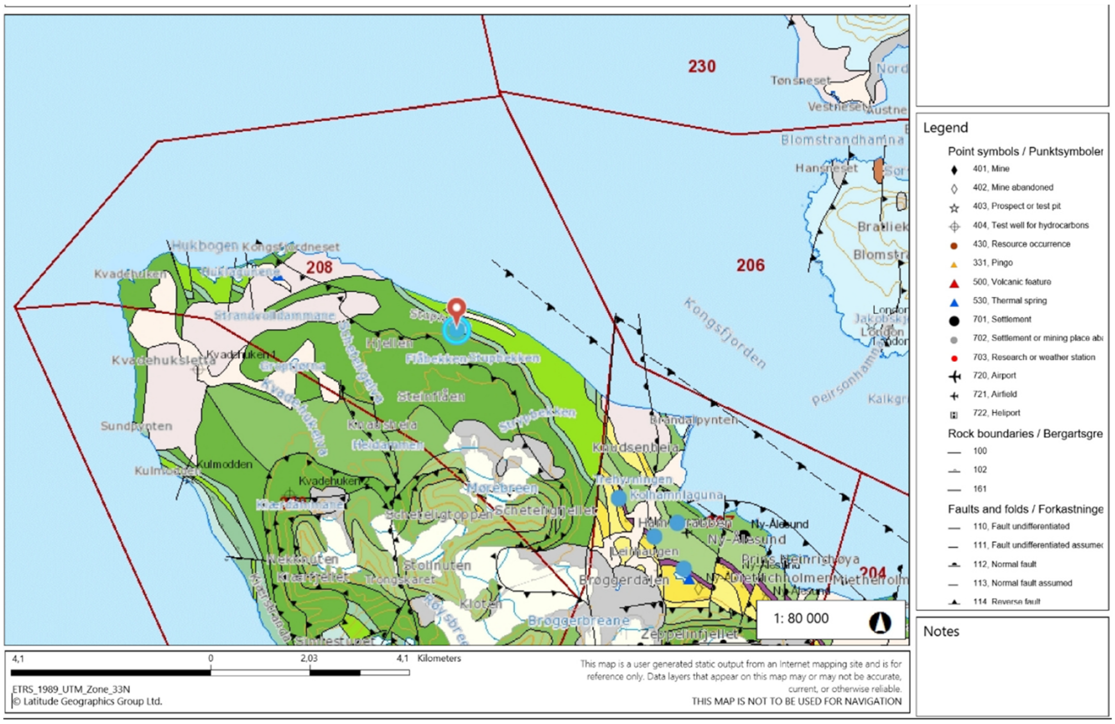

Airport area

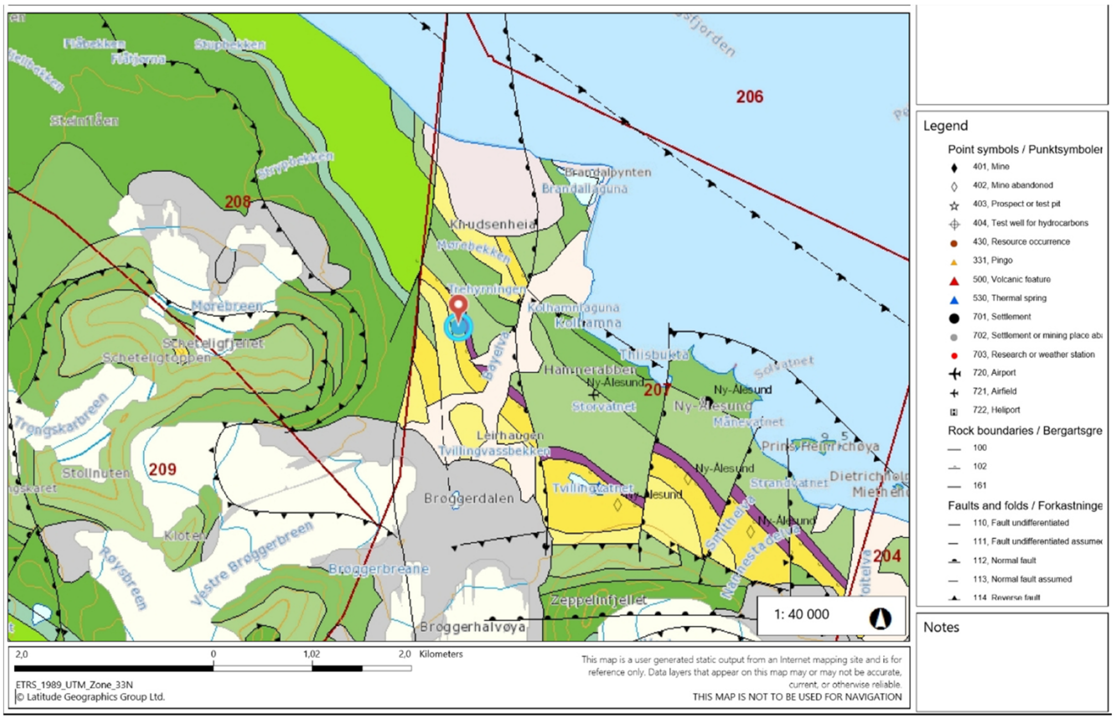

A 12: The data of temperature and carbon dioxide (CO_2) in Svalbard within 20 years [Environmental monitoring of Svalbard and Jan Mayen (MOSJ)].

Year	Temperature (℃)	CO_2 (ppm)
1988	-5.9458	358.7
1989	-5.8965	357
1990	-5.8153	355.2
1991	-5.7294	356.1
1992	-5.6613	360.9
1993	-5.6157	357.8
1994	-5.5788	359.1
1995	-5.5284	381.3
1996	-5.4465	362.3
1997	-5.3278	363.2
1998	-5.1804	365.5
1999	-5.0194	370.9
2000	-4.858	372
2001	-4.701	370.9
2002	-4.5456	374.7
2003	-4.3882	378
2004	-4.2318	378.9
2005	-4.0877	380.5
2006	-3.9687	383.1
2007	-3.8793	384.1
2008	-3.8096	386.4
2009	-3.7387	387
2010	-3.6452	390.3
2011	-3.5168	392.5
2012	-3.3545	394.8
2013	-2.5759	397.3
2014	-2.982	399.6
2015	-2.806	401.2
2016	-2.654	404.4
2017	-2.5314	408
2018	-2.4385	ND